1994

Adaptive power system stabiliser

Amin Khodabakhshian
University of Wollongong

ADAPTIVE POWER SYSTEM STABILISER

A thesis submitted in fulfilment of the requirements for the award of the degree of

DOCTOR OF PHILOSOPHY

from

THE UNIVERSITY OF WOLLONGONG

BY

AMIN KHODABAKHSHIAN, M.Sc.

Department of Electrical and Computer Engineering

1994

Contents

"...To my parents

and my wife..."

ABSTRACT

This thesis investigates a satisfactory stabiliser to damp out low frequency oscillations which occur in power systems for different operating conditions. A fixed gain power system stabiliser is inadequate to provide acceptable damping characteristics as the operating point changes. Adaptive stabilisers which are equipped by the identification process to recognise these changes can then be used to overcome this problem.

In adaptive control, which is a digital control strategy, the parameters of the discrete-time model of a continuous-time power plant are estimated through continual sampling of the input and output signals. In this regard, different methods for obtaining a discrete-time mathematical model for adaptive control of a single-machine infinite-bus power system are first presented. The usual approach has been to use the shift operator q, or its equivalent z transform, but this gives numerical difficulties with the small sampling periods which are now becoming usual with modern control hardware. It is shown, by means of the example of the identification of a generator excitation control system for both single-machine infinite-bus and multimachine power systems, that these problems can be avoided by the use of the delta operator instead. Calculations show that the delta operator formulation also reflects the frequency and dynamic response of the system more accurately and conveniently.

The adaptive Pole Assignment controller, which has not been applied to power systems as a stabiliser, is developed by fixing the poles of the transfer function $G_d(s) = \Delta\delta/\Delta P_m$ which reflects the effect of the load

disturbances (ΔP_m) on the power angle ($\Delta\delta$). The development of the control algorithm has been made using the delta operator rather than the shift operator as this removes numerical problems at fast sampling rates. The delta operator also gives transfer functions very similar to those of the continuous system and, therefore allows simplification of the control design by reducing the order of the numerator of the discrete-time transfer function. Comparative results for the adaptive Pole Assignment controller and a fixed parameter stabiliser show the improvement in response obtained with the adaptive algorithm as the operating point changes for a single-machine infinite bus power system.

In the Pole Assignment adaptive controller, the system response somewhat varies although the settling time of the system is fixed since the location of the zeros is not considered. Therefore, this technique is modified such that the new adaptive power system stabiliser is able to locate both the poles and the zeros. The control strategy is based on a new type of model reference adaptive technique in which the transfer function $G_d(s)$ is modified to a standard form based on explicit system identification. This avoids having to compare the actual plant output with a model following the usual model reference adaptive approach. Controller design is simplified by reducing the number of controller parameters to be identified and controller performance is improved by the use of the delta operator rather than the more usual shift operator for discretization. The similarity between continuous-time and discrete-time systems using the delta operator also allows the design of the adaptive controller based on a continuous-time control strategy. Simulation studies performed on a typical excitation control system model are presented. Comparative results of the Model Reference Adaptive controller, the Pole Shifting and the adaptive Pole-Assignment controllers

and a fixed parameter stabiliser clearly show the benefits of the proposed adaptive controller for stability enhancement of a single-machine infinite-bus power system, especially where there are large changes in operating point. This adaptive controller also provides better damping characteristics than a fixed parameter stabiliser for a multimachine power system.

Declaration

This is to certify that the work reported in this thesis was done by the author, unless specified otherwise, and that no part of it has been submitted in a thesis to any other university or similar institution.

.....

Amin Khodabakhshian

Acknowledgments

I am indebted to my supervisor, Associate Professor V.J. Gosbell, for his constant guidance and encouragement during the preparation of this thesis.

I would like to express my gratitude to:

The Ministry of Culture and Higher Education of Iran for their sponsorship, Dr A.L. Shafei for his valuable help, Dr M.A. Magdy for his guidance in the beginning of this work, and Pacific Power (NSW) for supplying information on system parameters.

I would also like to express my gratitude to the members of staff of the Department of Electrical and Computer Engineering, particularly Professor Chris D. Cook, Ms Maree J. Fryer and Mr. Peter Costigan.

I thank my wife Fereshteh, for her patience, understanding and support throughout the completion of this work.

Finally, I am greatly indebted to my parents, especially my father whom I recently lost, brother and sisters for their support and encouragement.

List of symbols and abbreviations

Power Systems

$A(s)$	denominator of $G_d(s)$
$a_1 ... a_4$	coefficients of denominator of $G_d(s)$
$B(s)$	numerator of $G_d(s)$
$b_1 ... b_3$	coefficients of numerator of $G_d(s)$
$C(s)$	numerator of $G_c(s)$
$c_1 ... c_2$	coefficients of numerator of $G_c(s)$
D	damping factor of synchronous machine
$G_d(s)$	transfer function relating $\Delta\delta$ to ΔP_d (or ΔP_m)
$G_c(s)$	transfer function relating $\Delta\delta$ to ΔV_{ref}
H	generator constant of inertia
K_d	damping factor of synchronous machine
K_e	Exciter gain
K_s	PSS gain
K_1	parameter representing a change in electrical torque for a change in rotor angle with constant flux linkages in the d-axis
K_2	parameter representing a change in electrical torque for a change in d-axis flux linkages rotor angle with constant rotor angle
K_3	parameter representing impedance factor
K_4	parameter representing demagnetising effect of a change in rotor angle

K_5	parameter representing a change in terminal voltage with change in rotor angle for constant E'_q
K_6	parameter representing a change in terminal voltage with change in E'_q for constant rotor angle
M	generator constant of inertia (= 2 H)
P	real power
Q	reactive power
P_a	accelerating power
t	time variable
T_a	time constant of PSS
T_1	time constant of PSS
T_2	time constant of PSS
T'_{do}	field open circuit time constant
V_t	terminal voltage
V_o	infinite bus voltage
X	equivalent system reactance
x'_d	transient reactance, direct axis component
x_d	reactance, direct axis component
x_q	reactance, quadrature axis component
$\Delta\delta$	change in rotor angle
ΔP_d	change in tie-line power
ΔP_m	change in mechanical power
ΔV_{ref}	change in reference voltage
$\Delta\omega$	change in rotor speed

ω_n	natural angular frequency of oscillation
ζ	damping ratio

Control and Identification

A/D	analog to digital converter
D/A	digital to analog converter
e	error signal
f_s	sampling rate
h	sampling time
L(k)	gain vector
P(k)	covariance matrix
t_k	time index
t_p	time required to reach the first peak
u(t), u(q), u(δ)	input variable
y(t), y(q), y(δ)	output variable
ε(k)	prediction error
ϕ(k)	observed vector
λ	forgetting factor
θ	parameter vector
$\hat{\theta}$	estimate of θ
ν_δ	measure of numerical sensitivity associated with frequency response evaluation for delta model
ν_q	measure of numerical sensitivity associated with frequency response evaluation for shift model

$v(t)$	guassian noise

Mathematical operators

$D=d/dt$	differential operator
Π	product of factors
q	forward shift operator
q^{-1}	backward shift operator
z	frequency domain operator
δ	delta operator
w	w operator
$\lambda_i( )$	eigenvalue of matrix ( )
Σ	summation of factors

Abbreviations

AER	automatic excitation regulator
ANN	Artificial neural network
APSS	Adaptive power system stabiliser
AVR	automatic voltage regulator
FLPSS	Fuzzy logic power system stabiliser
GMPS	Generalised Multivariable Pole Shifting
GMV	Generalised Minimum Variance
MIMO	Multi-Input Multi-Output
MRAC	Model Reference Adaptive Controller
MV	Minimum Variance
PA	Pole Assignment
PSS	power system stabiliser

RLS	Recursive Least Squares
SISO	Single-Input Single-Output
SMIB	Single-machine infinite-bus
STC	Self Tuning Control
STR	Self Tuning Regulator
SVC	static var compensator

CHAPTER 1

Chapter 1

INTRODUCTION

1.1 OVERVIEW

This thesis sets out to provide an adaptive controller able to damp out low frequency oscillations which appear on an interconnected power system over a wide range of operating points.

The Pole-Assignment adaptive controller is applied for the first time as a power system stabiliser, with the modification of the use of the delta operator rather than the shift operator to give improved performance at high sampling rates. The performance is shown to be marginally acceptable when the operating point changes because of shifts in the zeros. A further modification is given by fixing both poles and zeros using a new type of Model Reference Adaptive Controller and is shown to be robust against large changes in operating point. The final controller is tested for both single-machine infinite-bus and multimachine (Two-machine) power systems.

In this chapter a review of different techniques including classical and adaptive ones for damping out low frequency oscillations is given. A brief description of discretization with major contributions of this work is also presented.

1.2 A REVIEW OF LOW FREQUENCY OSCILLATIONS IN POWER SYSTEMS

In an interconnected power system, individual or groups of generating

plants are connected together via tie-lines. In order to maximise the efficiency of the overall interconnected system, it is desirable that all generating plants operate and transfer power through transmission and/or tie-lines without limitation.

However, in practice, sudden changes in load may produce low frequency oscillations which can severely limit the transfer of power within the system. Once started, they can decay, or continue to grow such that they cause two or more parts of power system to be disconnected. These oscillations that are of concern to the dynamic stability of a power system typically occur in the frequency range of approximately 0.2 to 2.5 Hz [1] and are usually recognised as being of two distinct types "local plant mode" and "inter-area mode". The local mode is associated with units at a generating station swinging with respect to the rest of the power system. Typically, this mode of oscillation occurs at the upper end of the frequency range mentioned above. In an interconnected network, various groups of synchronous generators are connected over tie-lines. Oscillations of any one machine group against other groups are reflected in the power flow over the tie-lines. This gives rise to the inter-area mode of oscillation. Typically, these oscillations occupy the lower end of the frequency range of interest [2].

At any given oscillation frequency, the major concern of dynamic stability is to improve both synchronising and damping torques [3]. Although the automatic excitation regulator (AER) can provide a significant improvement in the part of synchronising torques as its dc gain increases, it will increase the magnitude of negative damping torque causing instability especially for moderate to high system transfer impedances, and heavy loadings. With more experience, power system engineers are now convinced that in these circumstances, additional

damping can be provided by a "fixed" parameter supplementary excitation control, namely a power system stabiliser (PSS) [3-6]. In essence, the aim of a power system stabiliser is to produce a component of electrical torque in phase with speed variations. This causes an increase in damping torque produced by the generator and this in turn helps to damp out rotor oscillations. Therefore, a positive damping signal, derived from either the speed or frequency or accelerating power [1,7], with adequate gain and phase advance is injected at the summing junction where AER is connected.

The 'fixed' type of PSS performs well for a medium range of operating conditions. Where large changes in the parameters of the load and network configuration occur, the conventional PSS becomes less effective in providing the required damping signals [8]. One possible way to overcome this problem is to use adaptive techniques [8]. These types of controllers are equipped by the identification process to identify these changes and this in turn helps to change the controller parameters for increasing the damping.

Owing to the use of different methods for the design of fixed and adaptive PSSs, a separate review of classical and adaptive techniques will be given.

1.3 CLASSICAL TECHNIQUES

The dynamic stability study is undertaken to obtain the damping requirements for a satisfactory system performance. It is used to identify troublesome modes of oscillations, develops rules for determining which generators in a system should be equipped with stabilisers, determines the general characteristics of those stabilisers and decides on tentative stabiliser and regulator parameter settings [9]. Since in the dynamic

stability study the stability of a power system is subjected to a relatively small and sudden disturbance like a small step change in load, the system can be described by linear differential equations, and the system can be stabilised by a linear and continuous supplementary controller. Therefore, different methods of analysis based on linear control have been used by various investigators.

The Routh-Hurwitz criterion tests stability by examining the sign of the real part of the denominator polynomial of the closed-loop transfer function. The system is unstable if any root has a positive real part. This method has been used by investigators such as Gove [10] and Booth et al [11]. Whilst it gives a simple means of determining asymptotic stability, its main disadvantage is that it gives no indication of the degree of stability of the system, since no information is available on how the poles of the closed-loop transfer function move with variations in gain constants.

A method which is capable of indicating how the stability of a system relates to the variations in gain constants is the Root-Locus method. This method is quick to implement and involves plotting the poles and zeros of a transfer function on an Argand diagram. By varying the value of the gain constants, the migratory paths of the poles and zeros are charted. Poles tending towards the right-hand plane of the diagram lead to an unstable system. This method has been employed successfully by Bollinger et al [12] and Oradat et al [13] in evaluating parameter settings for PSS design. Stapleton [14] used this method to investigate the effect of voltage regulator parameter settings on the stability and dynamic response of an excitation control system. One drawback with this method is the presence of a large number of poles and zeros, which makes the establishment of any rules difficult.

The Nyquist criterion gives a test for the right-half plane poles of a closed-loop system. Its advantage is that stability considerations can be performed on a closed-loop system based on open-loop frequency response data. Given a closed-loop system with forward path transfer function G(s) and unity negative feedback, a necessary and sufficient condition for asymptotic stability is that the map of the Nyquist contour on the G(s)-plane, corresponding to a clockwise traverse, should make a number of anticlockwise encirclements of the point (-1, 0) equal to the number of poles possessed by G(s) in the right-half plane. The Nyquist contour is a path in the s-plane consisting of a segment of the imaginary axis, from -jR to jR, together with a semicircle of radius R in the right-half plane to close the contour, where there are poles on the imaginary axis, the contour is indented so as to avoid them [15].

This method has been used by Ewart et al [16] and Aldred et al [17] for determining the stability of synchronous machines. It is capable of assessing the degree of stability in the system and is useful for practical compensation studies [18]. However, it involves extensive computation.

Heffron et al [19] used the analogue computation approach to determine stability. This approach is based on the realisation of an electric circuit using adders, multipliers and integrators or differentiators to represent the dynamical system under investigation. This hardware set-up essentially solves a differential equation which reflects the characteristics of the dynamical system. The coefficients of the equation can be adjusted for optimum output using potentiometers. With this approach, close to real system performance can be observed. However, it is a lengthy process.

A method which is well suited for the selection of the parameter values of stabilising devices is the domain separation one, which was developed by

Venikov [20]. The method rests on the establishment of the characteristic equation of a system and its separation into real and imaginary parts, explicitly in terms of the parameters under investigation as functions of frequency and damping. Two parameters are studied at a time. These are plotted as a function of frequency for particular values of damping in a coordinate system with the two parameters as axes. It is then possible to establish the optimum values for these parameters based on curves which allow a separation of improved damping domain from a domain with worse damping. Yu et al [21] and Surana et al [22] have applied this method for selecting optimum values for regulator parameters.

Eigenvalue analysis is, so far, the most common method used for large interconnected power systems and lends itself readily to digital computer applications. Eigenvalues are roots of the characteristic polynomial of a system and as such characterise its performance. They may be real numbers or more often complex ones for dynamical systems. The real part conveys information about the amount of damping, while the imaginary part is related to the natural frequency of oscillation of the corresponding mode [23]. Eigenvalues are functions of the design and control parameters of the system so eigenvalue sensitivity analysis, whereby eigenpatterns are mapped out in the s-domain for small changes in parameter values, give a good indication of the degree of stability of the system. Obata et al [24], Martins [25] and Ajjarapu [26] are among many investigators who have used this approach in studies on power system dynamic stability.

Both domain separation and eigenvalue analyses are suitable for off-line stability analysis in system planning. However, it is very difficult to apply them to on-line stability assessment in system operation because they require too much computational time.

The methods of analyses described above aim at establishing relative stability measures for control purposes. Whilst classical methods rely on phase and gain margins, modern control design aim at locating the eigenvalues at well damped positions. A method which is able to locate the poles of the system at desirable locations is pole placement [27]. In this technique the unstable mechanical modes, from eigenvalue analysis of the open-loop power system, are first identified. To find out what these modes are and to which machines they belong, participation factor analysis [28] is used for a matrix of the same open-loop system. This helps to indicate which machine has a dominant effect on the unstable modes and then the decision for installing PSSs in some sites can be made. The PSSs are designed according to the desirable eigenvalues. The results shown in [27] indicate that the unstable modes are well damped as intended. To improve the damping of the poorly damped modes due to the dynamic interaction between machines damping factors for individual subsystems are varied. The results show an improvement in the damping of such modes [27]. However, this needs an extensive effort and time.

Linear Optimal Control (LOC) was first applied by Yu et al [29,30] to design a stabiliser for a hydroeletric power plant. The concept behind this class of regulators is to minimise a linear performance index which represents the system state variation. One of the main advantage of this method in comparison with the conventional PSS designs is that both damping and synchronising torques are being improved. Whereas, the conventional PSS has been designed with a single input signal using phase compensation and for a narrow band of oscillating frequencies, the LOC synthesises the control input from many state variable signals that themselves have different phases, has no need of compensation blocks, and is good over a wide band of frequencies. The drawback of this method is to find a suitable weighting factor Q which is very important in

LOC design. It is very difficult to find a general rule for the choice of all elements of the weighting matrix because most state variables are different physical quantities, like speed, flux linkage, and so on. To solve this problem Aldeen et al [30a] have tried to obtain a systematic method based on the Moore's [30b]. In this method the controllable and observable modes of the state vector in an ordered form are obtained by calculating the balance transformation matrix. However, their proposed method regarding the relationship between the state vector modes and the weighting matrices is not clear and fails to give rigorous systematic method. They also do not give a clear way how the first m states of the balanced system are weighted according to their contribution. To obtain the desirable characteristics a larger computational burden must be taken. Among other users of this method has been Habibullah et al [31].

The parameters of a power system change with load and operating conditions, and, therefore, its dynamic behaviour also changes. However, the conventional stabiliser mentioned above is designed to work most satisfactorily at a particular operating point, and its performance may deteriorate as operating point changes [8,32-35]. Therefore, autotuning stabilisers are required for effective control over a wide range of operating conditions.

1.4 ADAPTIVE CONTROL

Adaptive control is a subject of control theory which deals with a system that can modify its behaviour in response to changes in the dynamics of the process and the disturbances. In recent years, power engineers have considered employing adaptive control techniques for enhancing dynamic stability measures [8]. Among these, two main adaptive control schemes,

namely Model Reference Adaptive Control (MRAC) and Self Tuning Control (STC), have been well developed in control engineering as explained in Sections 1.4.1 and 1.4.2 and applied to power systems as explained in Section 1.4.3 [32-36]. These techniques lead to different ways of adjusting the controller parameters.

1.4.1 Model Reference Adaptive Control

Among the various types of adaptive control configurations, Model Reference Adaptive Control is important since it leads to relatively easy-to-implement systems with a high speed of adaptation which can be used in a variety of situations.

In MRAC the desired performance is expressed in terms of a reference model, which gives the desired response to a command signal. The output of the controlled plant (y(t)) is continually compared to that of the model ($y_m(t)$). The error signal ($e = y_m(t) - y(t)$) is used to adjust the parameters of the regulator in such a way that the error becomes zero.

A block diagram of the MRAC method is shown in Figure 1.1 where the system can be thought of as consisting of two loops: an inner loop consisting of the plant and the regulator and an adaptive outer loop.

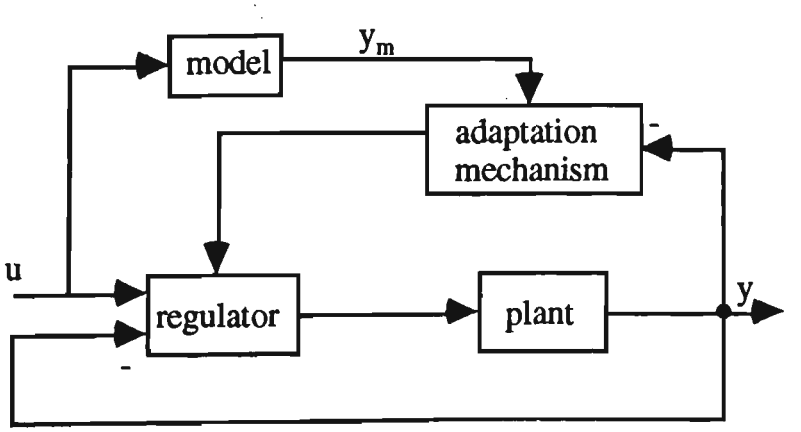

Figure 1.1 Configuration of the usual Model Reference Adaptive Control

The most important problem in such a control loop is to determine the adjustment mechanism so that a stable system, which brings the error to zero, is obtained.

The advantage of this loop-configuration is that, in the event of the adaptive loop failing, the controller will still function at a sub-optimum level. The original controller adjustment rule, called the 'MIT rule' [37] is given by:

$$\frac{d\theta}{dt} = -\gamma e \frac{\partial e}{\partial \theta} \qquad (1\text{-}1)$$

where e is the error between the model output and the actual plant output. The components of the vector $\frac{\partial e}{\partial \theta}$ are the sensitivity derivatives of the error with respect to the adjustable parameters θ. The parameter γ is a design parameter which determines the adaptation rate.

The MIT rule was motivated by the assumption that the parameters θ change much slower than the other system variables. To make the square of the error small, the parameters are changed in the direction of the negative gradient of e^2.

Equation (1-1) can be rewritten as:

$$\theta(t) = -\gamma \int_0^t e(s) \frac{\partial e(s)}{\partial \theta} ds \qquad (1\text{-}2)$$

The MRAC method discussed above is called a direct method because the adjustment rules tell directly how the regulator parameters should be updated.

1.4.2 Self-Tuning Control

A different scheme is obtained if the process parameters are updated and

the regulator parameters are obtained from the solution of a design problem. A controller of this construction is called Self Tuning Control (STC). It relates to a controller which automatically tunes the controller to the desired performance according to the changing system conditions.

A block diagram of STC is shown in Figure 1.2. The adaptive regulator may be regarded as consisting of two loops. The inner loop consists of the process and an ordinary linear feedback regulator. The parameters of the regulator are adjusted by the outer loop, which is composed of a recursive parameter estimator and a design calculation.

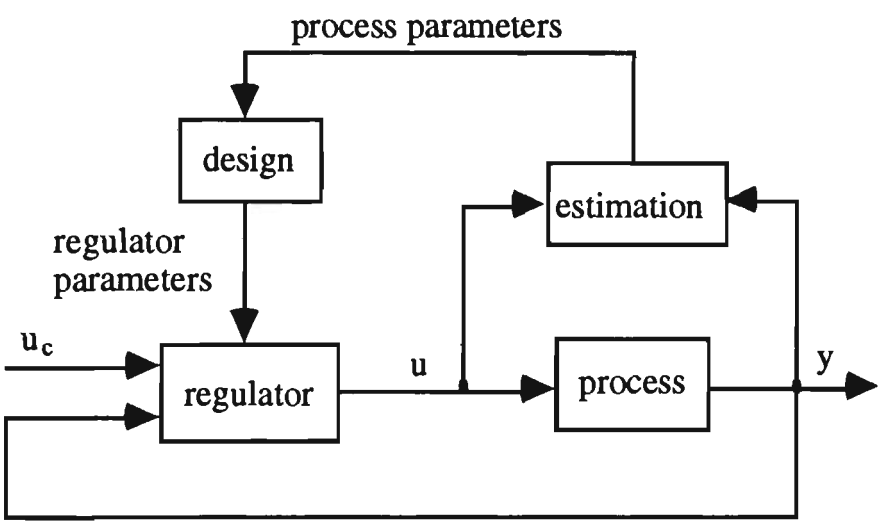

Figure 1.2: General Self-Tuning Control structure

In Figure 1.2 where the parameters of the open-loop transfer function of the process are estimated from sampled input/output data, an indirect adaptive algorithm is obtained. The regulator parameters are not updated directly, but rather indirectly via the estimation of the process model. This type of STC is called explicit STC. It is possible to calculate the parameters of the plant model so that it is expressed in terms of the controller parameters. The controller design step is thus eliminated and the controller parameters, rather than the plant model ones, are estimated. This method is known as the implicit STC.

The identification process in the STC scheme of Figure 1.2 is performed for an open-loop system where the input signal could be chosen freely with the exception that at least the condition of persistent excitation has to be satisfied [38]. This condition is usually performed by superimposing a pseudorandom noise on the input signal [32]. However, in the proposed adaptive controller in this work as explained below it is not possible to select the input signal of the open-loop system freely. Therefore, the indirect STC scheme of Figure 1.2 is modified and shown in Figure 1.3 where ΔV_{ref}, ΔP_d, ΔP_m, and $\Delta\delta$ show the voltage reference, the power swing disturbances, the change in load and the power angle swings respectively.

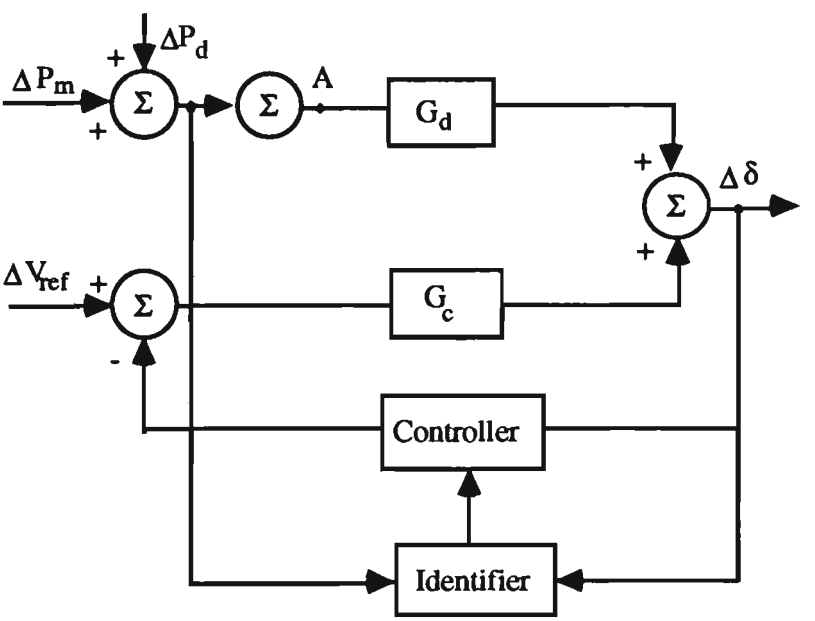

Figure 1.3: The adaptive controller scheme

The aim in this work is to design an adaptive controller such that the poles and the zeros of the closed-loop system ($G_d=\Delta\delta/\Delta P_m$) are placed at preselected locations by using explicit system identification. However, the point A shown in Figure 1.3 corresponding to that summing junction of the linearized model where the machine mechanical loop is connected (see Figure 2.1 in Chapter 2) is not accessible. Therefore, the closed-loop system has to be estimated rather than the open-loop system, which

includes the generator model and the excitation system, directly. In this scheme it is not necessary to add any additional noise to the system for identification.

Indirect STC, based on least squares estimation, was first proposed by Kalman in 1958 [39]. No analysis was given of the properties of the closed loop system. A prototype special-purpose computer was built to implement the controller, but the development was impeded by hardware problems. A similar controller, based on least-squares estimation and Minimum Variance (MV) control, in which the uncertainties of the estimates were considered, was published by Wieslander and Wittenmark in 1971 [40]. Astrom and Wittenmark [41] made a direct STC using MV for the control strategy and the RLS parameter estimation. The objective of this regulator is to minimise the variance of the output, without putting any constraints on the magnitude of the control signal. Similar Self-Tuning Controllers were developed by Clarke and Gawthrope [42-43] using Generalised Minimum Variance (GMV) control. This algorithm gives a considerable amount of freedom for adjusting the parameters of the controller but is more complicated than the MVSTC. Pole Assignment STC was the next development of STC, and was given by Wellstead et al [44]. In such STCs, the controller parameters are determined through a Recursive Least Square estimation such that the closed-loop poles are placed at desired locations. All these techniques have been developed in control engineering and some of them have been applied to power system. Now, a review is given of adaptive stabilisers in which some of these techniques have been used.

1.4.3 Adaptive stabilisers in power system applications

An increase in the damping of the system response is desirable, not only

because it reduces the fluctuations in the controlled variables and hence improving the quality of the electricity supply, but mainly because this damping is translated into an increase in the power transmission stability limits. Higher stability limits bring significant economic savings as the need for the expansion of the transmission system can be postponed.

Fixed gain controllers are widely used to improve the damping of power systems. However, these fixed-parameter controllers have been designed for a specific operating point and, therefore, they cannot, in general, maintain the same quality of performance at other operating points. It is for this reason that adaptive control has so much potential to improve system performance.

Kanniah, et al [45-46] use an STC approach on the excitation control of a single-machine infinite-bus (SMIB) model. Their self tuner is of the implicit type using Minimum Variance technique resulting in simple calculations to form the adaptive control output. However, STCs based on MV control concept suffer some serious drawbacks. They cannot handle non-minimum phase systems without excessive computations. Their attractive feature of simplicity is based on identifying the power system with minimum phase models, however, during the recursive identification process non-minimum phase models may occur which will result in excessive controls and possibly system instability [47]. They are also sensitive to the initial values of the parameters of the identifying model [35].

Xia and Heydt [48] develop an STC approach for a generator connected to an infinite bus through a long transmission line. Their difference equation model relates the present terminal voltage of the machine to past sampled values of that voltage, to past excitation voltages, and to

disturbance values. They augment the excitation control with Guassian noise to aid in the Recursive Least Square (RLS) estimation process. The identified parameters are used to form the control action as a function of past control actions, current and past terminal voltages, as well as desired terminal voltages, and a constant disturbance bias. Integral action is built into the control to eliminate steady-state error. A weighting factor on the control action is selected to enhance system stability. But their particular strategy is limited to use on minimum-phase systems.

Generalised Minimum Variance Self-Tuning Regulator (GMV-STR) was then used by Gu, et al [33] on a SMIB model to solve the difficulties associated with non-minimum phase situations. However, GMV-STR has a constrained control structure, in which the suitable values of two auxiliary polynomials S and Q should be selected to ensure that the closed-loop stability is achieved [33-35], and in this regard no direct method is given how to choose these polynomials such that the instability does not occur. Moreover, this method is more complex than MV control and requires more computation. Reference [33] has not given the superiority of this adaptive stabiliser to the fixed gain one as operating point changes. In [49] Bollinger et al also apply the GMV-STR in a 9-Machine system. A comparison of rotor damping from the proposed adaptive controller and a conventional PSS is given in the paper. The conventional PSS is designed using basic Root-Locus methods described in [50-52]. The simulation results under different conditions show that the system damping is improved when the adaptive PSS replaces the conventional PSS. Norum et al [53] use the same GMV-STR given by [33] to show the effectiveness of adaptive PSS in a real-time laboratory test.

Fan et al [54] use GMV-STR for a multimachine case. They apply this controller on individual subsystems through excitation control. They use a trial-and-error method for the selection of the order of the model to be identified. Using extensive simulations shows that a fourth-order discrete model is the best choice. The GMV control law is based on an one-step optimisation method and the control action at each step attempts directly to drive the system output to its steady-state point. However, this may result in high control burden and system response overshoots in the transient period [42,43]. In order to avoid this problem a dynamic model, which generates an improved trajectory, is obtained for the open-loop form of the identified model by shifting its open-loop poles by a factor α towards the origin. The simulation results show that the proposed GMV-STR is superior to the conventional PSS. However, as mentioned above the drawback of GMV technique is that there is no direct method to find the suitable weighting polynomials Q and R and any wrong selection of these polynomials causes instability [42,43].

An alternative self-tuning method which looks at the strategy of locating closed-loop poles to desired locations is the Pole Assignment (PA) control. Despite this attractive feature of PA controller, it has not been used as an adaptive stabiliser in power system. This method is dismissed in [32] as requiring good insight in selecting the characteristic equation such that a stable feedback controller is achieved. However, as shown later in Chapter 5, this is not a major problem [55].

Then, Ghosh et al [32] introduce a modified version of Pole Assignment, called Pole Shifting for supplementary excitation control. In Pole Shifting control, controller parameters are selected on the basis that closed-loop poles are moved a short distance from identified open-loop

poles in a stabilising direction (radially inward away from the unit circle). The amount of Pole Shifting is controlled by one parameter which can be adjusted to keep controller gains within a reasonable range. The exciter system considered in [32] has an automatic voltage regulator (AVR) with fixed parameters as a primary feedback control system. Superimposed on this is a secondary adaptive loop. The adaptive controller provides an auxiliary input to the AVR exciter loop, and a pseudorandom noise is superimposed on this auxiliary input to aid in the identification. The output of the difference equation model (and the input to the adaptive controller) is taken to be electrical power (with DC component removed). A third-order difference equation model is identified based on the input and output that are sampled every 100 msec. Simulation results on a SMIB model given in this work indicate that the adaptive controller's performance is superior to that of a fixed gain stabiliser and the Linear Optimal Controller.

Chandra et al [36] modify a generalised self tuning controller with Pole Assignment given in control engineering [56] to a self searching Pole Shifting algorithm which is the same as the method explained above. They point out that the most suitable sampling rate in this work , where the shift operator is used, is 100 msec. The simulation results on a multimachine case show a good improvement in dynamic response of the power system in comparison with the conventional stabiliser.

Wu et al [57] describe a self tuning PID (proportional-integral-derivative) power system stabiliser using Pole Shifting technique for a multimachine case. Due to the communication difficulty between individual generators decentralised self tuning stabilisers have been used. Each generator is described by a second-order discrete transfer function and identified by

RLS estimation using the shift operator. This transfer function, though based on local signals, includes the effect of other machines in power system. The PID PSS gain settings are adjusted according to the Pole Shifting technique with the on-line measured generator speed deviation $\Delta\omega$ as the input signal of the adaptive stabiliser. The Pole Shifting factors are being held constant with different values for each generator. The simulation results show that the self tuning PID stabiliser provides a better dynamic response than the conventional stabiliser.

In the Pole Shifting algorithm, shifting the poles excessively towards the centre of the z-plane increases the likelihood of the control signal saturation and, as a result, this may cause a poor identification process, and sometimes greatly affects the closed-loop performance [34]. To avoid this problem Cheng et al [34] describe a self-searching variable Pole Shifting algorithm. In this method the Pole Shifting factor α shifts the closed-loop system poles as close as possible to the centre of the unit circle without violating the control constraints. Since identifying a high order system needs a high computational calculation they point out that the identifying of the system by a lower order (third-order) model gives good results for the proposed algorithm as used in [32]. The simulation results on a SMIB model using the shift operator illustrate the good steady state stability when is compared with a fixed stabiliser.

Cheng et al [58] also expand their method described above to a multimachine power system. They use a decentralised model to design the STR. Each generator is identified as a third-order discrete model using the shift operator. The rotor speed ω and the stabilising signals are used for the identification process as the input and output signals respectively. The analysis and results given in this paper show that the

problem of the stabiliser co-ordination synthesis in a multimachine case is solved with the advantage of the improvement in dynamic performance of the power system.

Chen et al [59] propose another Pole Shifting algorithm in which the shifting factor α is calculated on-line based on an optimisation technique given in [60]. This scheme simplifies the optimisation procedure and reduces the optimisation time. In order to reduce the computation time and enhance the real-time property of the stabiliser, a lower order discrete model (third-order) using the shift operator and sampling time of 50 msec is used. It is shown that the measured and identified frequencies obtained from the low order linear approximation are matched nicely and consistently. The results for various conditions of a SMIB model show that the proposed adaptive PSS provides better damping than fixed PSS over a wide frequency range.

In [61,62] Pahalawatha expand the SISO Pole Shifting adaptive controller algorithm to the MIMO controller. This extension combines and co-ordinates the action of governor and excitation system. Here they take the accelerating power and variation in terminal voltage as the input signals to the controller. They use a 'self-searching' variable Pole Shifting algorithm [34,63], as explained above, to avoid having a poor performance of the controller. The simulation and real-time implementation results using the shift operator and a sampling time of 150 msec on a SMIB model show that the proposed adaptive controller performance is better than a fixed PSS.

Pole Shifting techniques had been limited to Single-Input Single-Output (SISO) systems or Multi-Input Multi-Output (MIMO) systems with equal number of inputs and outputs. Ghandakly et al [64] then propose a

Generalised Multivariable Pole Shifting (GMPS) technique which is capable of handling MIMO systems with arbitrary numbers of inputs and outputs. In this method the Pole Shifting factor is self adjusted on-line such that the control constraints will not be violated. The algorithm using the shift operator is applied to a SMIB power system excitation control. Both shaft speed and accelerating power are employed as control inputs. Simulation results show that the system performance obtained by this method is superior to the conventional PSS and a MVSTR. The studies presented also reveal the inherent instability of MVSTR when the system identified model becomes non-minimum phase.

All STR techniques given in the literature, so far, do not guarantee that the exact desirable response always follows as the operating point changes. The reason for this is that there is no access to fix the location of the zeros as well as the poles. A new adaptive controller using a novel approach will be introduced in Chapter 6 which is able to provide a specified response by considering the location of both the poles and the zeros [65].

Among the other controller techniques the optimal control has been used by [66-69]. In [66-68] Mao et al describe a real-time laboratory scaled studies using an adaptive optimal excitation control (OEC) and an adaptive power system stabiliser. Both the proposed OEC and PSS are implemented on three Intel 8086 single board computers, one for identification calculation, one for control calculation and one for man-machine interface. The plant output is taken as the weighted sum of the deviations of the voltage and active power signals. The test results on a SMIB model using the shift operator show that the adaptive controllers improve the damping of the power system in different operating

conditions. In this controller the stability can always guarantee the stability of the closed-loop system when the controlled system is controllable and the output weighting matrix Q>=0 because of the property of the linear optimal control. However, the system performance in linear optimal control depends on the action of the output weighting matrix Q [67] and, in this regard no direct method is given for the selection of Q.

Lim [69] describes a new self tuning stabiliser based on the minimisation of a modified version of a conventional quadratic performance index [70]. This method is so designed that upon minimisation the resulting optimal stabiliser possesses an additional derivative term which is not found in the conventional one. A third-order discrete model of a SMIB power system using the shift operator is used for the identification process. The simulation results show that the proposed self tuning stabiliser provides better damping characteristics than the conventional self tuning stabiliser given in [48] and a fixed PSS. However, no direct method is given how to select the positive weighting constant q', r, B^*.

Wu et al [71] introduce a new STR for a multimachine case. A third-order model of each generator is identified. The controller strategy is based on minimising a performance index in which the weighting factors (Q and R) are to be considered. The simulation results show the superiority of the proposed STR to an AVR controller. However, they do not compare this controller with a conventional PSS. There is also no direct method to determine the weighting factors.

In [72] Ghandakly et al present a decentralised Model Reference Adaptive Control, in which a combination of the decentralised and MRAC theories is applied. The decentralised scheme provides means for coordinating the

generating unit inputs from the excitation and governor control loops in order to generate adequate damping torques. The reference model is represented as a linear dynamic system satisfying certain model-following conditions and also having realistic as well as achievable performance objectives. Adaptive signals are derived for the exciter and governor inputs to assure overall system stability as well as desired system performance. The Liapunouv function method is used to synthesise the feedback controller. The proposed method is applied to a SMIB power system and the simulation results show that the system performance is superior to the digital stabilisers proposed by the same author in [73].

In [32] it is explained that Model Reference Adaptive Controller (MRAC) is not easily applicable in power system because it is not easy to select a suitable model based on the adaptive controller scheme shown in Figure 1.1. Moreover, in the case of unpredictable control disturbance, the reference system will not respond immediately while the actual system will [32,74]. This performance difference will be interpreted as a system error, and the adaptation of system gains will occur. Irving et al [74] explore MRAC for generator voltage regulation to maintain an unconditionally stable adaptive loop using hyperstability theory [75]. In this theory conditions on each component of a system guarantee the unconditional stability of the whole system. They use what they call a 'series-parallel' model reference scheme to reduce the effects of sudden unmeasurable disturbances. Then controllers are analysed in continuous-time domain only, and thus require accurate high speed analog computers to perform complex computations.

The problems regarding the usual approach of MRAC can be resolved by using a new adaptive controller scheme as will be shown in Chapter 6. In

this scheme by using an explicit system identification a compensator is so designed that it forces the closed-loop system to be the same as the reference model without requiring to calculate the error between the plant and the model outputs. An easy method will be given to select the reference model.

1.4.4 Fuzzy logic and artificial neural network stabilisers

There have recently been some interest among researchers to use fuzzy logic and artificial neural network stabilisers rather than using adaptive techniques. Although these methods propose a promise for a considerable work to be carried out in power system, the details of such stabilisers are not given here because they are beyond the scope of this thesis which is mainly concentrated on adaptive stabilisers. However, it is apt to have a brief review of the work done so far in this area.

Hsu et al [76] use an artificial neural network (ANN) for tuning the PSS under different operating conditions. A multilayer feedforward neural network is employed to adapt PSS parameters according to generator loading conditions. The inputs to the neural network contain generator real power output (P) and reactive power (Q) or power factor (PF) which characterise generator loading conditions. The outputs of the neural network are the desired PSS parameters. In the training process, the desired PSS parameters for some typical loading conditions are computed and stored. These input-output patterns constitute the training set. The connection weights are then obtained by using the generalised delta rule [77] with the input-output patterns in the training set as the training data. Once trained, the neural network provides the PSS parameters under any measured loading conditions. One of the important

difficulties in this method is to choose the proper value for the momentum constant and the learning rate. There is still no consensus as to what value of these parameters should be used in the learning process [77]. The simulation results on a SMIB model show the superior performance of the ANN PSS to the fixed PSS. However, the authors do not compare their results to another adaptive controller to show their claim regarding the superiority of this method to adaptive techniques.

Zhang et al [78] describe an artificial neural network (ANN) based adaptive power system stabiliser (APSS), in which the advantages of the self-optimising Pole Shifting adaptive control strategy [60] is combined with the quick response of the ANN. In this method a multi-layer perception with error back-propagation training method is employed. The ANN, trained by an adaptive PSS, has been applied to a single-machine infinite-bus (SMIB) power system. During training, the ANN learns to memorise and simulate the control strategy of APSS in order that it gives, in practice, the same performance as the APSS. A third-order discrete model of the generating unit using the shift operator with time-varying coefficients is used for the study. The speed of generator ω is used as the PSS input. For ANN, a fourth-order input signal is used for the four inputs of ANN, i.e. $\omega(n)$, $\omega(n-1)$, $\omega(n-2)$, $\omega(n-3)$. Since the main purpose of the paper is to make the ANN based PSS function as close to the APSS as possible, they consider a wide range for the generator output (0.1 to 1.0 p.u), and the power factor ranging for 0.7 lead to 0.1 lag for training the ANN. Simulation results show that there is not much difference between the performance of ANN PSS and APSS, but with the advantage that the ANN PSS requires a shorter time to produce the control signal for the system disturbance. However, as the authors state, no theory exists on how many neurones are required in a

specific problem. Researchers determine the number of neurones according to their experience and extensive simulation studies.

Hiyama [79] proposes a rule-based fuzzy logic power system stabiliser (FLPSS). The neural network is used to tune the FLPSS parameters under wide range of operating points. The neural network is composed of three layers, the input, the hidden, and the output ones. They input the real and the reactive power, measured in real time, and the external reactance of a SMIB model to the neural network to be able to set the FLPSS parameters as operating point changes. The sampled signals are obtained by using two digital reset filters in which the shift operator is used. The back propagation method is used for a predetermined learning set in the learning process of the neural network. The experimental results show that FLPSS improves the system performance in comparison with no controllers. However, there is no comparison with the conventional PSS.

Hsu et al [80] apply a fuzzy PSS to a multimachine system. Two real-time measurements $\Delta\omega$ and $\Delta\dot{\omega}$ (acceleration) are used as the input signals. These input signals are first described by some linguistic variables such as LP (large positive), MP (medium positive), SP (small positive) and so on, using fuzzy set notation to determine stabiliser output. A fuzzy relative matrix is developed using membership to find the relationships between stabiliser inputs and stabiliser output. Each generator is equipped with the stabiliser. The simulation results show a better power system performance than the conventional stabiliser. They claim this new PSS is better than a STR PSS since the method does not require real-time model identification. However, they do not compare their results with an adaptive PSS. The results also show that the settling time of the system is

comparatively large (about 10 sec), and in this regard the adaptive PSSs provide a much better performance.

1.5 A BRIEF REVIEW OF DISCRETIZATION

In all adaptive techniques, both the control algorithm and the identification scheme are based on a linear discrete-time model. Since a power system is a continuous-time system, an equivalent discrete-time model should be calculated. One common way of describing discrete-time models is to use the shift operator (q). With this operator, which is often expressed using the z-transform, the linear difference equations with constant coefficients can be readily manipulated [81]. It allows systems to be represented by a transfer function which is often a ratio of polynomials in (q).

Despite its wide use in adaptive control, it is apparent that the transfer function which is obtained using the shift operator is not at all like the transfer function in the s-domain. To obtain a better correspondence between continuous and discrete-time systems, a difference forward operator (delta operator) has been suggested by Middleton et al [82-83]. This advantage allows the designer to ignore the sampling zeros arising from the sampling process and, therefore, to simplify the control strategy [55,65]. This important advantage will be used in Chapters 5 and 6 for designing adaptive controllers.

When the poles and zeros of a stable continuous-time system are mapped to the discrete-time model (shift model) they are located inside a unit circle in the z-plane [81]. For the delta model, those poles and zeros are located inside a circle centred on -1/h of radius 1/h where h is the

sampling time in seconds [83].

One cause of numerical difficulties in the shift operator representation of discrete-time systems is the clustering of the poles and zeros around the point (1, 0) in the z-domain at the short sampling periods usually required to meet high performance controller specifications. A related problem is that the shift operator transfer function loses consistency with the continuous case for frequency response calculations. It will be demonstrated that the delta operator is a simple way of resolving these problems, giving more accurate and consistent results [84]. The other advantage of using the delta operator is that at short sampling periods there is a close resemblance between the continuous and discrete models as well as improved numerical properties compared with the shift operator.

The major advantages of the delta operator approach to discretization are as follows:

(a) It is possible to use short sampling periods without incurring numerical difficulties such as a high sensitivity to round-off errors in coefficient representation.

(b) The coefficients of the discrete-time transfer function of the power system are closely similar to the corresponding ones in continuous-time and it becomes easier to tune controller parameters for improved dynamic performance.

(c) The frequency and transient response of the continuous system can be accurately estimated from the discretized system.

1.6 THESIS REVIEW AND ORGANISATION

The thesis is organised as follows;

The thesis first describes the power system model used in this study. The concepts of discretization of continuous-time systems will be introduced in Chapter 3. The numerical difficulties associated with the shift operator when discretizing at small sampling periods are given. Two power system transfer function examples are used to show the advantages of the delta operator compared to the shift operator. Chapter 4 presents a modified method of Recursive Least Square estimation in which the delta operator is used for identifying the parameters of a power system [85].

Chapter 5 introduces a new adaptive Pole Assignment controller in which the delta operator is used. In this algorithm, the controller parameters are adjusted so that the poles of the closed-loop transfer function $G_d(s)=\Delta\delta/\Delta P_m$, which shows the effect of the load disturbances (ΔP_m) on the power angle ($\Delta\delta$), are placed at preselected locations ensuring that the settling time is satisfactory for a wide range of operating points. Simulation studies performed on a typical excitation control system model, demonstrating clearly the benefits of the proposed adaptive stabiliser, are presented. Results are compared with a fixed gain stabiliser.

A new adaptive controller using the delta operator is proposed in Chapter 6 which is able to provide a specified system response for all operating points. The control strategy is based on a new type of model reference adaptive technique in which the transfer function $G_d(s)$ is used as a reference model. In this model reference adaptive technique there is no need to calculate the error between the plant output and that of the model.

The controller parameters are adjusted so that the poles and zeros are placed at a preselected location using explicit system identification [65]. Comparative results will be given for the adaptive stabiliser based on the two alternative control algorithms and for a fixed parameter stabiliser and a Pole Shifting adaptive controller. The last chapter presents the general conclusions.

1.7 ORIGINAL CONTRIBUTIONS OF THIS THESIS

The major contributions given in this work can be summarised as follows:

1- A comparison of different techniques for obtaining a discrete-time mathematical model for digital control design of a power system is given. It is known that to meet the requirement for high performance of a digital controller a short sampling time should be used. But this leads to considerable numerical difficulties in the discretization of power system transfer functions if the shift operator is used. The delta operator suggested by Middleton et al in control engineering is then applied for the first time to power system to avoid these problems.

2- The usual Recursive Least Square estimation is modified by using the delta operator having the advantage that a short sampling time can be used without incurring numerical difficulties. This modification and its advantages have not been previously noted, even in control literature.

3- A new Pole Assignment adaptive controller using the delta operator improves the dynamic behaviour of a single-machine infinite-bus power system as operating point changes when compared with a conventional stabiliser and the Pole Shifting controller.

4- A new type of Model Reference Adaptive Controller is shown to be able to provide specified damping characteristics over a wide range of operating conditions for both single-machine infinite-bus and multimachine power systems. The major advantages of this adaptive controller in comparison with the other adaptive techniques are summarised as follows;

(i) It does not suffer from non-minimum-phase problem because of the use of the delta operator.

(ii) It gives a better damping characteristics than the Pole Shifting control which has been the best adaptive controller given so far in the literature.

(iii) Unlike the usual approach of MRAC it is not necessary to calculate the error between the model and plant outputs. It uses the same explicit identification as the Pole Assignment controller to place both the poles and the zeros of the system at specified locations.

(iv) An easy method is given to obtain a reference model for a power system.

(v) It provides a flat gain characteristics over most of the frequency range of concern confirming that a desirable damping can be achieved for both local and inter-area modes [34].

(vi) Unlike GMV-STR and adaptive optimal control it does not have a constrained control structure.

CHAPTER 2

Chapter 2

POWER SYSTEM MODELLING

2.1 INTRODUCTION

With progress in microprocessor technology, the development of stabilisers based on adaptive control techniques becomes a feasible way to track the changes in operating point of a power system [8]. In these techniques, a model of the system to be controlled is continually identified in real-time and the control is calculated using a selected strategy. In all these proposals, the emphasis has been to maintain good damping characteristics as the operating conditions change.

When the behaviour of a power system using adaptive control is to accurately simulated, it is essential that a sufficient detail for mathematical model be chosen. For adaptive feedback control design, especially for identification part it is most desirable to choose a low order open-loop model which must be suitable for representing the actual system. However, after designing the feedback controller computer simulations should be carried out when a high order model of the actual open-loop system is used.

In this study where the effect of low frequency oscillations is of concern there are a limited number of system components important such as the synchronous generator, the excitation system and supplementary controllers [4]. For each of them several basic models are recommended by IEEE, and can be adapted for the studies of specific problems.

In this chapter a suitable open-loop model for the design of the adaptive controller is presented. It will be shown that this model sufficiently represents the actual system. A suitable model is also given for discretization purpose and is taken up further in Chapter 3 where the effect of mathematical discrete operators such as the delta operator and the shift operator introduced in Section 1.5 is discussed.

2.2 GENERAL SYSTEM MODEL

In general, a power plant connected to the rest of the power system is described by nonlinear equations. Computer simulations using standard numerical integration algorithms are used to obtain the dynamic behaviour of such a system. In many cases, however, linearization of the nonlinear equations is appropriate, and in such cases the valuable insights into general behaviour over a variety of operating conditions can be gained by the powerful techniques of linear system analysis.

The phenomena of the dynamic stability and damping of synchronous machines for the mode of small perturbations around the operating point can be studied by a linearized block diagram. This is shown in Figure 2.1 for a single-machine infinite-bus (SMIB) [4] where the blocks are.

(i) Excitation system : $\dfrac{K_{e1}}{1 + T_e\, s}\ \dfrac{1 + T_a\, s}{1 + T_b\, s}$

(ii) field flux decay: $\dfrac{K_3}{1 + K_3\, T'_{do}\, s}$

(iii) machine mechanical dynamics loop: $\dfrac{1}{M\, s^2 + K_d\, s + K_1}$

The ΔP_d shown in Figure 2.1 shows the electrical power swings reflected in the flow of power in transmission and/or tie-lines [6].

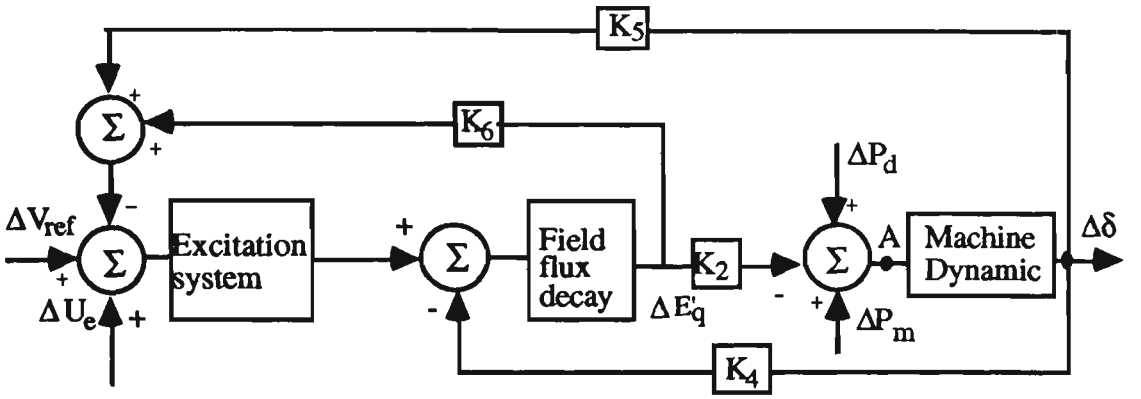

Figure 2.1: Block diagram of transfer functions used for low frequency oscillation studies without stabiliser for a SMIB model [4]

Although the design of any supplementary controller on a one machine system is logically the best place to begin an evaluation of the controller, it would be more desirable if a more through investigation can be done with a multimachine model. For a multimachine case the linearized block diagram which is an extension of Figure 2.1 is shown in Figure 2.2 [4]. Because of the interaction among machines, the state variables become multiplied, for instance, $\Delta\delta$ becomes $\Delta\delta_i$, i=1,...,n. The branches and loops also become multiplied; for instance, K_1 becomes K_{1ij}, i=1,...,n, j=1,...,n.

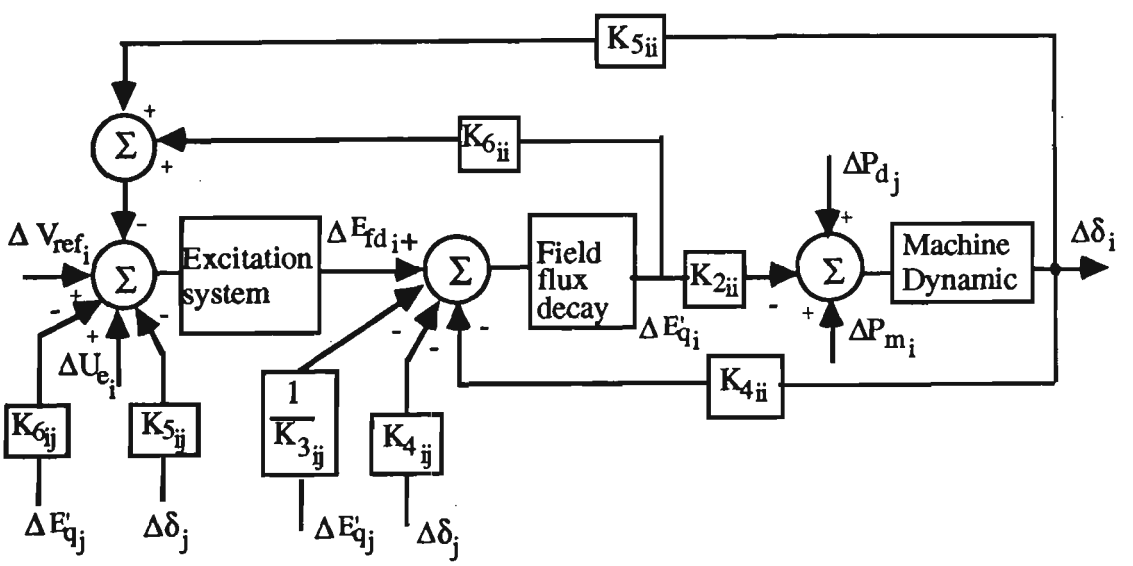

Figure 2.2: Basic model of a multimachine case for low frequency oscillation studies without stabiliser [4]

The blocks shown in Figure 2.2 are:

(i) Excitation system : $\frac{K_{e1_i}}{1 + T_{e_i} s} \frac{1 + T_{ai} s}{1 + T_{bi} s}$

(ii) field flux decay: $\frac{K_{3ii}}{1 + K_{3ii} T'_{doi} s}$

(iii) machine mechanical dynamics loop: $\frac{1}{M_i s^2 + K_{di} s + K_{1ii}}$

The ΔP_{d_j} shown in Figure 2.2 represents the electrical power swings due to dynamic interaction between the ith machine and the other machines and reflected in the flow of power in transmission and/or tie-lines [6] and is equivalent to

$$\Delta P_{dj} = \Sigma K_{1ij} \Delta\delta_j + \Sigma K_{2ij} \Delta E'_{qj} \qquad (2\text{-}1)$$

where $\Delta E'_{q_j}$ is the internal voltage of the stator of a third-order generator (see Appendix I).

"During low-frequency oscillations, the current induced in a damper winding is still negligibly small, hence the damper windings can be completely ignored in system modelling" [4]. However, in the models given in Figures 2.1 and 2.2 an approximate damping factor $K_d = D/\omega_b$ has been considered. The effect of the governor is ignored because its speed is not fast enough in comparison with the modern excitation system during low frequency oscillations [3,4].

An IEEE excitation system model type AC4 with a high initial response described in [86] and shown in Figure 2.3 has been used. In this model which represents the modern exciters overall equivalent gain and the time constant associated with the regulator and/or firing of the thyristors are represented by K_e and T_e respectively.

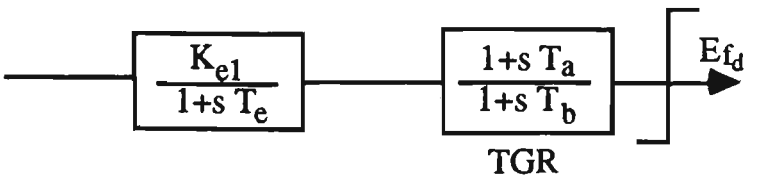

Figure 2.3: IEEE excitation system type AC4

For well-damped performance of the regulating loop, as shown in [3,87], it is desirable to maintain the crossover frequency less than $1/(2T_e)$ which would mean that the steady-state gain K_e is limited to a value less than $T'_{do}/(2T_e)$. However, this imposes a restriction on exciter performance because the steady-state gain is directly related to the exciter regulation. To have a desirable voltage regulation (say, less than 1%), the exciter gain may be selected as a considerably higher value than $T'_{do}/(2\,T_e)$ [87]. Transient gain reduction (TGR) is then widely used in industry to resolve this conflicts of objectives between a stable well-damped voltage-regulating loop, and a low value of exciter regulation. TGR is usually implemented as a lead-lag filter $[(1 + T_a\,s)\,/1 + T_b\,s)]$.

By selecting $1 / T_a$ as considerably lower than the crossover frequency (e.g., $T_a=1$), as described in [3], the effects of concern during low frequency oscillations are not significantly different if the assumption is made that the regulator is represented by $[K_e/(1+T_es)]$ rather than $[(K_{e1}/(1+T_es))\ (1+T_a\,s)/(1+T_bs)]$, where $K_e=K_{e1}\,(T_a / T_b)$ is the transient gain. Therefore, it is assumed that the equivalent gain of the excitation system can be represented by a dc gain K_e and $T_a=T_b=0$.

2.3 A PARTICULAR MODEL FOR DESIGN OF THE ADAPTIVE CONTROLLER

The problem under study is the stability of the torque angle loop, i.e., the

behaviour of the rotor angle ($\Delta\delta$) (not to be confused with the delta operator) and speed following a small disturbance such as a sudden change in load, which can be represented equivalently by a sudden change in mechanical power (ΔP_m) and power swing disturbances (ΔP_d) [3-6]. Dynamic stability can be investigated by considering the location of the poles of the closed-loop transfer function including the stabiliser which relates ΔP_m to $\Delta\delta$:

$$G_d(s) = \frac{\Delta\delta}{\Delta P_m} \qquad (2\text{-}2)$$

The fixed parameter stabiliser is usually designed either through eigenvalue analysis for a particular dominant frequency usually associated with the local mode [1,4,6,27,35,73] or using other methods such as pole placement [27] and Linear Optimal Control [29]. Although it has been shown by [88] that static var compensator (SVC) may improve system stability, it must be kept in mind that the most inexpensive 'fixed' parameter controller to damp low frequency oscillations is a well located and tuned power system stabiliser [89]. The possibility of damping these oscillations through static compensators should be only considered once the PSS option has been exhausted [89]. However, if in a power system the SVC has been included to control the voltage at a particular bus, computer simulations should consider the effect of the SVC in system stability performance.

The parameters of the power system change with operating point, yielding a different transfer function for each change, while the stabiliser parameter settings are optimum for only one of these operating points. Therefore, it is desirable that the system is equipped by an adaptive controller to identify the changes.

These changes are not fast and significant changes would not be expected over a time scale of a few minutes [90]. It would thus be feasible to identify the operating point in terms of "K" parameters by examination of appropriate input and output waveforms such as $\Delta\delta$, ΔP_m and ΔP_d [5]. The first signal can be obtained from a rotor encoder on the generator shaft or measuring the speed ($\Delta\omega$) and passing it through an integrator. The second signal can be obtained by measuring accelerating power ($\Delta P_m = P_a = P_m - P_e$) [7]. The third signal for both single-machine infinite-bus and multimachine power systems is included in the measurement of electrical power reflected in the flow of power in transmission and/or tie-lines and appears in ΔP_m. These signals could be used to allow the computer to identify the transfer function G_d and to adjust the stabiliser parameter settings to match the changing operating point. The widely used method of identification is Recursive Least Squares (RLS) estimation described in many control texts [91-92].

In order to identify the parameters of the system a discrete model with a suitable order must be selected. In practice, the higher the order of the model is chosen, the closer the model approaches the real power system. However, in real-time application it is neither practical nor necessary to use a high order model to identify the system because (i) the least-square identification technique automatically fits the model parameters to the actual input-output characteristics [91-92], (ii) a high order model involves a heavy calculation burden which is undesirable for the on-line computer control [32,34,54,57,58].

As mentioned earlier the aim of this study is to design an adaptive controller which is able to damp out low frequency oscillations over a wide range of operating points. To simplify the analysis it is desirable to

choose a low order model of the open-loop system in the first step of the design. Obviously, this depends on the model to be considered being able to reasonably represent the actual system. To decrease the order of the model shown in Figures 2.1 and 2.2 it is assumed that the voltage control system is very fast compared with the dynamics of the rest of the system. Therefore, the block diagram representation of the excitation system can be shown simply by its dc gain (i.e., K_e) [2,5]. This is a reasonable assumption as shown below because the time constant of the modern exciters is very short (say, 0.01sec [34,49]).

Consider, for example the transfer function of the electrical loop (G(s)) between ΔU_e and $\Delta E'_q$ of Figures 2.1 and 2.2 in the following cases;

(i) Excitation system : including T_e

$$G(s) = \frac{K_e K_3}{(1+T_e s)(1+K_3 T'_{do} s) + K_e K_3 K_6}$$

(ii) Excitation system : neglecting T_e

$$G(s) = \frac{K_e K_3}{(1+K_3 T'_{do} s) + K_e K_3 K_6}$$

It should be noted that since the component of the torque produced by the K_4 branch (see Figure 2.1) is negligible [3] its effect has been ignored for calculating the electrical loop.

The stabilisers are mainly designed to compensate the phase lag produced by the electrical loop transfer function G(s). By using an illustrative example taken from [3] where K_3=0.36, K_6=0.417, K_e=25, and T'_{do}=5 (see Appendix II) the transfer function G(s) for two cases is:

(i) $$G(s) = \frac{9}{(1+0.01 s)(1+1.8 s) + 3.753}$$

(ii) $G(s) = \dfrac{9}{(1+1.8\ s) + 3.753}$

The Bode diagram of both transfer functions are shown in Figures 2.4 and 2.5. As can be seen from Figures 2.4 and 2.5 there is a negligible difference between the phase characteristics of two cases in the frequency range of 13-15 rad/sec and there is no difference between the magnitude of two cases in the whole frequency range of concern. Consequently, for the design of the adaptive controller given in Chapters 5 and 6 the excitation system is considered simply as a dc gain.

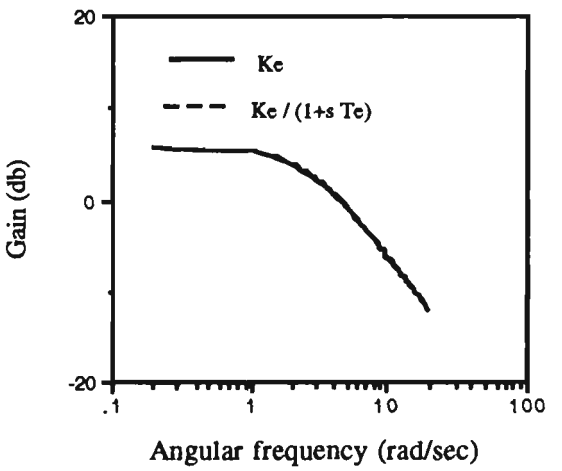

Figure 2.4: Gain characteristics of transfer function G(s) for two different cases

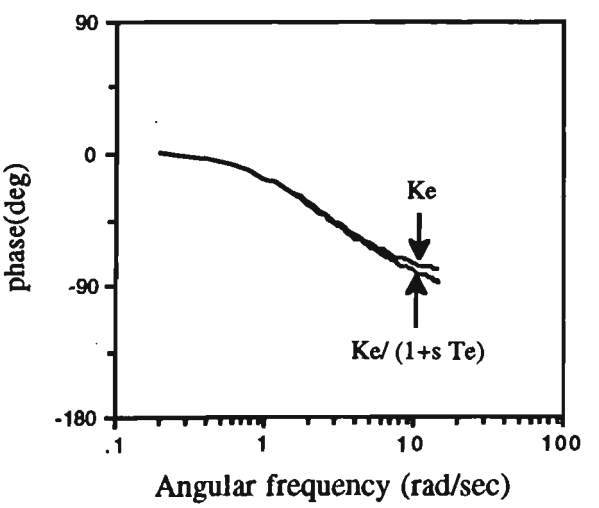

Figure 2.5: Phase characteristics of transfer function G(s) for two different cases

However, there should be distinction between the model to be used for the design purpose and identification and the model to be used for simulations. Computer simulations are carried out for the case where the excitation system is $[K_e/(1+T_e s)]$.

2.4 DISCRETIZATION MODEL

When a digital control is to be applied in power system it is imperative that the continuous-time system be discretized by using a suitable mathematical operator such as the delta operator introduced in Section 1.5. The transfer function to be used for discretization will be the closed-loop transfer function G_d. As explained in Section 1.4.2 this transfer function will be the basic model for the identification and the design of the adaptive controller. As an example before using the proposed adaptive controllers it is assumed that the power system is equipped by a conventional stabiliser to improve the damping characteristics. This situation is shown in Figure 2.6.

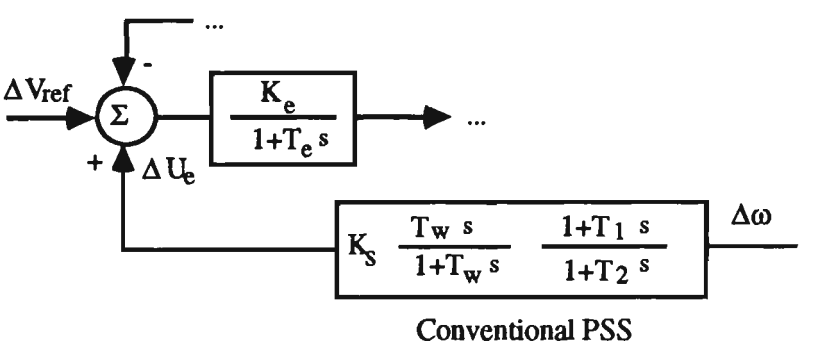

Figure 2.6: Excitation control system with power system stabiliser

The aim in this section is to provide a simple example of a low order transfer function for discretization purposes given in Chapter 3. This model should represent the actual system sufficiently. In order to simplify the analysis and reduce the order of the closed-loop system the

PSS used by [5] and shown in Figure 2.7 has been considered rather than using the conventional PSS applied to power utilities [4].

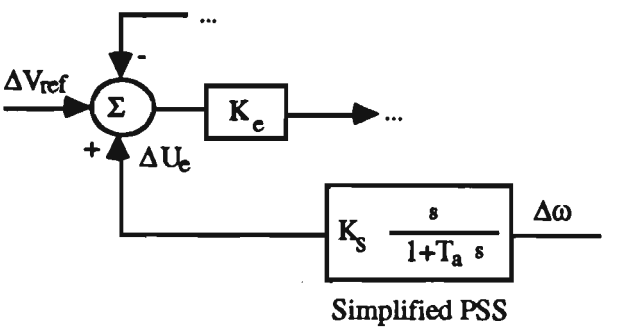

Figure 2.7: Excitation control system with simplified PSS

The question which may arise is that whether this simplified model is close to the high order power system. An illustrative power system given in [3] is now used to discuss this point. The high order model includes the excitation system by $[K_e/(1+T_e s)]$ and the conventional PSS represented in Figure 2.6. The low order model of the excitation control system is a dc gain K_e and simplified PSS shown in Figure 2.7. The parameters of both models are given in Appendices II and III. Then $G_d(s)$ can be determined as:

(i) high order model:

$$G_d(s) = \frac{125s^4 + 18932s^3 + 666993s^2 + 1730372s + 166386}{s^6 + 152s^5 + 5624s^4 + 120927s^3 + 774506s^2 + 1896218s + 182730} \quad (2\text{-}3)$$

(ii) low order model

$$G_d(s) = \frac{125s^2 + 2830s + 6601}{s^4 + 23.89s^3 + 595s^2 + 2953s + 7226} \quad (2\text{-}4)$$

The gain and phase characteristics and transient response to a 5% step change in load for both models are shown in Figures 2.8, 2.9, and 2.10 respectively.

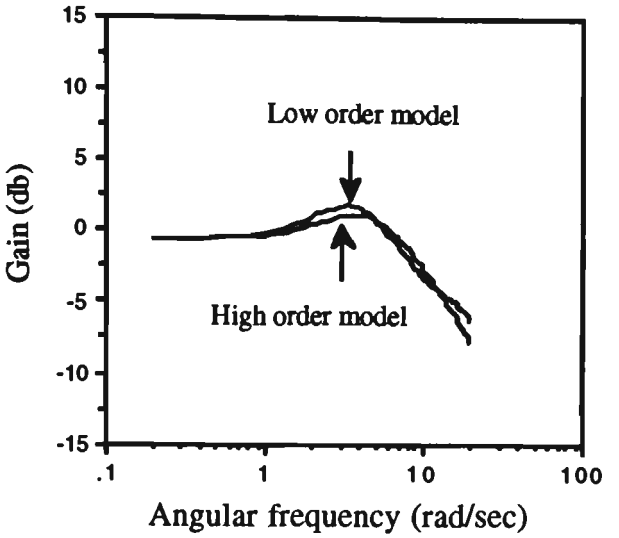

Figure 2.8: Gain characteristics of high and low order models

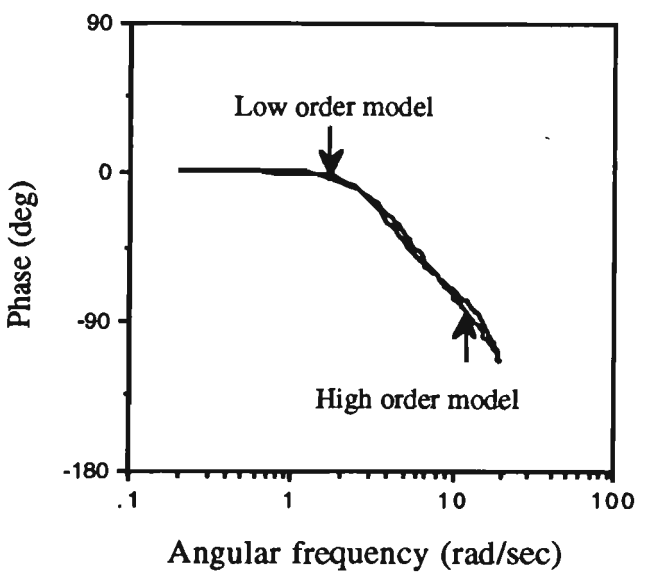

Figure 2.9: Phase characteristics of high and low order models

As can be seen from Figures 2.8 to 2.10 the characteristics of both systems are close to each other confirming that the low order model can be used as an example to show the robustness of the delta operator for discretization.

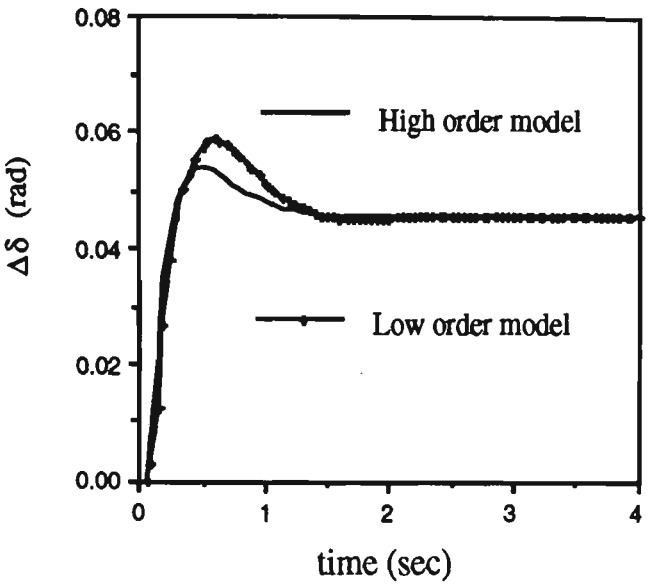

Figure 2.10: Transient response of high and low order models to a 5% step change in load

2.5 CONCLUSIONS

Linearized models of single-machine infinite-bus and multimachine power systems have been presented. The synchronous generator is represented by a third-order model. For modern exciters it was shown that considering the excitation system as a dc gain could sufficiently represent the actual open-loop system. This reduces the order of the model for the design of the adaptive controller and identification. However, computer simulations will be carried out for the system where the excitation system is fully represented. A simplified PSS was given rather than the full PSS used in industry for discretization purposes. This allows a reduction in the order of the closed-loop system transfer function. A transfer function ($G_d(s)$) was introduced for dynamic stability study. This will be the basic transfer function for further study in this thesis.

CHAPTER 3

Chapter 3

DISCRETIZATION OF POWER SYSTEM TRANSFER FUNCTIONS

3.1 INTRODUCTION

There has been increasing interest in utilising digital techniques for controlling power systems with the introduction of low cost digital controller hardware. Digital control systems are highly reliable, self-diagnostic, and can be readily reconfigured to implement advanced control strategies. One such digital control strategy which has been demonstrated to be suitable for enhanced performance of a power system is adaptive control [32,36]. Adaptive techniques involve the identification of the parameters of the discrete-time model of the plant through continual sampling of the input and output signals, thus keeping track of operating conditions. The calculation of the control action is made during each sampling time based on the selected control strategy.

A power system is a continuous-time system. Nevertheless, where a digital controller is to be applied, it is desirable to develop a discrete-time model for analysis purposes. The forward shift operator q has been a convenient tool to describe discrete-time models. This operator converts linear difference equations into simple algebraic equations.

Despite its wide use, it will be shown that because of the clustering effect there would be numerical difficulties in the shift operator representation of discrete-time systems when short sampling times are involved. When

the poles and zeros of a stable continuous-time system are mapped to the shift model using short sampling times, they cluster around the point (1,0) in the z-plane [82,84]. A problem regarding numerical difficulties is that the shift operator transfer function loses consistency with the continuous case for frequency response calculations.

The other alternative for calculating a discrete-time model is to use the w-transform. This method was developed to allow continuous system design techniques to be applied to discrete systems and is usually calculated from the shift operator. It will be shown that since there is no direct method for calculating w-model from a continuous-time system, it would also have numerical difficulties as the shift operator does.

The delta operator [84] is a simple way of resolving these problems, giving more accurate results. The advantage of this alternative representation is that at short sampling periods there is a close resemblance between the dynamic behaviour of the continuous and discrete models. It also retains the similarity between continuous-time and discrete-time systems that has been one of the advantage of using w-transform.

The chapter is organised as follows: Section 3.2 reviews how to obtain the discrete-time model of a continuous-time system. Section 3.3 gives the relationship between the poles and zeros of the continuous-time system and the discrete ones. The difficulties which arise when discretizing at small sample periods are given in Section 3.4. Section 3.5 gives a comparison between the delta and shift operators when applied to the discretization of the power system transfer functions involving a typical excitation control system with stabiliser.

3.2 DISCRETIZATION OF CONTINUOUS-TIME SYSTEMS

Consider, for example, a digital control system as shown in Figure 3.1. The plant is taken to be a generating unit under study, its excitation system and the power system to which it is connected including other generators and their controllers. The plant will typically have continuous signals at its input and output. However, the controller input and output are discrete signals because of the sampling nature of analog to digital (A/D) converter at the input and the discrete nature of the digital output.

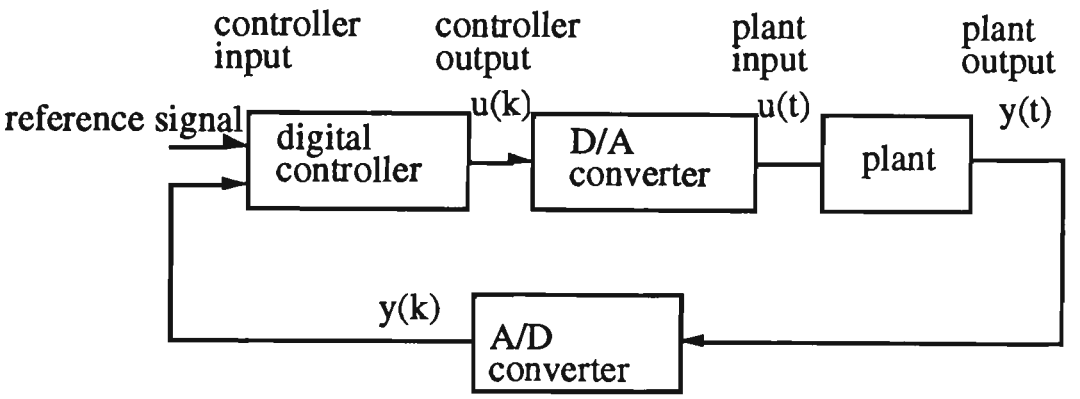

Figure 3.1: Digital control system

The common characteristics of these seemingly different types of systems is that their dynamic behaviour may be analysed by applying discrete-time mathematical concepts. In general, difference equations are the mathematical language utilised in the description of discrete-time systems [81].

In order to find the discrete-time equivalent of a continuous-time system, the underlying continuous-time system equations have to be solved over the sampling intervals [81]. The key problem is then to find the relationship between the sampled output y(k) and the sampled input u(k) as shown in Figure 3.1. For general nonlinear systems, there are various numerical techniques to approximate the solution (for example, Euler

approximation). However, in the case of linear systems, one can obtain an exact description of the sampled response using linear state space models [81].

3.2.1 Zero-order hold sampling of continuous-time system

Consider a continuous-time linear state space model of the form

$$\begin{cases} \dfrac{dx}{dt} = A\,x(t) + B\,u(t) \\ y(t) = C\,x(t) \end{cases} \tag{3-1}$$

The zero order hold sampling model of the continuous-time system is given by,

$$\begin{cases} x(t_{k+1}) = \emptyset(t_{k+1}, t_k)\,x(t_k) + \mu(t_{k+1}, t_k)\,u(t_k) \\ y(t_k) = C\,x(t_k) \end{cases} \tag{3-2}$$

where $\emptyset$ and μ are matrix functions of A and B as shown in standard control texts [81].

It should be noted that it is assumed that the input is generated by a zero-order hold, that is

$$u(t) = u(k\,h) \quad \text{for} \quad k\,h \le t \le (k+1)\,h \tag{3-3}$$

3.2.2 Discrete-time operator models

In order to manipulate linear difference equations such as (3-2), it is most convenient to use operator calculus. Operator calculus gives a compact description of systems and makes it easy to derive relationships among system variables and the manipulation of difference equations is reduced

to a purely algebraic operation. It would be then easy to show the relationships between the input and output signals by a transfer function. Three operators which have been used in discrete-time systems are as follows [83,84,93].

1-Shift operator

The most commonly used operator calculus is the forward shift operator q, defined by $q\,x(k) = x(k+1)$ where k is the discrete-time index and x(.) stands for any sampled signal. Using the shift operator calculus allows Equation (3-2) to be written compactly as a simple form of

$$\begin{cases} q\,x(t_k) = \emptyset\,x(t_k) + \mu\,x(t_k) \\ y(t_k) = C\,x(t_k) \end{cases} \tag{3-4}$$

2-w operator

Sometimes discrete frequency design is carried out by using a bilinear transformation, also called the w-transform. The essential idea of the method is to transform the discrete model of the plant by substituting a new variable w, using the bilinear mapping,

$$w = \frac{2}{h}\,\frac{q-1}{q+1} \tag{3-5}$$

where q is the conventional shift operator and h is the sampling interval in seconds, and to perform the compensator design in the w-plane [93]. The interesting idea of using this method is that the stability boundary in the w-plane is the imaginary axis, just as for the s-plane of continuous-time system.

However, using Equation (3-5) for calculating the w-transform would transfer numerical difficulties from the shift model to the w model.

Therefore, the w-transform of the continuous-time system given in Equation (3-1) should be calculated directly. For the w operator, Equation (3-2) can be written as

$$\begin{cases} w\, x(t_k) = \emptyset''\, x(t_k) + \mu''\, x(t_k) \\ y(t_k) = C\, x(t_k) \end{cases} \tag{3-6}$$

where

$$\emptyset'' = \frac{\emptyset - I}{\frac{h}{2}(q+1)} \quad \text{and} \quad \mu'' = \frac{2}{h}\frac{\mu}{q+1} \tag{3-6 a}$$

As can be seen from Equations (3-6 a) the shift operator q appears in the denominator. This means that the matrices $\emptyset''$ and μ'' cannot be calculated numerically from continuous-time system matrices. Therefore, w-transform has to be calculated through either the shift operator or the delta operator introduced further.

3-Delta operator

Despite the wide use of the shift operator in digital control, it is apparent that there is no resemblance between the shift operator q and the continuous-time operator d/dt. In order to obtain an operator calculus which is more like a derivative, Middleton et al [83] has suggested a difference operator, namely, delta operator δ, defined by $\delta = \frac{q-1}{h}$, where q is the conventional shift operator and h is the sampling interval in seconds. Using this operator, the linear discrete state space model of (3-2) can be written as

$$\begin{cases} \delta\, x(t_k) = \emptyset' x(t_k) + \mu' x(t_k) \\ y(t_k) = C\, x(t_k) \end{cases} \tag{3-7}$$

where

$$\emptyset' = \frac{\emptyset - I}{h}, \text{ and } \mu' = \frac{\mu}{h}$$

Note that the delta operator provides the same flexibility as the shift operator does because the relationship between δ and q is a simple linear function. The choice of which operator is to be used is a function of particular application. This concept will be discussed further in Section 3.5 for two power systems.

3.2.3 Selection of sampling rates

The selection of sampling rate is normally based on the bandwidth or, equivalently, on the rise time of the closed-loop system [81]. It has been suggested that the sampling rate be at least ten times the bandwidth of the closed-loop system or there will be a loss of information related to intersample behaviour [81,83]. Consider, for example, the step response of a closed-loop transfer function $\frac{s+3}{(s+2)(s+1)}$, in which the bandwidth is 0.15 Hz. The output signal is

$$y(t) = 1.5 + 0.5\, e^{-2t} - 2\, e^{-t}$$

Figures 3.2 (a), (b) and (c) show the sampled data version of this signal with sampling rates of f_0 = 0.3, 0.6, 1.5 Hz. Note that reconstruction of the signal is impossible with the 0.3 Hz sampling rate, a little difficult with the 0.6 Hz sampling rate but can be approximately achieved by the 1.5 Hz sampling rate.

Consequently, in practice, sampling rates in excess of ten times the controller bandwidth should be chosen. Middleton et al [83] have suggested sampling rates to be between ten times and fifty times the

closed-loop bandwidth for modern, fast, high precision digital control systems. Very fast sampling rates above fifty times the desired closed-loop bandwidth offer no advantages [83].

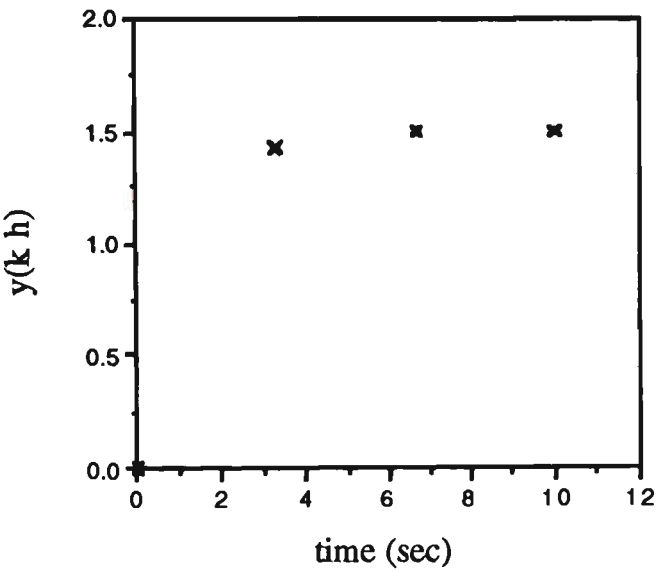

(a) $f_0 = 0.3$ Hz

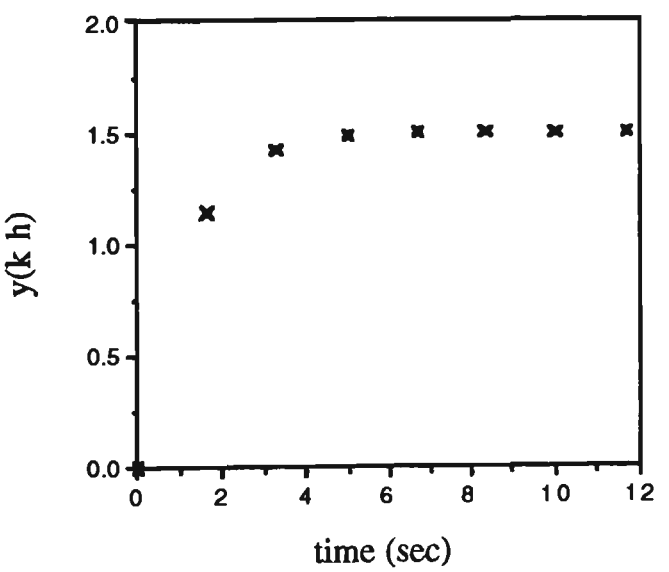

(b) $f_0 = 0.6$ Hz

Figure 3.2 : Sampled 0.15 Hz bandwidth signal

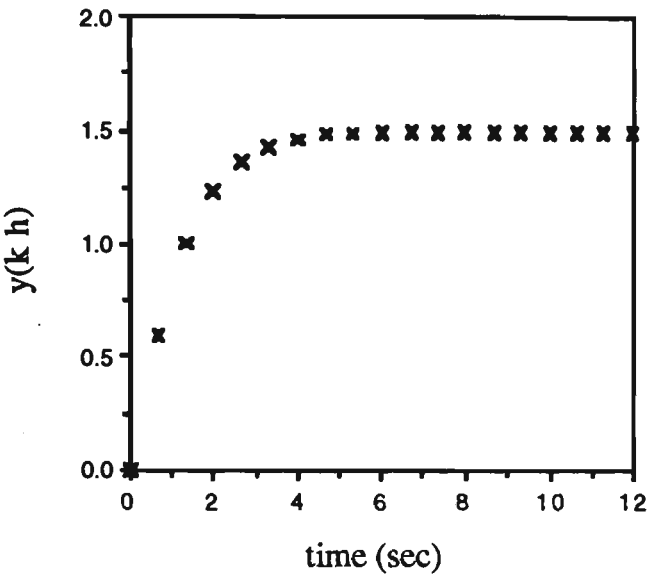

(c) $f_0 = 1.5$ Hz

Figure 3.2: Sampled 0.15 Hz bandwidth signal

Note that this conclusion may also be motivated by careful consideration on the sampling theorem which states that if the Fourier transform of a continuous-time signal f(t) is zero for all ω outside the interval $(-\omega_0,\omega_0)$, that is

$$F(\omega) = 0 \quad \text{for} \quad |\omega| > \omega_0$$

then f(t) can be uniquely determined from its sampled values {f(k h)} if the sampling period is selected to satisfy

$$h \leq \frac{\pi}{\omega_0} = \frac{\pi}{2\ \pi\ f_0} = \frac{1}{2\ f_0} \qquad (3\text{-}8)$$

This theorem states that no loss of information is incurred through the process of the sampling if a signal is sampled at a rate at least twice as fast as the signal's highest frequency content (bandwidth). However, all signals of practical interest will have Fourier transforms for which there does not exist a finite value of ω_0 so that $F(\omega) = 0$ for $|\omega| > \omega_0$ [81]

(there are still frequency components outside the bandwidth). If the sampling theorem is then directly applied, this leads to h=0 ($\omega_0=\infty$) which is clearly unrealistic. For this reason the theoretical lower limit on the sampling rate of twice the bandwidth suggested by the sampling theorem is not useful in control applications and should be extended to at least ten times the bandwidth as in the preceding example [81].

3.2.3.1 Sampling time selection in power system

Despite the fact that the changes in load, or configuration is not very fast, to obtain the best controller performance a short sampling time, as shown above, should be chosen. Moreover, the modern exciter has a very short time constant and any additional digital controller should be able to respond to the sudden changes (like a 3-phase fault) as fast as possible with the other controllers and this can be only achieved by using a short sampling time. This will be more important when the use of a digital exciter with a very fast response becomes popular in industry [94].

3.3 TRANSFER FUNCTION

One convenient feature of using operator calculus in discrete-time systems was that the linear difference equations could be converted into algebraic equations. This insight allows one to link the system input to the system output with a quantity which is commonly known as the system transfer function.

To provide motivation for the concept of the transfer function consider, for example, the state-space model of (3-4). In order to obtain the input-output relationship, the state vector must be eliminated. It follows from

(3-4) that

$$(q\,I - \emptyset\,)\,x(t_k) = \Gamma\,u(t_k)$$

This gives

$$y(t_k) = C\,x(t_k) = C\,(q\,I - \emptyset\,)^{-1}\,\Gamma\,u(t_k)$$

The system transfer function for the system (3-4) is then given by

$$H(q) = \frac{B(q)}{A(q)} = C\,(qI - \emptyset)^{-1}\,\mu \qquad (3\text{-}9)$$

For the delta operator, the system transfer function can be written as

$$H(\delta) = \frac{C(\delta)}{D(\delta)} = C\,(\delta\,I - \emptyset')^{-1}\,\mu' \qquad (3\text{-}10)$$

The polynomials A-D shown in Equations (3-9) and (3-10) [83] are degree of m for B and C and degree of n for A and D so that $m \leq n$.

As will be shown further in Section 3.5.2 since there is no advantage of using w-operator in digital control systems compared with the other operators, the system transfer function using w-transform is not given here. Accordingly, the analysis given further will focus on only the shift and delta operators.

3.3.1 Poles and zeros of continuous-time system

Consider the continuous-time system of (3-1). The transfer function of (3-1) is given by

$$H(s) = \frac{E(s)}{F(s)} = C\,(sI - A)^{-1}\,B \qquad (3\text{-}11)$$

where E is a polynomial of degree m and F a polynomial of degree n.

The poles of the transfer function are the n roots of the equation F(s)=0, and the m zeros of the transfer function are the m roots of the equation E(s) = 0. The poles of the system can be also obtained by evaluating the eigenvalues of matrix A, which is denoted by $\lambda_i(A)$, i=1, ..., n.

3.3.2 Poles of sampled system

The zero-order-hold sampling of (3-1) gives the discrete-time system of either (3-4) for the shift model or (3-7) for the delta model. Its poles are the eigenvalues of Φ ($\lambda_i(\Phi)$, i=1,...,n) for the shift model and the eigenvalues of Φ'($\lambda_i(\Phi')$, i=1, ..., n) for the delta model. Because $\Phi = e^{Ah}$ and $\Phi' = \frac{e^{Ah} - I}{h}$, it follows from the properties of matrix functions [95] that

$$\lambda_i(\Phi) = e^{\lambda_i(A)h} \qquad \text{shift model} \qquad (3\text{-}12)$$

$$\lambda_i(\Phi') = \frac{e^{\lambda_i(A)h} - I}{h} \qquad \text{delta model}$$

Equation (3-12) gives the mapping from the continuous-time poles to the discrete-time poles. In other words, a continuous-time system with poles, at $s = p_i$, i = 1, ..., n, when sampled with period h gives a discrete-time system with poles at $q = e^{p_i h}$ for the shift model and $\delta = \frac{(e^{p_i h} - 1)}{h}$ for the delta model.

3.3.3 Zeros of sampled system

It is not possible to give a simple formula for the mapping of the zeros. Suppose the continuous-time system transfer function (3-11) has m zeros

and r zeros at infinity, where r is the difference between the number of the poles and the number of the zeros (i.e., r = n-m). The discrete-time system, for short enough sampling time, then has zeros at

$$q_i \approx e^{s_i h} \qquad \text{shift model} \tag{3-13}$$

$$\delta_i \approx \frac{(e^{s_i h} - 1)}{h} \qquad \text{delta model}$$

where s_i's are the zeros of the continuous-time system [96]. The r-1 sampled zeros that correspond to the zeros of infinity of the continuous-time system will go to the zeros of the polynomial B_r as the sampling time goes to zero [96]. The polynomial B_r is listed below for a few values of r.

shift model	delta model	(3-14)
$B_1(q) = 1$	$B_1(\delta) = 1$	
$B_2(q) = q+1$	$B_2(\delta) = \delta h + 2$	
$B_3(q) = q^2 + 4q + 1$	$B_3(\delta) = \delta^2 h^2 + 6\delta h + 6$	

For the shift model, the polynomial B_r has unstable zeros outside or on the unit circle for $r \geq 2$. The unstable zeros are listed below

r	unstable zeros	(3-15)
2	-1	
3	-3.732	

For the delta model, the zeros of the polynomial B_r go to infinity as h tends towards zero.

3.4 THE EFFECT OF SMALL SAMPLING PERIODS

When using small sampling periods, it was shown that unstable zeros would appear as the sampling period decreased, even though all zeros of the continuous-time system were stable. The sampling period also has a considerable influence on the numerical sensitivity such that a short sampling period requires a high precision in the coefficients [81]. This aspect is related to the increased clustering of the poles and zeros around the point (1, 0) in the z-plane with decreasing sample period as shown in references [83,84]. These problems can be overcome by replacing the shift model by one based on the delta operator.

One convenient feature of the delta operator is that the poles and zeros approach those of the continuous system at short sample periods. This has the advantage that there is an increasingly close consistency between the coefficients of the continuous-time and discrete-time systems as the sampling time reduces. It will be shown in Chapters 5 and 6 that this advantage allows to simplify the design of the adaptive controller.

3.4.1 Clustering effect

The effect of small sampling times can be seen by taking the limit of h approaching zero in Equation (3-12). The poles of the shift model converge to the fixed point (1, 0) while those of the delta model converge to the poles of the continuous-time system.

Consider, for example, a continuous-time system with transfer function

$$G(s) = \frac{s^2 + 2s + 2}{s\,(s+0.5)\,(s^2 + 3s + 6.25)} \qquad (3\text{-}16)$$

The poles and zeros of the corresponding discrete-time models for different sampling times h = 1.0, 0.3, 0.1, 0.03, 0.01 second are shown in Figures 3.3 (a), (b) for shift and delta models respectively.

In the case of the shift operator model, the sampling zeros slowly vary with sampling time and move to the unstable region of the unit circle (-1, 0), while the plant poles and zeros vary considerably and converge to the point (1, 0) independently of the corresponding continuous-time system as h tends towards zero.

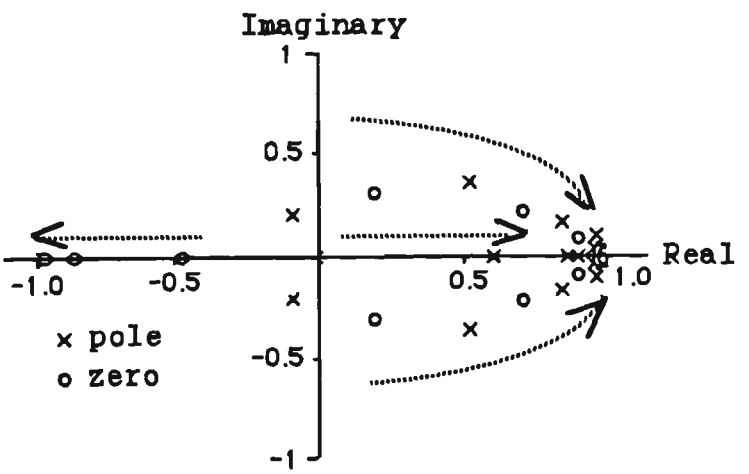

(a) Shift model

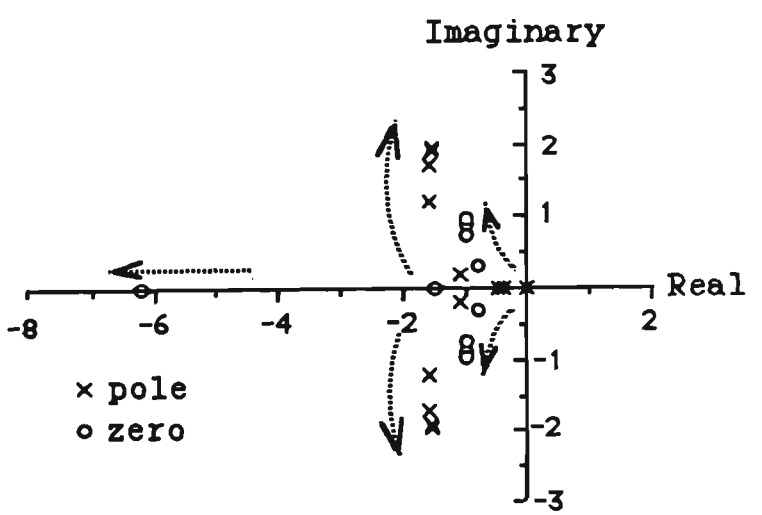

(b) Delta model

Figure 3.3: Variation of sampled poles and zeros as sampling period decreases

Comparing Figures 3.3 (a) and 3.3 (b) shows the consistency of the delta model poles and zeros which correspond one-for-one with the continuous poles and zeros and converge to them as the sampling time decreases to zero. There are additional zeros which arise from the sampling process and these go to $-\infty$ as h tends towards zero.

3.4.2 Numerical difficulties

Numerical round-off in the coefficients of the transfer function gives an error in the poles and zeros [81]. Consider a transfer function with distinct poles p_i and characteristic polynomial:

$$A(q) = (q-p_1) \ldots (q-p_n) = q^n + a_1 q^{n-1} + \ldots + a_n$$

The sensitivity of the kth root of a polynomial with respect to changes in the ith coefficient can be shown to be [81]:

$$\Delta p_k \approx - \frac{p_k^{n-i}}{\prod_{j \neq k} (p_k - p_j)} \Delta a_i \qquad (3\text{-}17)$$

where Δa_i and Δp_k are the change of the coefficient and the root respectively. As shown earlier, when a short sampling time is used for discretizing a transfer function, the poles and zeros of the shift model closely approach the point (1, 0). In this situation the denominator of Equation (3-17) is very small and even a very small change in a coefficient gives a large error in the poles and zeros. This numerical difficulty causes the frequency response and time response of the corresponding digital algorithm to vary significantly from that which would be given by an infinite precision implementation. As will be illustrated further in Section 3.5, the delta model does not give this

problem. The following analysis gives the value of the sampling period at which this problem becomes significant.

Let $\nu_q(\omega)$ and $\nu_\delta(\omega)$ denote the measure of the numerical sensitivity associated with frequency response evaluation for the shift and delta models respectively as defined in Appendix IV [83]. The condition for

$$\nu_\delta(\omega) << \nu_q(\omega) \tag{3-18}$$

is shown in Appendix IV to be satisfied when

$$|q - 1| < \frac{1}{2}|q| \tag{3-19}$$

where q is the pole of the shift model having the smallest magnitude. This derivation assumes the system to be at least fourth-order as would be normal with a power system transfer function.

It is possible to determine directly from the continuous-time poles if a discretized system gives significant numerical difficulties. Let a stable continuous-time system have its ith pole $s_i = -a_i + jb_i$ where a_i is a positive number. It follows that the corresponding shift model has a pole at $q = e^{p_i h} = e^{(-a_i+jb_i)h} = e^{-a_i h}(\cos b_i h + j\sin b_i h)$ lying inside the unit circle. By considering the largest dominant pole of the continuous-time system the assumption in Equation (3-19) implies that

$$|e^{-a_i h}(\cos b_i h + j\sin b_i h) - 1| < \frac{1}{2}|e^{-a_i h}(\cos b_i h + j\sin b_i h)| \tag{3-20}$$

A straightforward manipulation of Equation (3-20) gives

$$0.75\, e^{-2a_i h} - 2\, e^{-a_i h}\cos b_i h < -1 \tag{3-21}$$

If the sampling time has been selected from bandwidth considerations and is sufficiently small that it satisfies Equation (3-21) then significant numerical difficulties will occur and it is most desirable to use the delta model. This will be illustrated next with examples concerning power system steady state stability.

It will now be shown by two different power system examples that the method of discretization has a considerable impact on the accuracy of identifying the transfer function.

3.5 POWER SYSTEM TRANSFER FUNCTION EXAMPLES

3.5.1 Example I

The use of the delta and shift operators in the discretization of a power system is now illustrated using the illustrative power system given in [3,5] and shown by Equation (2-4).

The system bandwidth is found from the 3 dB points to be ω_0=10.3 rad/sec suggesting a sampling rate in the range $\frac{10 \times 10.3}{2 \times 3.14} \leq f_s \leq \frac{50 \times 10.3}{2 \times 3.14}$ Hz, giving a suggested range for the sampling period of $0.013 \leq h_S \leq 0.06$ second. As explained in Section 3.2.3, the shorter sampling period of 0.013 second is more suitable because of better intersample behaviour and will be used here. It is useful to recall that a sampling period of 0.0125 second has been used for the design of a digital PSS [97].

The results of zero order hold discretization have been calculated for both shift and delta models and are shown in Equations (3-22) and (3-23). The shift model has been evaluated by a commercial package CODAS II [98] with the highest precision that the software allowed.

$$G_d(q)=\frac{0.010433\,q^3 - 0.0077555\,q^2 - 0.010243\,q + 0.0077259}{q^4 - 3.6444\,q^3 + 5.0275\,q^2 - 3.116\,q + 0.73303} \quad (3\text{-}22)$$

$$G_d(\delta)=\frac{0.8\,\delta^3 + 139\,\delta^2 + 2524\,\delta + 5627}{\delta^4 + 27\,\delta^3 + 558\,\delta^2 + 2679\,\delta + 6160} \quad (3\text{-}23)$$

Table I

	continuous-time system	discrete-time system (delta model)	discrete-time system (shift model)
zeros	-2.64, -19.99	-2.59, -17.66, -153.49	-0.99, 0.97, 0.77
poles	-2.8 ± j 2.7 -9.14 ± j 19.84	-2.8 ± j 2.6 -10.85 ± j 17.44	0.86 ± j 0.23 0.96 ± j 0.02

The poles and zeros of three different systems have been shown in Table I. The third zero of the delta model has been introduced by the sampling process and can be considered as a zero in continuous-time system which goes to $-\infty$. The other poles and zeros are very close to the corresponding ones for the continuous-time case, illustrating the consistency between the continuous-time system and the delta model. Considering the largest dominant pole of $G_d(s)$ (i.e., -9.14 + j 19.84) and Equation (3-21), it can be seen that $-1.126 < -1$. It follows that the controller transfer function in the form of the delta operator is preferable to the shift model. It can also be seen that $G_d(q)$ is on the verge of being non-minimum phase because one zero (-0.99, 0) is located close to the point (-1, 0).

Calculations have been performed on the excitation control system described earlier to compare the continuous frequency response $G_d(j\omega)$ with that of the discretized systems using the delta and shift operators.

The trapezoidal approximation method has been used to calculate the frequency response of the discrete-time systems. This involves substituting $(2+j\omega h)/(3-j\omega h)$ for q in the shift operator form and substituting $j\omega/(1-\frac{jh\omega}{2})$ for δ in the delta operator form. This method is known to give good correspondence between the continuous-time and discrete-time frequency responses at low frequencies [83]. Figures 3.4 (a) and (b) depict the gain characteristics of $G_d(s)$ when modelled by the shift and delta operators respectively, with the continuous-time model also shown for comparison.

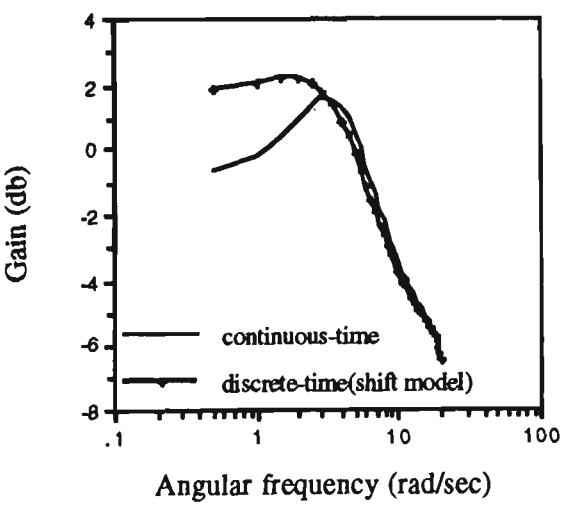

(a) Shift operator

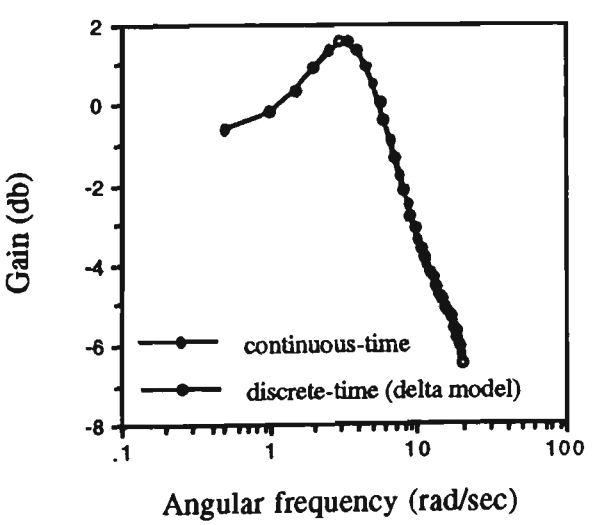

(b) Delta operator

Figure 3.4: Calculated frequency responses

Referring to Figures 3.4 (a) and (b) it is clear that, at low frequencies, the gain characteristics of the excitation control system, when modelled by the shift operator, deviates from that of the continuous-time model. On the other hand, almost identical characteristics are obtained for the delta and continuous-time models over the whole frequency range of interest, confirming the accuracy of the delta model when short sampling periods are involved.

The sensitivity of $G_d(q)$ to numerical rounding off was investigated further by evaluating the frequency response using lower decimal point accuracy. Figures 3.5 (a) and (b) show the gain characteristics of $G_d(q)$ for four and three decimal point accuracy respectively. The shift model is seen to be extremely sensitive to round off errors for short sampling periods with very large changes in the frequency response calculation for changes in coefficients as small as 0.001 representing changes of less than 1%. However, the delta model gives consistent results irrespective of the accuracy of the coefficients.

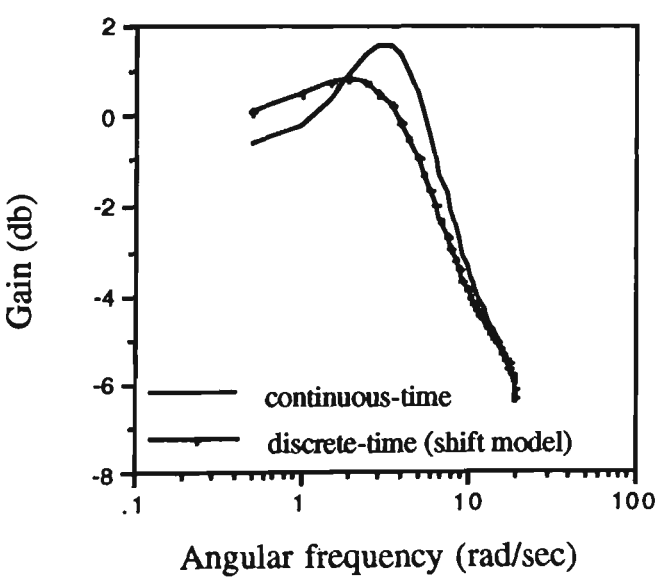

(a) Four decimal point accuracy

Figure 3.5: Effect of round-off on shift model frequency response (sampling time = 0.013 sec)

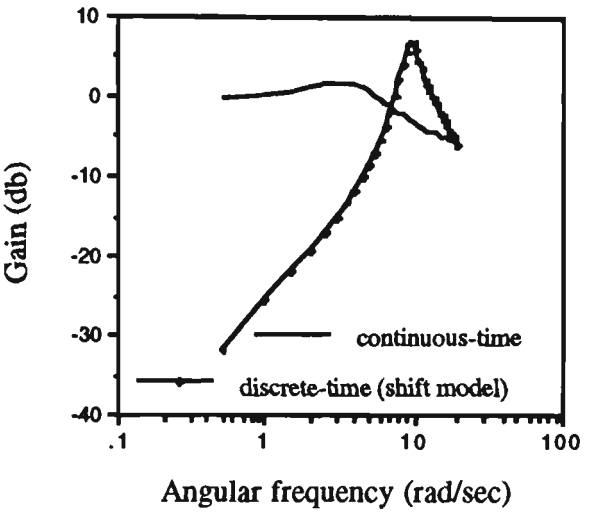

(b) Three decimal point accuracy

Figure 3.5: Effect of round-off on shift model frequency response (sampling time = 0.013 sec)

Further calculations have been conducted to compare the step response of the excitation control system when modelled using the shift and delta operator based on Equations (3-22) and (3-23) respectively. The transient response of both models to a unit step input with zero initial condition is shown in Figure 3.6. The shift model loses its accuracy after the initial part of the transient response and in the steady state because of the limited accuracy of representing its coefficients.

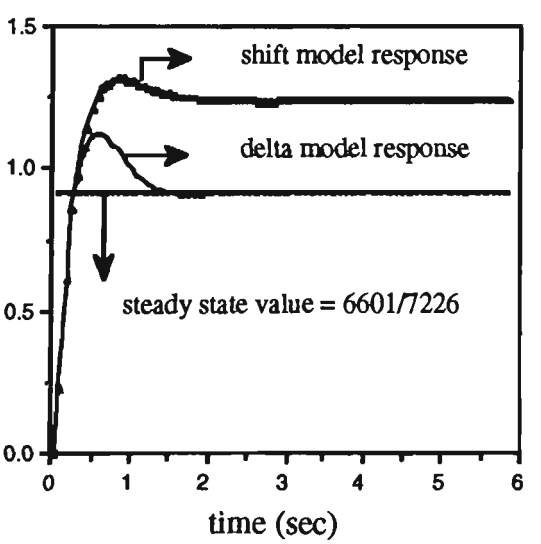

Figure 3.6: The unit step responses for the two discrete models using Equations (3-22) and (3-23)

The above calculations show that implementing a discrete-time system by the delta model has distinct advantages over the commonly adopted approach of the shift model for short sampling periods as would often be required to give adequate bandwidth.

3.5.2 Example II

An Australian power system example is used to show the advantages of the delta operator in power system analysis. The w-model of continuous-time system is calculated through both the shift and the delta operators and the results are compared.

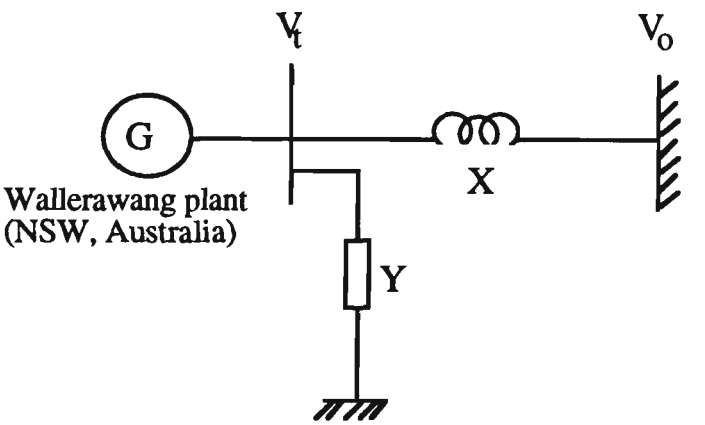

Figure 3.7: A single-machine infinite-bus model

Consider a synchronous generator supplying power to an infinite bus through a series transmission impedance with a shunt load admittance Y, as shown by Figure 3.7. V_o and V_t represent the terminal and infinite bus voltages respectively. The parameters of the power system model shown in Figure 3.7 for the (i) 1993 medium load and (ii) 1993 high load cases have been given in Appendix V.

The same transfer function given in Section 3.5.1 ($G_d(s)$) and the block diagram of Figure 2.1 are used here. By considering the 1993 high load case and the parameters of the excitation control system as K_e = 50, K_s=4.8 and T_a = 0.05, $G_d(s)$ is calculated as follows;

$$G_d(s) = \frac{9.52\,s^2 + 216\,s + 518}{s^4 + 23.8\,s^3 + 493\,s^2 + 2344\,s + 6110} \qquad (3\text{-}24)$$

Using the procedure given in Section 3.5.1 and the system bandwidth of $\omega_0 = 12$ rad/sec give a suggested range for the sampling period of $0.01 \le h_S \le 0.05$ second. As mentioned earlier the shorter one is used for discretization.

The results of zero order hold discretization are shown in Equations (3-25) and (3-26).

$$G_d(q) = \frac{0.00047392q^3 - 0.00037564q^2 - 0.00047112\,q + 0.00037746}{q^4 - 3.7511\,q^3 + 5.3005\,q^2 - 3.3455\,q + 0.79612} \qquad (3\text{-}25)$$

$$G_d(\delta) = \frac{0.047\,\delta^3 + 10.5\,\delta^2 + 199\,\delta + 461}{\delta^4 + 25\,\delta^3 + 471\,\delta^2 + 2197\,\delta + 5441} \qquad (3\text{-}26)$$

The w-models which have been calculated using the shift operator and the delta operator are shown in Equations (3-27) and (3-28) respectively.

$$G_d(w) = \frac{-6.125e\text{-}16\,w^4 - 4.25e\text{-}10\,w^3 + 7.5401e\text{-}84\,w^2 + 1.9012e\text{-}6\,w + 4.62e\text{-}6}{8.8707625e\text{-}9\,w^4 + 3.0334e\text{-}7\,w^3 + 4.393e\text{-}6\,w^2 + 0.0000216\,w + 0.00002} \qquad (3\text{-}27)$$

$$G_d(w) = \frac{3.3e\text{-}6w^4 - 0.05\,w^3 + 8.56\,w^2 + 214\,w + 520}{w^4 + 23.1\,w^3 + 495\,w^2 + 2356\,w + 6139} \qquad (3\text{-}28)$$

Calculation of frequency responses have been performed using the frequency domain approximation [83]. This involves substituting $e^{j\omega h}$ for q in the shift operator form, substituting $\frac{e^{j\omega h} - 1}{h}$ for δ in the delta

operator form and substituting $j \frac{2}{h} tg (\frac{\omega h}{2})$ [81,93] for w in the w operator form. Figure 3.8 (a) and (b) depict the gain characteristics of $G_d(s)$ (case iv) when modelled by the shift and delta operators respectively, with the continuous-time model also shown for comparison. Figures 3.9 (a) and (b) also show the gain characteristics of $G_d(s)$ when modelled by the w operator using Equations (3-27) and (3-28) respectively.

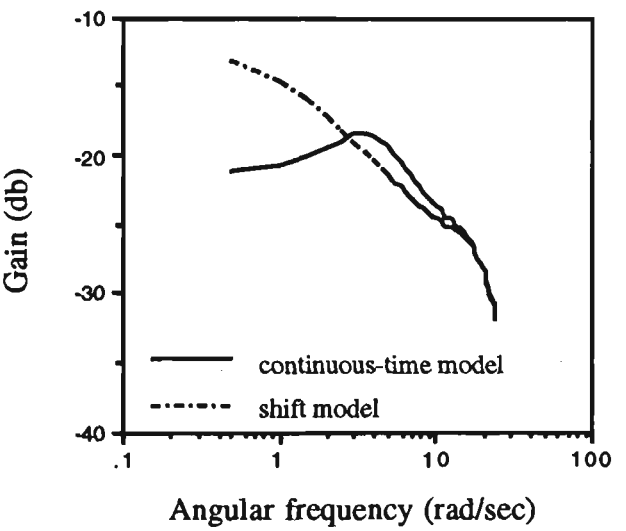

(a) shift model

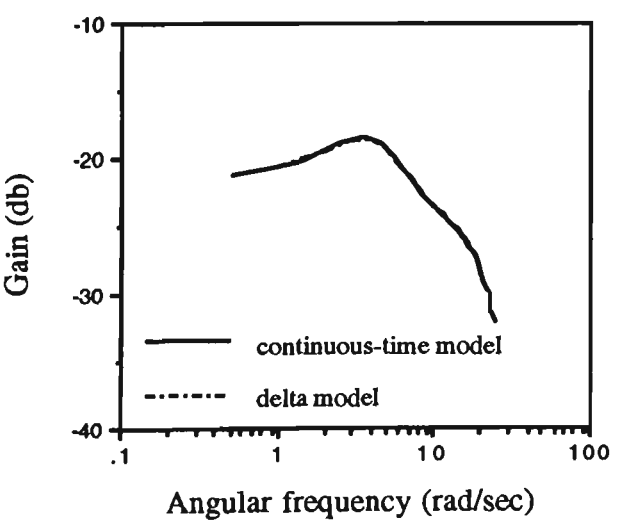

(b) delta model

Figure 3.8: Calculated frequency response

(sampling time =0.01 sec)

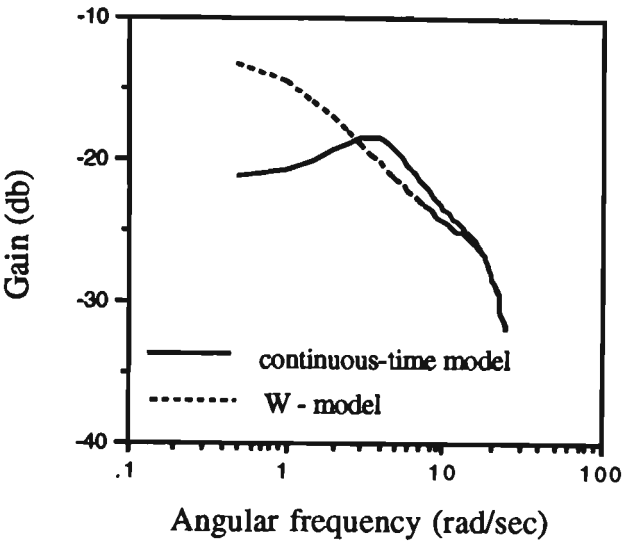

(a) w-model has been calculated by using the shift operator

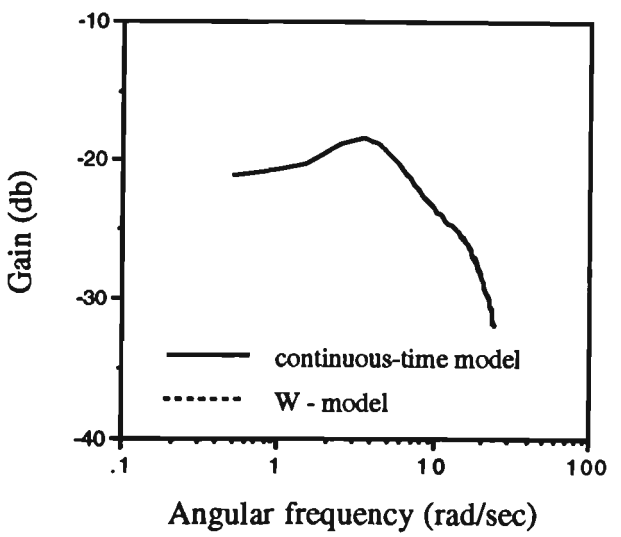

(b) w-model has been calculated by using the delta operator

Figure 3.9: Calculated frequency response

(sampling time =0.01 sec)

Referring to Figures 3.8 (a) and (b), it can be seen that the same results have been obtained as mentioned in Section 3.5.1. The shift model loses its accuracy when short enough sampling time is used. However, the results confirm the accuracy of the delta operator when used in power system. Figures 3.9 (a) and (b) also show that the w-model gives accurate

results only when it is calculated through the delta operator. Using the delta operator gives not only the accurate results but also a close resemblance between continuous-time and discrete-time system coefficients. Therefore, the w operator has no distinct advantages over the delta operator and it is not necessary to be calculated.

3.6 CONCLUSIONS

High performance will be achieved from modern digital controllers if shorter sampling periods can be used, but this leads to difficulties in the discretization of transfer functions. A comparison has been given of the use of the shift, delta, and w operator methods for the discretization of two power system transfer functions at typical short sample periods. The shift model representation has been shown to be very sensitive to numerical round-off. This has several unfortunate consequences such as incorrect steady state and frequency responses. It has been shown that the delta operator model does not have these problems with the added convenience that its transfer function bears a close correspondence to the continuous-time system. The w operator had no distinct advantages rather than the delta operator because it had to be calculated through the delta operator to avoid the numerical difficulties.

CHAPTER 4

Chapter 4

SYSTEM IDENTIFICATION

4.1 INTRODUCTION

Adaptive control techniques such as self-tuning control involve the identification of the parameters of the plant model through continual sampling of the input and output signals. The process of constructing models and estimating unknown plant parameters from the experimental data is called system identification [81].

System identification comprises both model structure and parameter identification. Since the model structure of a power system is usually known as shown in Section 2.2, it is only necessary to perform parameter identification. There are various algorithms which can be used for this purpose. These can be implemented on-line or off-line. The off-line algorithms require the accumulated data which are processed several times. This makes the off-line algorithms more accurate than on-line ones but more computationally burdensome. On-line algorithms are necessary in adaptive schemes because the data must be processed in real time.

Recursive Least Squares (RLS) estimation is the most commonly method used in adaptive control. With this method, the computation is relatively simple and parameter convergence is fast [91].

In adaptive control both the control algorithm and the identification scheme are based on a linear discrete-time model. The usual approach

for discretizing is using the shift operator. However, it will be shown that because of numerical difficulties arising from clustering effect when a short sampling time is used, the identified model loses consistency with the continuous case for frequency response calculation. The delta model is shown to give a model which is accurate over the frequency range [85].

This chapter is organised as follows: Section 4.2 describes the concept of the predictive model. Recursive Least Squares estimation is described in Section 4.3 followed by introducing a new technique for identification of power system parameters in Section 4.4. Section 4.5 gives a comparison between the shift and delta operators in which the parameters of a generator excitation control system for both SMIB and multimachine power systems are estimated. Conclusions will be given in Section 4.6.

4.2 PREDICTIVE MODEL

One of the important aspects of an adaptive scheme is to choose a predictive model which is properly structured in order to represent the actual dynamic behaviour of the system [99]. Following the development in [92], consider, for example, a dynamical system with the input signal u(t) and the output signal y(t). The Laplace domain transfer function which relates the input signal to the output signal may have the form of

$$G(s) = \frac{B_0 s^m + B_1 s^{m-1} + \ldots + B_m}{s^n + A_1 s^{n-1} + A_2 s^{n-2} + \ldots + A_n} = \frac{Y(s)}{U(s)}; \quad m \le n \qquad (4\text{-}1)$$

The discrete-time transfer function of Equation (4-1) is of the form:

$$G(q) = \frac{C_0 q^{n-1} + C_1 q^{n-2} + \ldots + C_{n-1}}{q^n + D_1 q^{n-1} + D_2 q^{n-2} + \ldots + D_n} = \frac{Y(q)}{U(q)} \qquad (4\text{-}2)$$

The forward shift operator q can be replaced by the backward shift operator, q^{-1}. The latter is defined such that

$$q^{-1}\, x(k) = x(k-1)$$

where k is the discrete-time index and x(.) stands for any discrete signal.

Equation (4-2) may be rearranged to give

$$y(k) = q^{-1}\,\frac{C_0 + C_1 q^{-1} + C_2 q^{-2} + \ldots + C_{n-1}\, q^{-n+1}}{1 + D_1 q^{-1} + D_2 q^{-2} + \ldots + D_n\, q^{-n}}\; u(k) \qquad (4\text{-}3)$$

In compact form

$$y(k) = q^{-1}\,\frac{C(q^{-1})}{D(q^{-1})}\; u(k) \qquad (4\text{-}4)$$

where

$$C(q^{-1}) = C_0 + C_1 q^{-1} + C_2 q^{-2} + \ldots + C_{n-1} q^{-n+1}$$

$$D(q^{-1}) = 1 + D_1\, q^{-1} + D_2\, q^{-2} + \ldots + D_n q^{-n}$$

If there is any time delay associated with the system, which is represented in Laplace domain as $e^{-\tau s}$, then the above model modifies to the following form

$$y(k) = q^{-L}\,\frac{C(q^{-1})}{D(q^{-1})}\; u(k) \qquad (4\text{-}5)$$

where L=m+1 and m = the integer part of $\frac{\tau}{h}$. Note that the zero order hold of $e^{-\tau s}$ can be obtained using the transformation $q = e^{sh}$ [81]. Equation (4-5) is the general discrete-time transfer function representation of a continuous-time transfer function.

The predictive model of (4-5) for the case, where Gaussian noise ($\upsilon(k)$) is included, is given by

$$y(k)= -D_1\, y(k-1) - D_2\, y(k-2) - \ldots + C_0\, u(k-L) + C_1\, u(k-L-1) + \ldots + C_{n-1}\, u(k-L-n) + \upsilon(k) \quad (4\text{-}6)$$

Consider, for example, the parameter vector of

$$\theta^T = (D_1 \ldots D_n\, C_0 \ldots C_{n-1}) \quad (4\text{-}7)$$

and the observed vector of input-output data of

$$\phi^T(k) = (-y(k-1) \ldots -y(k-n)\; u(k-L) \ldots u(k-L-n)) \quad (4\text{-}8)$$

Then, in compact form, Equation (4-6) can be written as

$$y(k) = \theta^T \phi(k) + \upsilon(k) \quad (4\text{-}9)$$

Equation (4-9) is the estimation model and describes the observed variable y(k) as an unknown linear combination of the components of the observed vector $\phi(k)$ plus noise.

4.3 RECURSIVE LEAST SQUARES ESTIMATION

Recursive Least Squares is a basic technique for parameter estimation. The method is particularly simple if the model has the property of being linearly on the unknown parameters. Following the development in [92], the main features of RLS method are summarised as follows.

Consider the Equation (4-9). The parameter vector θ is to be estimated from measurements of y(k), $\phi(k)$, k= 1, ... , N. A common way is to choose this estimate by minimising what is left unexplained by Equation (4-9) $\upsilon(k)$. That is, to minimise the function

$$V_N(\theta) = \frac{1}{N} \sum_{1}^{N} \left[y(k) - \hat{\theta}^T \phi(k) \right]^2 \qquad (4\text{-}10)$$

with respect to θ [91]. This gives the RLS algorithm in which the unknown parameter vector $\hat{\theta}$ can be updated during each sampling time as follows;

$$\hat{\theta}(k) = \hat{\theta}(k\text{-}1) + L(k)\, \varepsilon(k) \qquad (4\text{-}11)$$

where $\hat{\theta}(k)$ is the new estimate of the parameter vector, $\hat{\theta}(k\text{-}1)$ is the old estimate of the parameter vector,

$$L(k) = \frac{P(k\text{-}1)\, \phi(k)}{[\, 1 + \phi^T(k)\, P(k\text{-}1)\, \phi(k)\,]} \quad \text{is the gain vector}$$

$P(k) = [\, I - L(k)\, \phi^T(k)\,]\, P(k\text{-}1)$ is the covariance matrix, and

$\varepsilon(k) = [\, y(k) - \hat{\theta}^T(k\text{-}1)\, \phi(k)\,]$ is the prediction error.

The initial value for diagonal covariance matrix is usually chosen as a very large number (α) (say, $> 10^5$) [100].

For time-invariant systems, $\hat{\theta}(k)$ converges to its 'true' value with time. The gain vector L(k), the prediction error $\varepsilon(k)$ and the covariance matrix also tend to zero. However, for some systems it is of interest to consider the situation in which the parameters change with time as is typical with a power system. There are two situations which can be covered by simple extensions of the least-squares method. In one case parameters are changing abruptly but seldom and in other case the parameters are changing slowly [91]. The case of abrupt parameter changes can be covered by resetting the covariance matrix to its initial value αI, where α is a large number. In doing so, the stored information in the L(k) matrix is lost. However, the other case where the parameters change slowly does

not have this problem. This method can be covered by a relatively simple mathematical model which is to replace the least-squares criterion of Equation (4-10) with

$$V_N(\theta) = \frac{1}{N} \sum_{1}^{N} \lambda^k \left[y(k) - \hat{\theta}^T \phi(k) \right]^2 \qquad (4\text{-}12)$$

where λ is a parameter such that $0 < \lambda \leq 1$ and is called the forgetting or discounting factor [91,100]. The λ is usually selected a value close to 1 (say, 0.95-0.999 [100]). By using this method the gain vector and the covariance matrix can be rearranged as [91]

$$L(k) = \frac{P(k-1)\,\phi(k)}{[\,\lambda I + \phi^T(k)\,P(k-1)\,\phi(k)\,]}$$

$$P(k) = [\,I - L(k)\,\phi^T(k)\,]\,P(k-1)\,/\,\lambda \qquad (4\text{-}13)$$

4.4 RLS ESTIMATION USING THE DELTA OPERATOR

Consider the linear system represented in the δ-domain as shown in Figure 4.1.

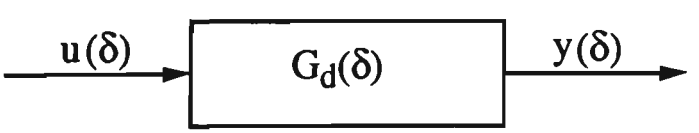

Figure 4.1

The transfer function $G_d(\delta)$ is in the form

$$G_d(\delta) = \frac{b_1\delta^{n-1} + b_2\delta^{n-2} + \cdots + b_n}{\delta^n + a_1\delta^{n-1} + \cdots + a_n} = \frac{y(\delta)}{u(\delta)} \qquad (4\text{-}14)$$

Since the synchronous generator is a zero time delay plant [33], the time delay τ (or m) considered in Equation (4-5) is assumed to be zero.

Considering $\delta = \frac{q-1}{h}$, straightforward algebraic modifications of Equation (4-14) lead to the simplified model

$$y_d(k) = \theta^T \phi(k) \qquad (4\text{-}15)$$

where

$$y_d(k) = q^{-n}(q-1)^n y(k)$$

$$\phi(k)^T = q^{-n}\{h(q-1)^{n-1}y,\ h^2(q-1)^{n-2}y,\ ...,\ h^n(q-1)y,$$

$$h(q-1)^{n-1}u,\ h^2(q-1)^{n-2}u,\ ...,\ h^n(q-1)u\}$$

and

$$\theta^T = \{-a_1, -a_2, ..., -a_n\ b_1, b_2, ..., b_n\}$$

Equations (4-15) have been written in the form of the models used for RLS estimation method as shown in Equation (4-9). The same Equations (4-13) are also used here to calculate the gain vector and covariance matrix.

4.5 PARAMETER ESTIMATION EXAMPLE

4.5.1 Single-machine infinite-bus example

The block diagram of Figure 1.3 is used to identify the closed-loop transfer function $G_d(s)$ given in Section 2.4. The sampled data of the output ($\Delta\delta$) are obtained by using a Fortran program in which the machine is modelled by a set of non-linear differential equations based on Park's equations (see Appendix I) [4,101].

The computer will be able to identify the system parameters based on the sampled values of the input and output if the system is excited enough [100]. In order to satisfy the condition a signal with the frequencies in the range of 0.2-2.5 Hz is used as an input (ΔP_d). Note that the low frequency oscillations occurring in power system are in the frequency range of approximately 0.2 to 2.5 Hz [1].

It is now shown that the identification method based on the sampled data using shift model gives inaccurate results when short enough sampling time is used to obtain a high performance for digital controllers used in power system. This problem arises from numerical difficulties related to the clustering effect in shift model and the necessary use of a finite precision in number representation as discussed in Section 3.4.2. To illustrate the problem the same order of the closed-loop transfer function of Equation (2-4) with two different sampling times 0.03 and 0.013 seconds is used for identification. However, it should be mentioned that computer simulations are carried out using the high order power system given by Equation (2-3) and shown in Figure 2.6 to obtain the sampled output of the power system.

The discrete-time transfer function will be taken to be:

$$G_d(\tau) = \frac{b_1\tau^3 + b_2\tau^2 + b_3\tau + b_4}{\tau^4 + a_1\tau^3 + a_2\tau^2 + a_3\tau + a_4} \qquad (4\text{-}16)$$

where τ can be q or δ for the shift and delta models respectively.

The parameters of $G_d(\tau)$ for two kinds of discrete-time representations have been obtained by RLS estimation with five decimal point accuracy and shown in Table 1. These parameters will be used to obtain the frequency response of G_d for different cases as explained below.

The linear discrete-time model should represent the essential dynamics of the actual plant when identified. Therefore, the frequency response of $G_d(s)$ is compared with that of the identified systems using the delta and shift operators using the trapezoidal approximation.

Table 1

parameters	sampling time = 0.03 sec		sampling time = 0.013 sec	
	shift model	delta model	shift model	delta model
a_1	-3.08663	30.29	-3.64409	27.35
a_2	3.71956	511	5.02724	561
a_3	-2.11544	2335	-3.11578	2691
a_4	0.48621	5010	0.73340	6190
b_1	0.10181	1.8	0.02075	1.6
b_2	-0.14822	150	-0.03611	141
b_3	0.04937	2143	0.01559	2553
b_4	0.00075	4450	-0.00006	5653

Figures 4.2, 4.3 (a) and (b) depict the gain characteristics of $G_d(\tau)$ using two different operators and two different sampling times, with the continuous model also shown for comparison. The convergence characteristics of the parameters for two different models are shown in Figures 4.4 (a) and (b).

Referring to Figures 4.2 and 4.3 it is clear that the gain characteristics of the excitation control system, when identified using shift operator, deviates from that of the continuous-time model. On the other hand, almost identical characteristics are obtained for the delta and continuous-

time models over the whole frequency range of interest, confirming the accuracy of the delta model when short sampling periods are involved.

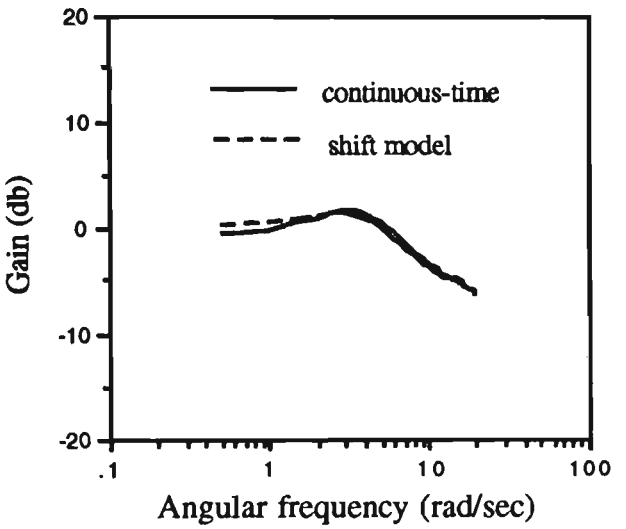

(a) shift operator

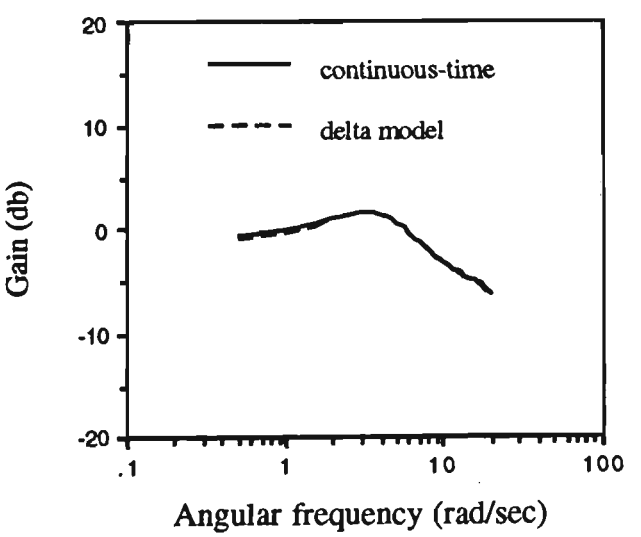

(b) delta operator

Figure 4.2: Calculated frequency responses

(sampling time = 0.03 sec)

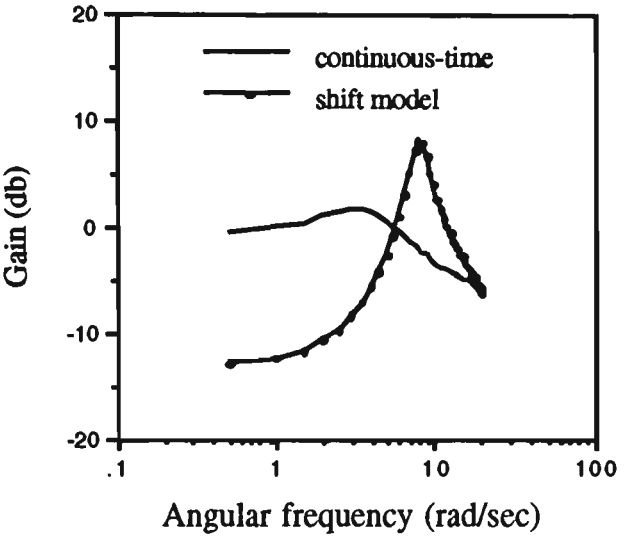

(a) shift operator

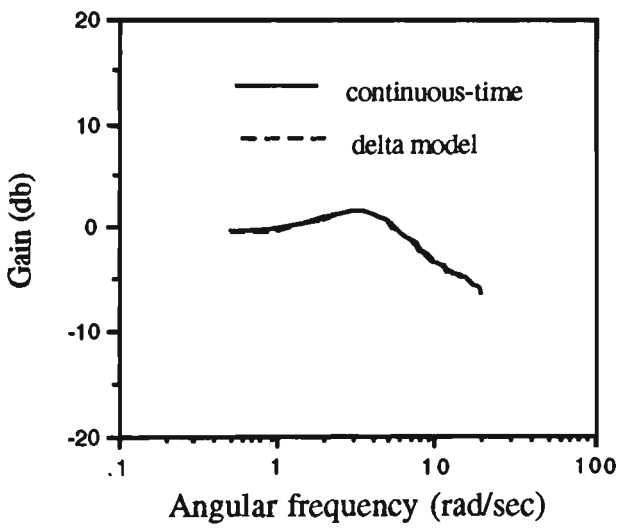

(b) delta operator

Figure 4.3: Calculated frequency responses

(sampling time = 0.013 sec)

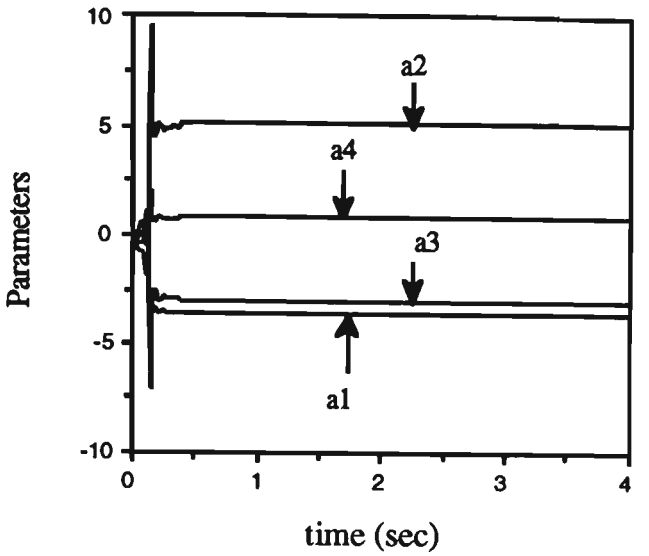

(a) shift operator

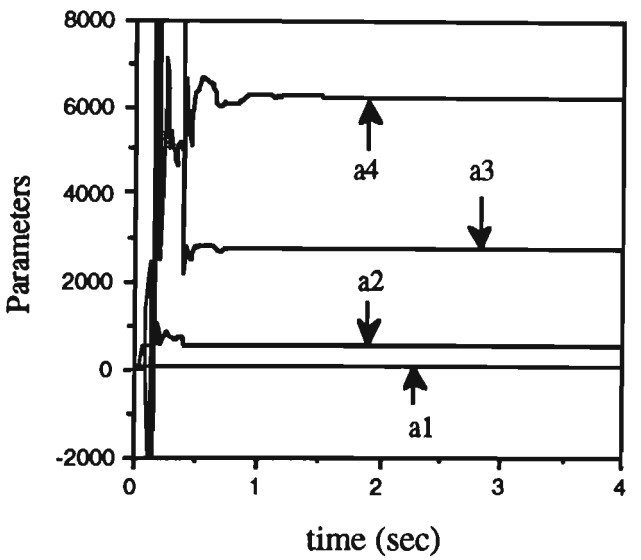

(b) delta operator

Figure 4.4: The convergence characteristics of the parameters (sampling time = 0.013 sec)

4.5.2 Multimachine example

Consider, for example, a two-machine system as shown in Figure 4.5. The parameters of this system are given in Appendix VI.

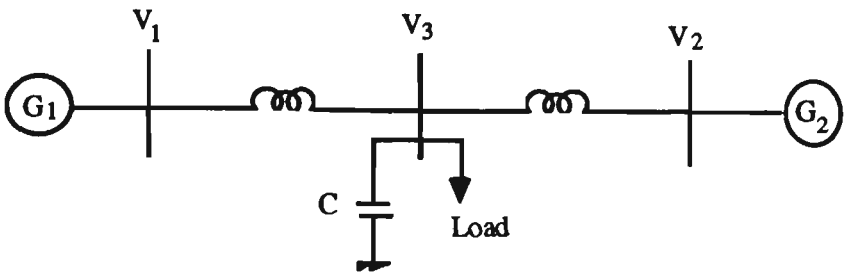

Figure 4.5: Two-machine system

The linearized equation of this system can be shown in the form

$$\dot{x} = A\,x + B\,u \tag{4-17}$$

where x is the state vector comprising $\Delta\omega_i$, $\Delta\delta_i$, $\Delta E'_{q_i}$, ΔE_{fd_i} for each machine, and u is the input vector comprising of ΔV_{ref} of each machine. The 8x8 matrix A and the 2x8 matrix B are given in Appendix VI. Eigenvalue analysis shows that the system is lightly damped and should be equipped by some means to improve the damping. The additional damping can be provided by a fixed PSS which inserts an appropriate signal at the voltage regulator summing junction. This situation is shown in Figure 4.6. Both machines are equipped by PSS because both are effective on the lightly damped modes.

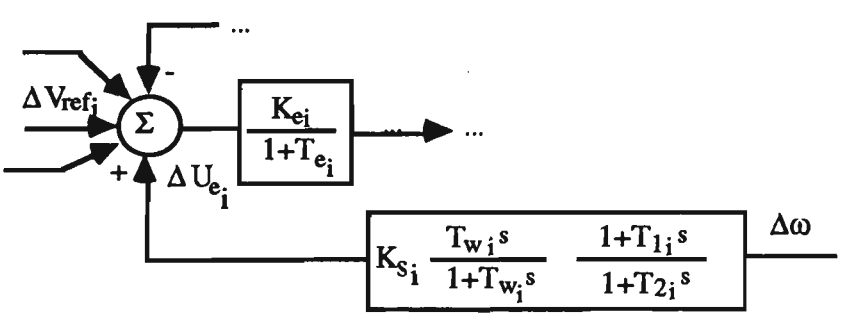

Figure 4.6: Excitation control system of ith machine with PSS

The PSS for each machine is so designed that the phase lag produced by excitation control system of each machine is compensated [4,102]. Since the phase lag of the voltage regulator is small, a lead-lag compensation

block is sufficient for the excitation control design. The PSS parameters are given in Appendix VI.

The transfer function G_{d1} of the generator G_1 with the same order as Equation (4-16) will be identified for two different cases (i) the dynamic interaction between machines is considered, and (ii) machine G_2 is considered as an infinite bus by enlarging its inertia (say, 9999) and reducing its reactance (say, 0.00001). The second case has been considered to see the effect of the dynamic interaction between machines on the identified transfer function. In principle, the coefficients of the transfer function G_{di} of the individual ith machine in terms of "K_{ii}" (not "K_{ij}") parameters (see Figure 2.2) should not be changed significantly for two cases mentioned above.

Although the output signal $\Delta\delta_i$ is affected by different input signals (see Figure 2.2), as will be explained further in Chapter 6 it is sufficient to consider only the input signal ΔP_{di}. The other input signals do not have any effect on the identified transfer function G_{di}. A sampling time of 10 msec is used for the parameter estimation.

Figures 4.7 (a) and (b) show the gain characteristics of G_{d1} using the delta and the shift operators, with the continuous model also for comparison. The convergence characteristics of two parameters for different cases are shown in Figures 4.8 (a) and (b).

Referring to Figure 4.7 (a) it is clear that the delta operator gives identical characteristics with the continuous-time system for the whole frequency range of concern. Figure 4.8 (a) also shows that there is a negligible difference between the identified parameters for two cases (i) and (ii) mentioned earlier. This confirms that the delta model is able to

identify the parameters of the individual ith machine accurately when there is dynamic interaction between machines.

On the other hand, the gain characteristics of the shift model deviates from that of the continuous-time model when a short enough sampling time is used, especially for low frequency range in which inter-area modes are the most dominant modes. Figures 4.7(b) and 4.8 (b) also show that the dynamic interaction between machines affects on the identified transfer function so that the gain characteristics change significantly.

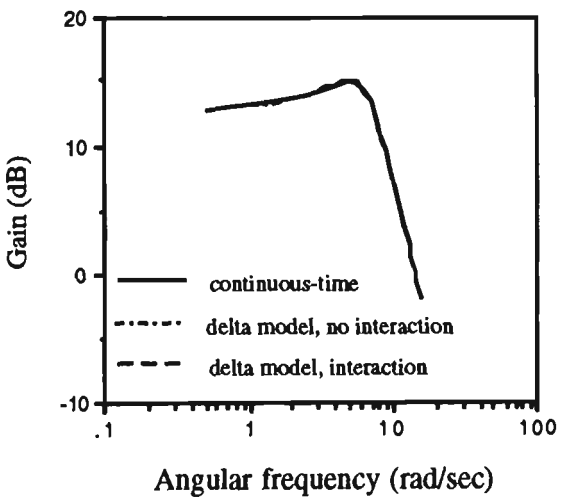

(a) delta model

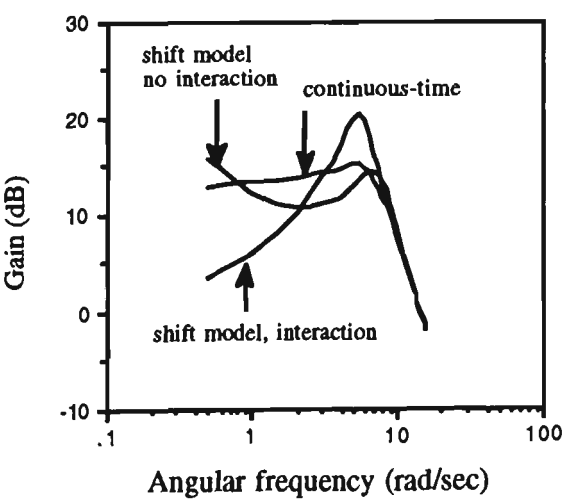

(b) shift model

Figure 4.7: Calculated frequency response

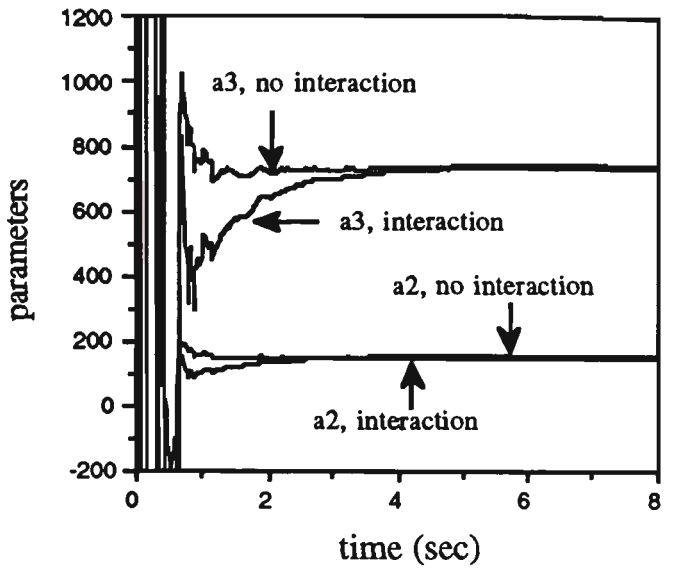

(a) delta model

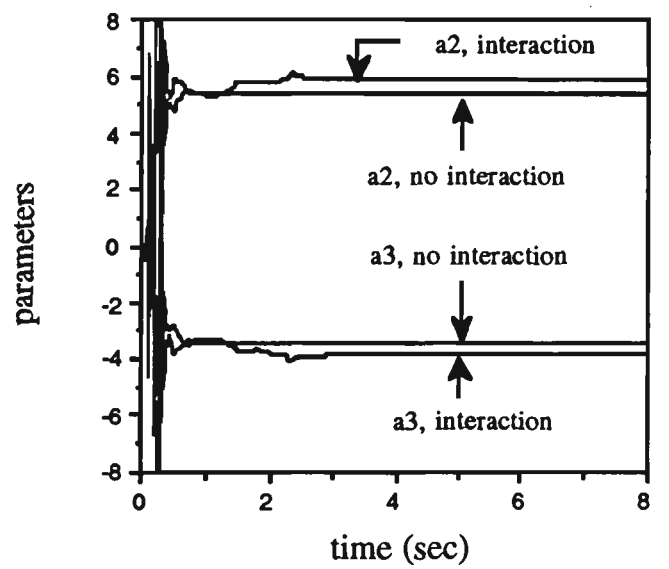

(b) shift model

Figure 4.8: The convergence characteristics of parameters

It should be mentioned that in both discrete models the dynamic interaction between machines may cause the parameter convergence to be slower than the SMIB model.

4.6 CONCLUSIONS

A perspective of the subject of identification in dynamical system has been presented with particular reference to the Recursive Least Squares method. A new technique of identification using the delta model has been obtained.

A comparison has been given of the use of the shift and delta operator methods for identifying the parameters of discrete-time model of the system at typical short sample periods. The shift operator gives poor results such as an incorrect frequency response and difficulties in identifying the power system model. The delta operator does not have these problems and gives accurate results. It was also shown that the identified transfer function of an individual subsystem in a multimachine case could be changed significantly using the shift operator when there is dynamic interaction between machines. However, the delta operator was shown to be accurate in all cases.

CHAPTER 5

Chapter 5

POLE ASSIGNMENT ADAPTIVE CONTROLLER

5.1 INTRODUCTION

Different methods [1-6] of designing supplementary excitation control known as power system stabilisers with fixed parameter settings have been reported for improving the power system stability. This works reasonably well over a medium range of operating points, but the damping may diminish as the generator load changes or the network configuration is altered through planned, or contingency outages [103-104].

One technique to solve this problem is a digital adaptive controller which tracks the changing operating point by identification and calculates the control action at each sampling time using the identified model. Previous studies [8,105] have shown a great improvement by the use of adaptive techniques.

The Pole Assignment (PA) controller first proposed by Edmonds [106] and was developed further by Wellstead, et al [44] in the field of control engineering by using the shift operator. In this algorithm, the controller parameters are adjusted so that the poles of the closed-loop transfer function are placed at preselected locations. This chapter applies this technique to a SMIB power system for the first time by adding a further contribution in which the delta operator is used to simplify the analysis and to avoid the numerical difficulties associated with the shift operator.

This chapter is organised as follows: Section 5.2 describes a derivation of a simplified block diagram to characterise the dynamic behaviour of the power system while Section 5.3 demonstrates the effect of the fixed gain PSS on single-machine infinite-bus power system performance. Section 5.4 gives the design of the Pole Assignment controller and simulation results which are compared with those for a fixed parameter power system stabiliser.

5.2 SYSTEM MODELLING

5.2.1 System block diagram

The same block diagram of Figure 2.1 is used here.

5.2.2 A simplified block diagram

For the analysis purposes of this work the block diagram of the linearized model shown in Figure 2.1 may be reconfigured to a simplified diagram as shown in Figure 5.1. This figure shows the effect of the disturbances such as a change in either load or voltage reference on the power angle changes ($\Delta\delta$). The coefficients of the polynomials A(s), B(s) and C(s) are given in Appendix VII. The denominator of $G_c(s)=\frac{\Delta\delta}{\Delta V_{ref}}$ is the same as the denominator of $G_d(s)$.

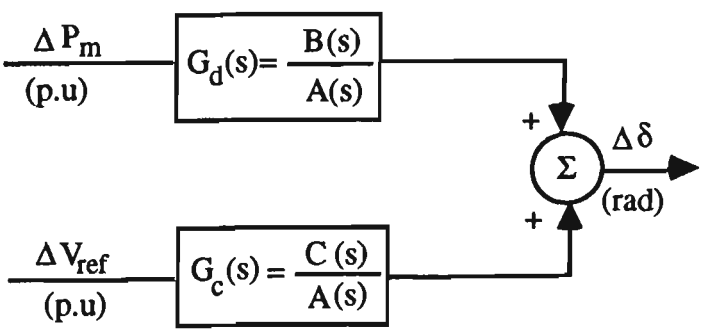

Figure 5.1: A modified block diagram of Figure 2.1

It should be noted that for the design of the adaptive controller, as explained in Section 2.3, the excitation system has been considered as a dc gain K_e. However, as will be shown further in Section 5.4.6 computer simulations are carried out for the case where the excitation system is $[K_e/(1+T_e s)]$. To compare the adaptive stabiliser given further in Section 5.4 with a conventional stabiliser the latter is first given.

5.3 FIXED GAIN PSS

5.3.1 Design operating point

Consider in particular a single-machine infinite-bus model as shown in Figure 5.2. The parameters of the system including the "K" parameters are given in Appendix II.

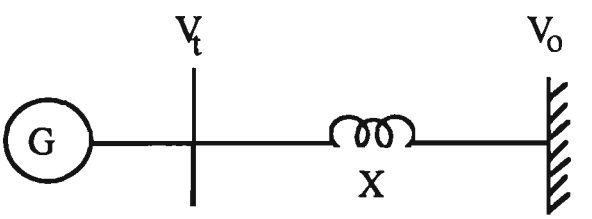

Figure 5.2: A single-machine infinite-bus model

By considering the operating point P+jQ=1+j0.5 p.u, X=0.4 p.u, V_t=1.0 p.u, $G_d(s)$ may be calculated using the block diagram of Figure 2.1.

$$G_d(s) = \frac{125\ s^2 + 12636\ s + 33277}{s^4 + 102\ s^3 + 518\ s^2 + 13358\ s + 36546} \qquad (5\text{-}1)$$

The poles of Equation (5-1) are $s_{1,2} = -0.53 \pm j\ 11.37$, $s_3 = -2.88$ and s_4=-97.86 showing that the system is lightly damped and should be equipped by some means to improve its damping. Figure 5.3 shows the situation where a PSS has been added to the block diagram given of Figure 2.1.

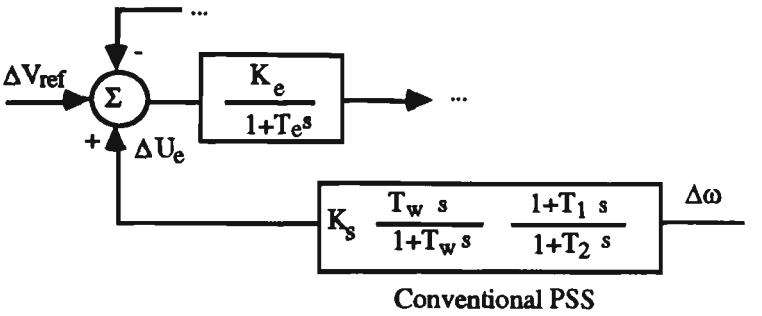

Figure 5.3: Excitation control system with PSS

As shown in Section 2.4 this leads to the closed-loop transfer function of:

$$G_d(s) = \frac{125s^4 + 18932s^3 + 666993s^2 + 1730372s + 166386}{s^6 + 152s^5 + 5624s^4 + 120927s^3 + 774506s^2 + 1896218s + 182730} \quad (5\text{-}2)$$

where the poles are $s_{1,2} = -16.64 \pm j\ 21.37$ and $s_{3,4} = -4.1 \pm j\ 2.39$, s_5=-110.4 and s_6=-0.1. By using partial-fraction expansion it can be seen that the residue corresponding to the pole -0.1 is -0.00038 which means that its effect in damping of the system is negligible. The location of other poles show that the damping of the system has been improved. Transient performance of the system to a 1% step change in load was tested and shown in Figure 5.4 for the cases before and after using the PSS. It is clear from Figure 5.4 that the damping of the system has been enhanced when the PSS is used.

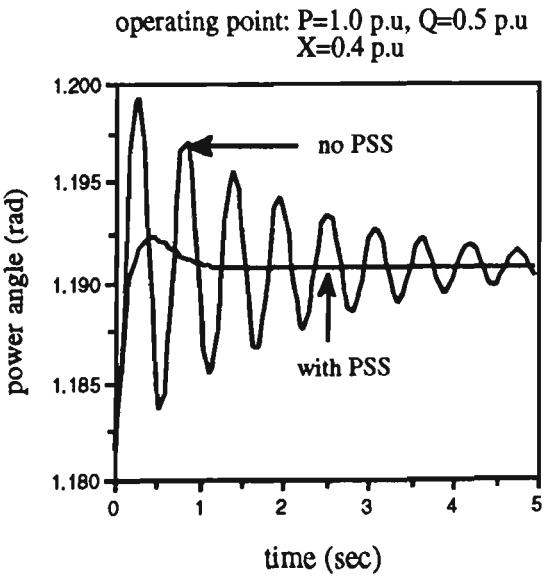

Figure 5.4: Time response of the system to 1% step change in load

5.3.2 Change in operating point

The PSS becomes less effective as the operating point changes [8]. For example, consider the case where the reactance line changes from X=0.4 p.u. to X=1.0 p.u [3] while the parameters of the PSS are fixed at the design values for X=0.4 p.u. Accordingly, this will affect the "K" parameters (K_1 to K_6) shown in Figure 2.1 giving a shift in the poles. Figure 5.5 shows the transient performance of the power system to a 1% step change in load at the new operating point. Comparing Figures 5.4 and 5.5 shows that the PSS is less effective as the system moves from its design operating point.

One possible way to improve the damping of the system is to change the excitation control system parameters as shown in Figures 5.6 (a-d) and 5.7 (a-d) for both operating points. In Figures 5.6 (a-c) and 5.7 (a-c) it is assumed that two parameters are fixed and then the system performance is tested by changing the third excitation control system parameter (i.e., K_e or K_s or T_1). Figure 5.6 (d) and 5.7 (d) depict the case where all three parameters are changed.

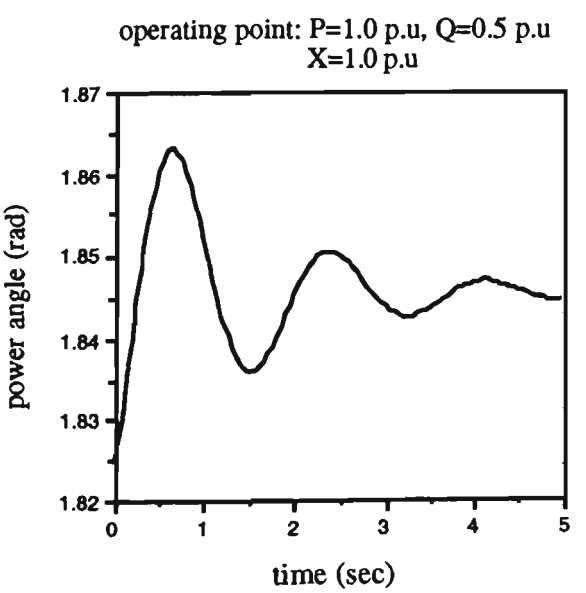

Figure 5.5: Time response of the system to 1% step change in load

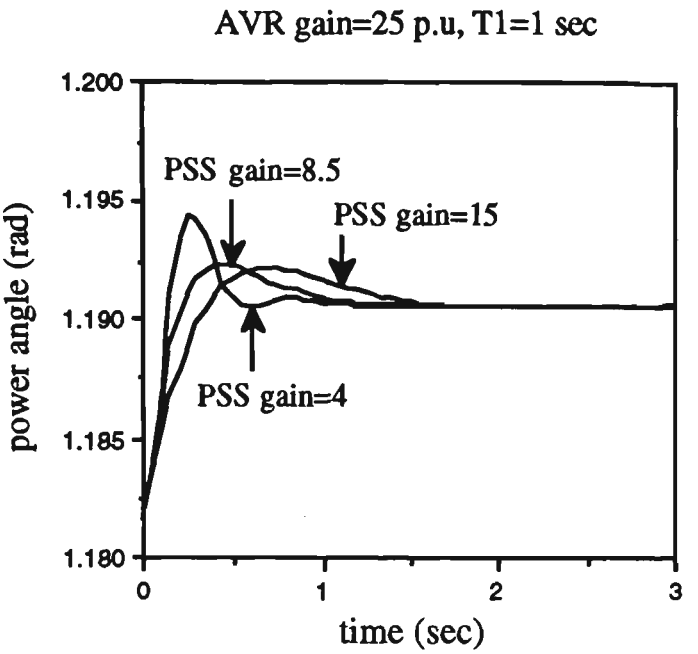

(a)

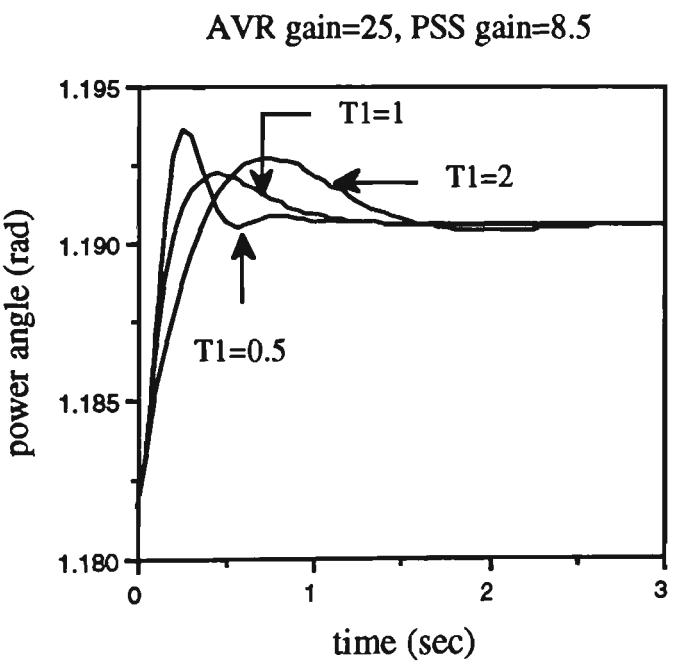

(b)

Figure 5.6: Time response of power system to 1% step change in load (P+jQ = 1+j 0.5 p.u, X=0.4 p.u, V_t=1.0 p.u)

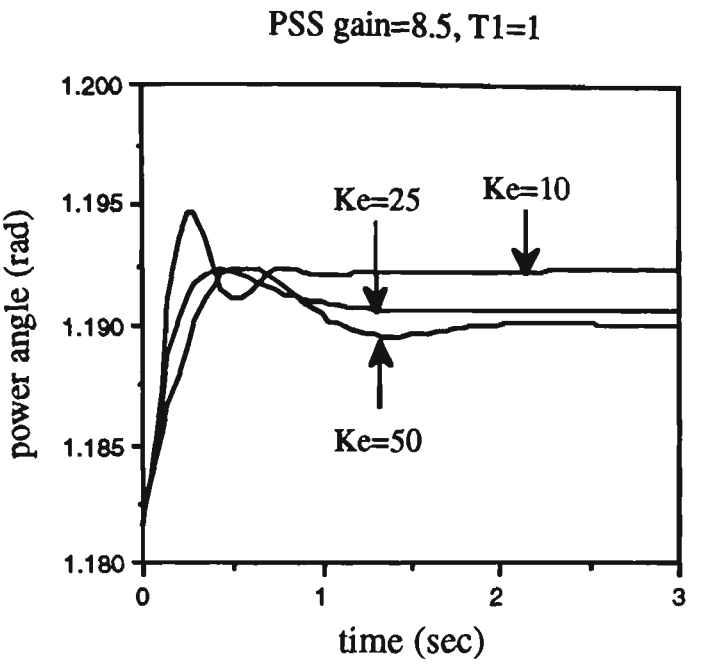

(c)

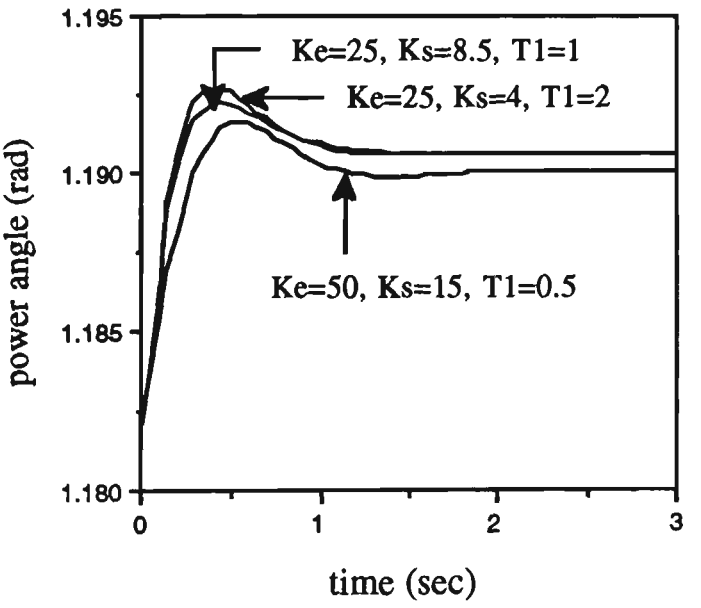

(d)

Figure 5.6: Time response of power system to 1% step change in load (P+jQ = 1+j 0.5 p.u, X=0.4 p.u, V_t=1.0 p.u)

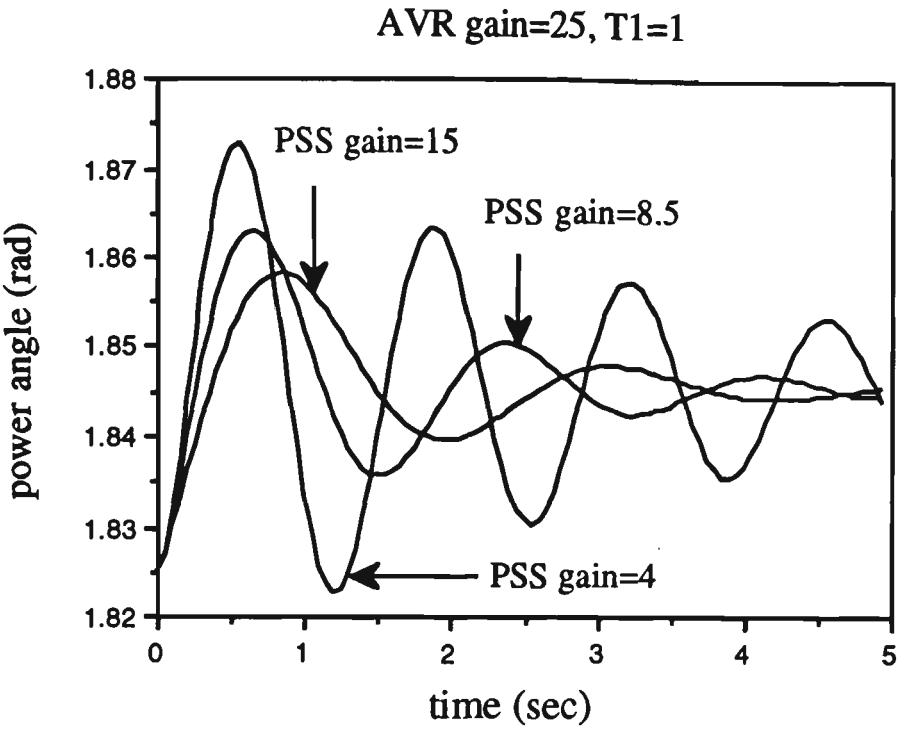

(a)

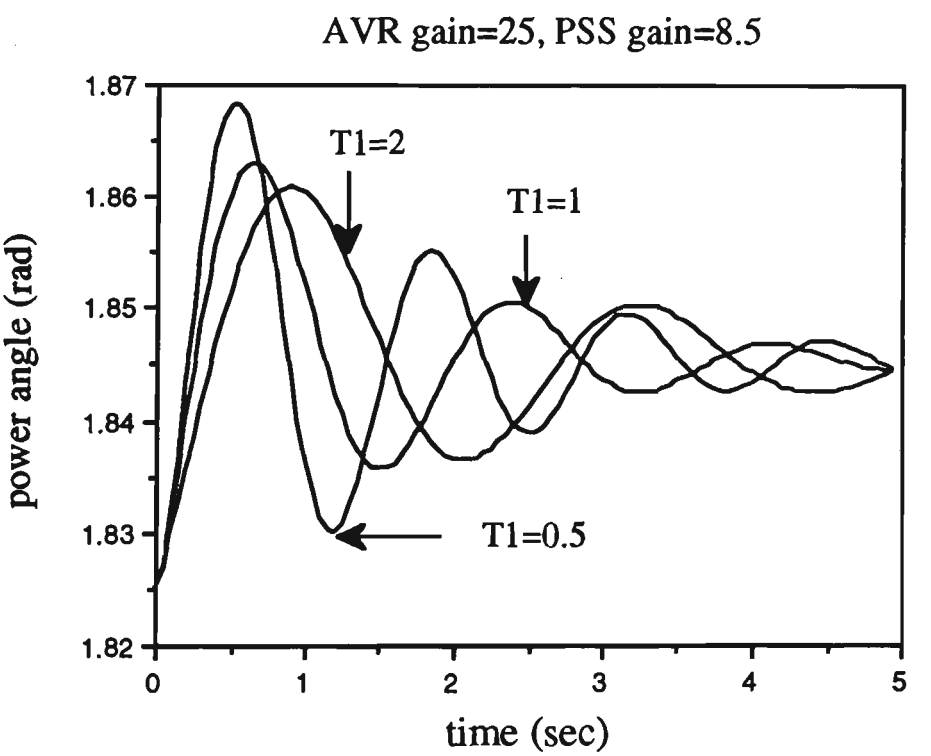

(b)

Figure 5.7: Time response of power system to 1% step change in load (P+jQ = 1+j 0.5 p.u, X=1.0 p.u, V_t=1.0 p.u)

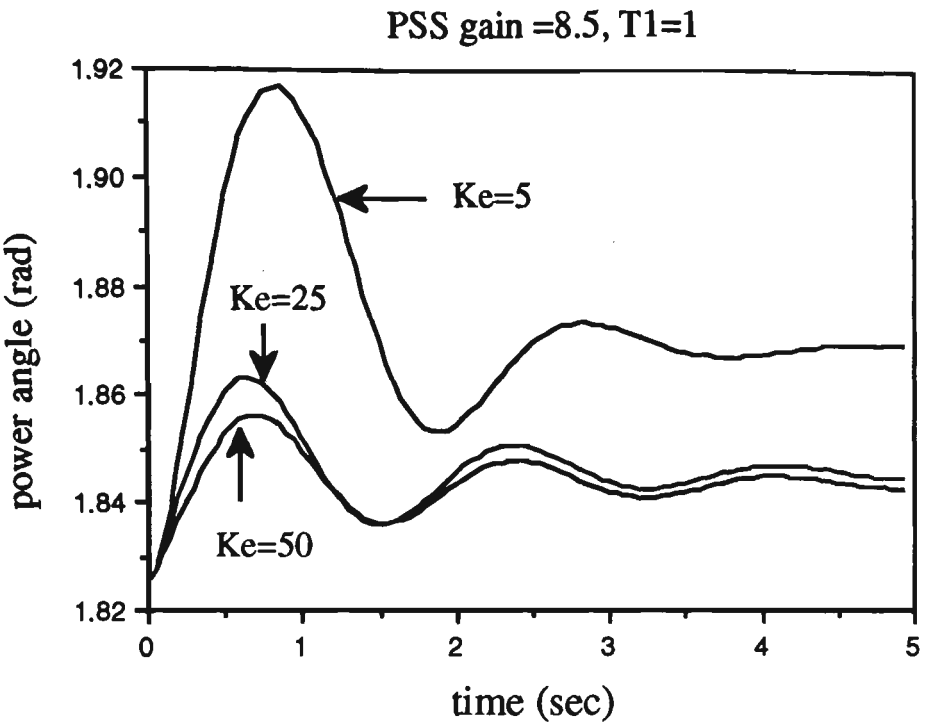

(c)

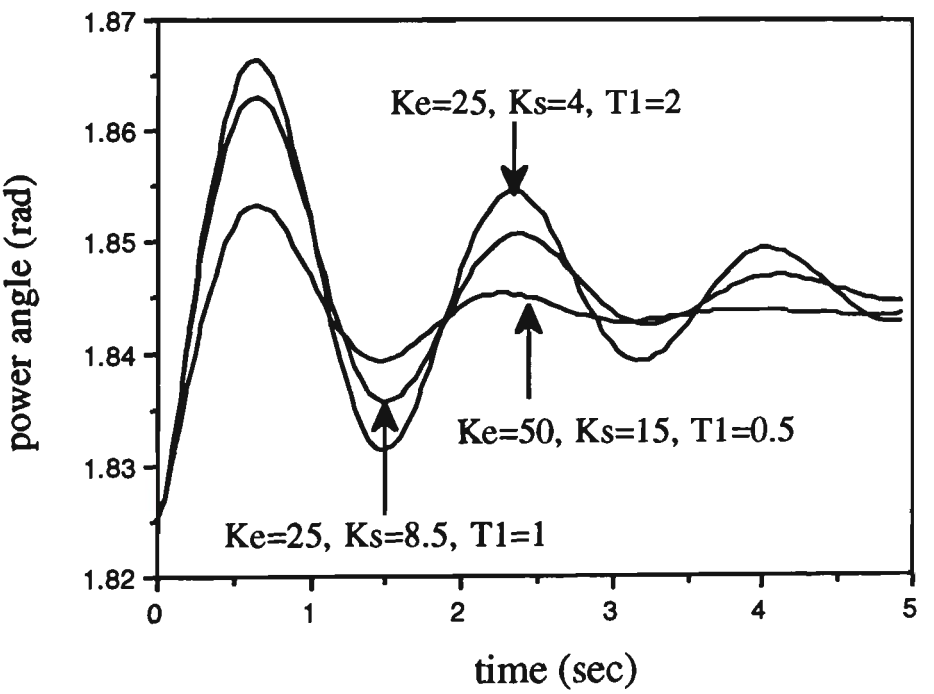

(d)

Figure 5.7: Time response of power system to 1% step change in load
(P+jQ = 1+j 0.5 p.u, X=1.0 p.u, V_t=1.0 p.u)

It is clear from Figures 5.6 (a-d) that the designed excitation control system parameters (i.e., K_e=25, K_s=8.5, T_1=1) gives the best transient performance for the initial operating point P+jQ=1+j 0.5 p.u, X=0.4 p.u, V_t=1.0 p.u. However, Figures 5.7 (a-d) show that there would be some improvements in damping of the system at new operating point (X=1.0 p.u) if the excitation control system parameters change. For instance, see Figure 5.7 (d) in which the parameters K_e=50, K_s=15 and T_1=0.5 have resulted in a better transient performance than the other cases.

Although the damping has been improved, it is still much inferior than the other operating point in which PSS has been designed. Moreover, there would be, in practice, very difficult to select the excitation control system parameters without having any information about the changes in parameters of the system unless they are identified by some means.

To cope with these changing conditions, an adaptive controller can be used such that its gain settings are automatically adjusted on-line in order to place the poles of the closed-loop system at well-damped locations.

5.4 POLE ASSIGNMENT CONTROLLER

5.4.1 Discrete model of open-loop system

Given a continuous-time system as shown in Figure 5.1, the problem is to design a digital controller which will maintain the output constant against changes in P_m. It is assumed that the open-loop continuous-time system given in Appendix VII is modelled in discrete form using the delta model as follows:

$$\Delta\delta(t_k) = \frac{B(\delta)}{A(\delta)}\Delta P_m(t_k) + \frac{C(\delta)}{A(\delta)}\Delta V_{ref}(t_k) \qquad (5\text{-}3)$$

where $\Delta\delta(t_k)$, $\Delta P_m(t_k)$ and $\Delta V_{ref}(t_k)$ are the sampled output and inputs of the system respectively. The polynomials A, B and C are given by

$$A(\delta) = \delta^3 + a_1 \delta^2 + a_2 \delta + a_3$$

$$B(\delta) = b_0 \delta^2 + b_1 \delta + b_2$$

$$C(\delta) = c_0 \delta^2 + c_1 \delta + c_2 \qquad (5\text{-}4)$$

In Chapter 3, it was shown that using the delta operator for discretization of a power system transfer function had the advantage of similarities between the coefficients of the polynomials of continuous-time and discrete-time transfer functions. As the coefficients b_0 and c_0 are zero for the continuous time system they are very small compared with b_1 and c_1 respectively for the discretised system when a short sampling time is used and can be ignored. Equations (5-4) as justified further in Section 5.4.5 (Table I) may be rewritten as:

$$A(\delta) = \delta^3 + a_1 \delta^2 + a_2 \delta + a_3$$

$$B(\delta) = b_1 \delta + b_2$$

$$C(\delta) = c_1 \delta + c_2 \qquad (5\text{-}5)$$

5.4.2 Determination of controller parameters

A supplementary excitation controller should be activated only when low-frequency oscillation begins to develop, and should be automatically terminated when the system oscillation stops so it does not interfere with steady-state operation [4]. This is achieved in a conventional stabiliser design by a washout circuit [3,4]. This circuit also has to be applied for a discrete model where the shift operator is used [32]. However, this can be ignored for the delta operator because this operator represents a

difference, it leads to models that are like models in d/dt [83]. This means that when the system is in steady-state the controller output will be zero if the numerator polynomial of the feedback controller is divisible by the delta operator (δ).

A standard feedback control law as shown in Figure 5.8 is assumed;

$$u(t_k) = - \frac{G(\delta)}{F(\delta)} \Delta\delta(t_k) \qquad (5\text{-}6)$$

where polynomials G and F are given by

$$F(\delta) = \delta^{n_f} + f_1 \delta^{n_f-1} + f_2 \delta^{n_f-2} + \ldots + f_{n_f}$$

$$G(\delta) = \delta (g_1 \delta^{n_f-1} + g_2 \delta^{n_f-2} + \ldots + g_{n_f}) \qquad (5\text{-}7)$$

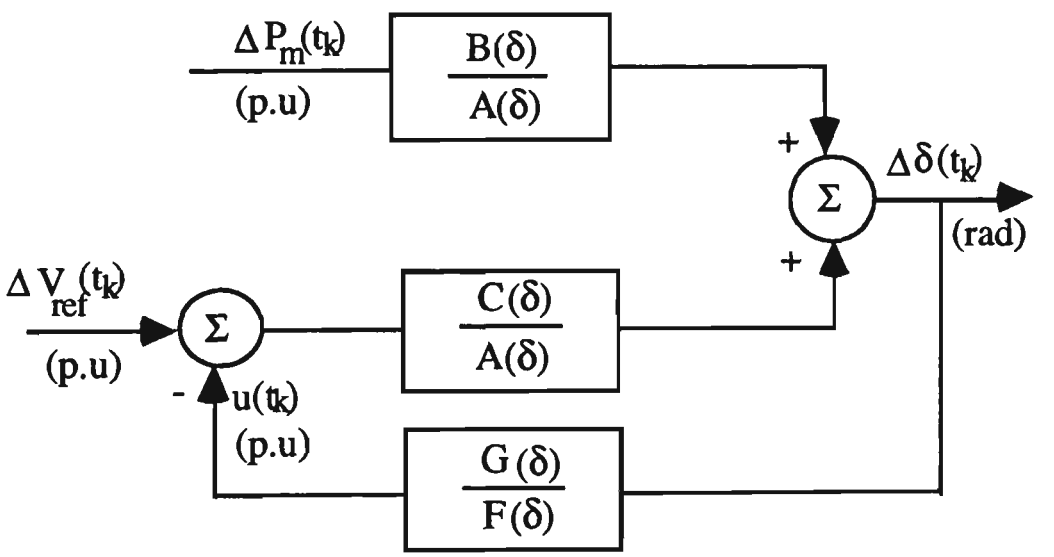

Figure 5.8: The modified block diagram with feedback controller

Substituting Equation (5-6) in (5-3) and rearranging gives

$$\Delta\delta(t_k) = \frac{BF}{AF + GC} \Delta P_m(t_k) + \frac{CF}{AF + GC} \Delta V_{ref}(t_k) \qquad (5\text{-}8)$$

For clarity, the polynomial argument δ has been dropped from Equation (5-8). This will also be the case elsewhere provided there is no

ambiguity. The next step is to choose the coefficient of G and F to satisfy the Diophantine equation:

$$AF + GC = T \tag{5-9}$$

where T is a polynomial whose roots are the desired poles of the system. There are no general guidelines on the choice of T [32,44] and a special study has to be made for each specific system as discussed further in Section 5.4.5.

Using the identity given by Equation (5-9), the closed-loop characteristics are then described by

$$\Delta\delta(t_k) = \frac{BF}{T}\Delta P_m(t_k) + \frac{CF}{T}\Delta V_{ref}(t_k) \tag{5-10}$$

Consider T in the general form:

$$T(\delta) = \delta^{n_t} + t_1\,\delta^{n_t-1} + t_2\,\delta^{n_t-2} + \ldots + t_{n_t} \tag{5-11}$$

and polynomials F and G given in Equation (5-7), where n_t and n_f are the degrees of polynomials T and F respectively. There are known coefficients of polynomial T and unknown coefficients of polynomials F and G in the right and left hand sides of Equation (5-9) respectively. It can be seen from Equations (5-7) and (5-11) that

The number of known coefficients = n_t = deg T and,

The number of unknown coefficients = 2 n_f = 2 deg F

In order to be able to solve the equations, the number of known coefficients should be equal to the number of unknown ones, that is

$$2 \text{ deg } F = \text{deg } T \tag{5-12}$$

Therefore, the degrees of polynomials G and F are obtained by solving the following equations:

$$\begin{cases} \deg A + \deg F = \deg T \\ 2 \deg F = \deg T \end{cases} \tag{5-13}$$

Considering Equations (5-5) and (5-7), solution of Equation (5-9) takes the form of

$$\begin{pmatrix} 1 & 0 & 0 & 0 & 0 & 0 \\ a_1 & 1 & 0 & c_1 & 0 & 0 \\ a_2 & a_1 & 1 & c_2 & c_1 & 0 \\ a_3 & a_2 & a_1 & 0 & c_2 & c_1 \\ 0 & a_3 & a_2 & 0 & 0 & c_2 \\ 0 & 0 & a_3 & 0 & 0 & 0 \end{pmatrix} \begin{pmatrix} f_1 \\ f_2 \\ f_3 \\ g_1 \\ g_2 \\ g_3 \end{pmatrix} = \begin{pmatrix} t_1 - a_1 \\ t_2 - a_2 \\ t_3 - a_3 \\ t_4 \\ t_5 \\ t_6 \end{pmatrix} \tag{5-14}$$

Equation (5-14) can be written as

$$M X = P \tag{5-15}$$

The solution of Equation (5-15) is

$$X = M^{-1} P \tag{5-16}$$

where the elements of matrix X are the coefficients of polynomials F and G. It is to be noted that since polynomials A and C have no common factors, the inverse of matrix M always exists [32,81].

5.4.3 Estimation of plant transfer functions

There are two methods for estimating the parameters of the open-loop system shown in Figure 5.1 and given by Equation (5-5), as illustrated below. Since the voltage reference, in practice, does not change very often [45], ΔV_{ref} is assumed to be zero in the following discussion of the

effect of load disturbances. This will also be the case for the multimachine system given further in Section 6.5.

5.4.3.1 Estimation of $G_d(s)= \frac{BF}{T}$

System identification can be performed by measuring the changes in power angle ($\Delta\delta$), accelerating power ($\Delta P_m = P_a = P_m - P_e$) and power swings ($\Delta P_d$) as shown in Figure 5.9 and explained in Section 2.3.

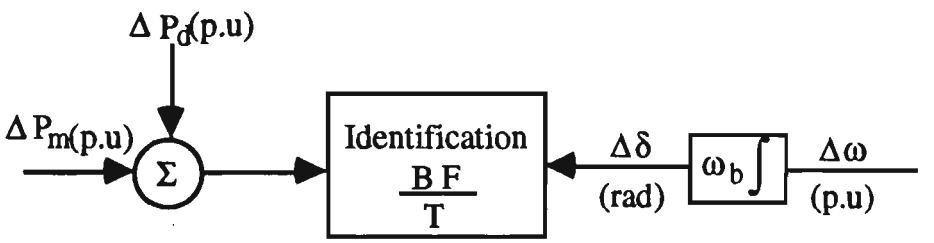

Figure 5.9: The identification block diagram

As explained in Section 1.4.2 the closed-loop system will be first estimated because the open-loop signals cannot be measured freely in this control design. The next step is to derive the coefficients of polynomials A and C. Let the identified denominator polynomial of the closed-loop system be as

$$T' = \delta^6 + t'_1\,\delta^5 + t'_2\,\delta^4 + \ldots + t'_6 \qquad (5\text{-}17)$$

By considering Equation (5-14) it will be seen that

$$\begin{pmatrix} a'_1 \\ a'_2 \\ a'_3 \\ c'_1 \\ c'_2 \end{pmatrix} = \begin{pmatrix} 1 & 0 & 0 & 0 & 0 \\ f_1 & 1 & 0 & g_1 & 0 \\ 0 & 0 & f_3 & 0 & 0 \\ 0 & f_3 & f_2 & 0 & g_3 \\ f_3 & f_2 & f_1 & g_3 & g_2 \end{pmatrix}^{-1} \begin{pmatrix} t'_1 - f_1 \\ t'_2 - f_2 \\ t'_6 \\ t'_5 \\ t'_4 \end{pmatrix} \qquad (5\text{-}18)$$

where a'_1, a'_2, a'_3, c'_1 and c'_2 are the coefficients of polynomials A and C at the new operating point. It should be mentioned that the controller

parameters will be fixed during the identification process, leaving the closed-loop system to perform its normal excitation control function. When the open-loop system parameters converge to their new values, the controller parameters are changed using Equation (5-16).

5.4.3.2 Estimation of $G_c(s)= \frac{CF}{T}$

System identification may be done by adding a sequence of pseudorandom noise ($\zeta(t_k)$) as shown in Figure 5.10. Equation (5-18) can also be used for obtaining the coefficients of polynomials A and C at the new operating point.

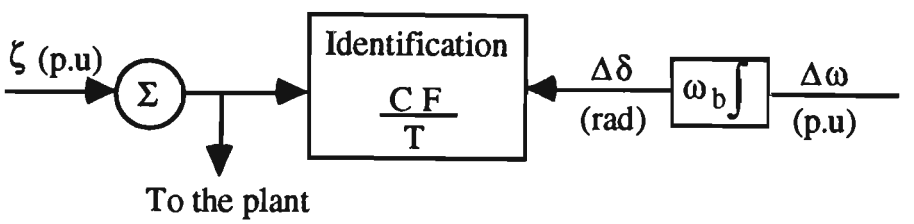

Figure 5.10: The identification block diagram

Among two methods of estimation given above, the first one, in which the transfer function $G_d(s) = \frac{BF}{T}$ is estimated, has been used here because there is no need to insert an additional disturbance into system.

The steps involved in PA controller design are summarised as follows;

(i) The linearized model of Figure 2.1 is rearranged in the modified block diagram as shown in Figure 5.8.

(ii) At each sample interval, the coefficients of polynomials A and C are estimated by recursive least-squares method using the delta operator.

(iii) Compute the control which will then place poles to preselected locations.

5.4.4 Sampling time selection

The sampling time has to be chosen sufficiently fast to enable the poles of G_d to be identified accurately. These will be the poles of the chosen polynomial T when the controller is working correctly. As will be illustrated further in simulation results the pole -20 will be the best choice for desirable polynomial T in power system. This polynomial will be tested on different power systems. The gain characteristics of $20^6/T$, in which $T=(s + 20)^6$, is shown in Figure 5.11 suggesting that the sampling time should be $\frac{2\ \pi}{50\ X\ 7}$ = 0.018 sec. Referring to Equation (3-21) in Section 3.4.2 and using sampling time of 0.02 sec it will be seen that

$$0.75\ e^{-2\ x\ 20\ x\ 0.02} - 2\ e^{-20\ X\ 0.02} \cos(0\ x\ 0.02) = -1.004 < -1$$

confirming the necessity of using the delta model.

It is also to be noted that the sampling time must be sufficient to determine the poles of G_d when the system is uncontrolled to allow the controller to begin its operation when first commissioned. These poles belong to the polynomial A shown in Figure 5.8. These poles have been examined for a wide range of operating points and confirm that sampling time of 20 ms will be satisfactory.

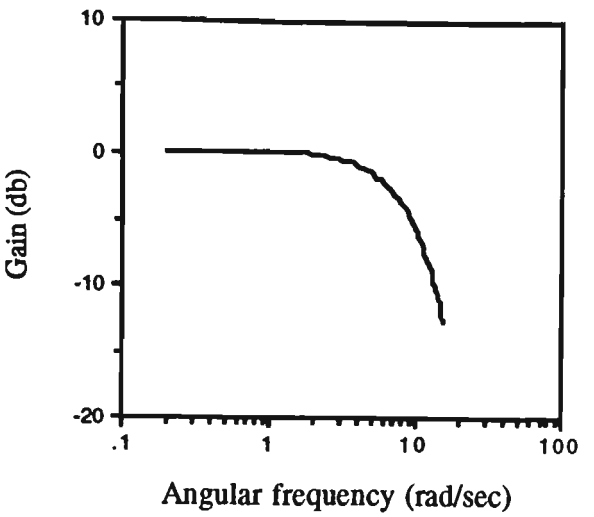

Figure 5.11: The gain characteristics of $20^6/T$

5.4.5 Choice of T

Simulation studies were performed on the excitation control system given in Section 5.3.1 with the generator modelled by a set of non-linear differential equations based on Park's equations [4,101]. For analysis purposes the system is represented by the transfer function given by Equations (5-4). The coefficients of transfer functions in both continuous-time and discrete-time systems are given in Table I for the initial operating point (X=0.4 p.u).

Table I shows that the discrete-time coefficients c_0 and b_0 are much smaller than c_1 and b_1 respectively and can be ignored as described in Section 5.4.1.

Table I

Parameters	a_1	a_2	a_3	b_0	b_1	b_2	c_0	c_1	c_2
Continuous-time system	3.9	130	365	0	125	333	0	0	-722
Discrete-time system	5.31	135	348.	0.5	125.8	319	-.05	-13.9	-691

Five different polynomials with their equivalent delta models were considered for T as follows:

(i) $(s + 10)^6$, $(\delta + 9.06)^6$

(ii) $(s + 20)^6$, $(\delta + 15.48)^6$

(iii) $(s + 30)^6$, $(\delta + 22.56)^6$

(iv) $(s^2 + 12.56\, s + 79.21)^3$, $(\delta^2 + 12.52\, \delta + 69.86)^3$

(v) $(s^2 + 25.7\, s + 317)^3$, $(\delta^2 + 25\, \delta + 245.3)^3$

Choosing any polynomial having the roots with a real part less than 10 gives a slower settling time than the fixed gain stabiliser and has not been investigated. It will be also shown that any polynomial with a real part more than 20 (say, 30) does not provide a better damping characteristics.

The power angle variation of the system for a 1% step change in load was obtained for different polynomials T and graphed in Figure 5.12 showing that the best choice of the polynomials is case (ii) as it gives a smaller overshoot and a fast settling time.

In order to see whether or not the polynomial $(s+20)^6$ can be used more generally, the same polynomials were tested for a variety of power systems which include a hydro system with a high inertia [3] and a thermal unit with a medium inertia (see Appendix V). Figures 5.13 (a), (b) and (c) show the changes in power angle following a 1% step change in load. Referring to the graphs shown in Figures 5.13 $(s+20)^6$ appears as a suitable choice in general for the polynomial T.

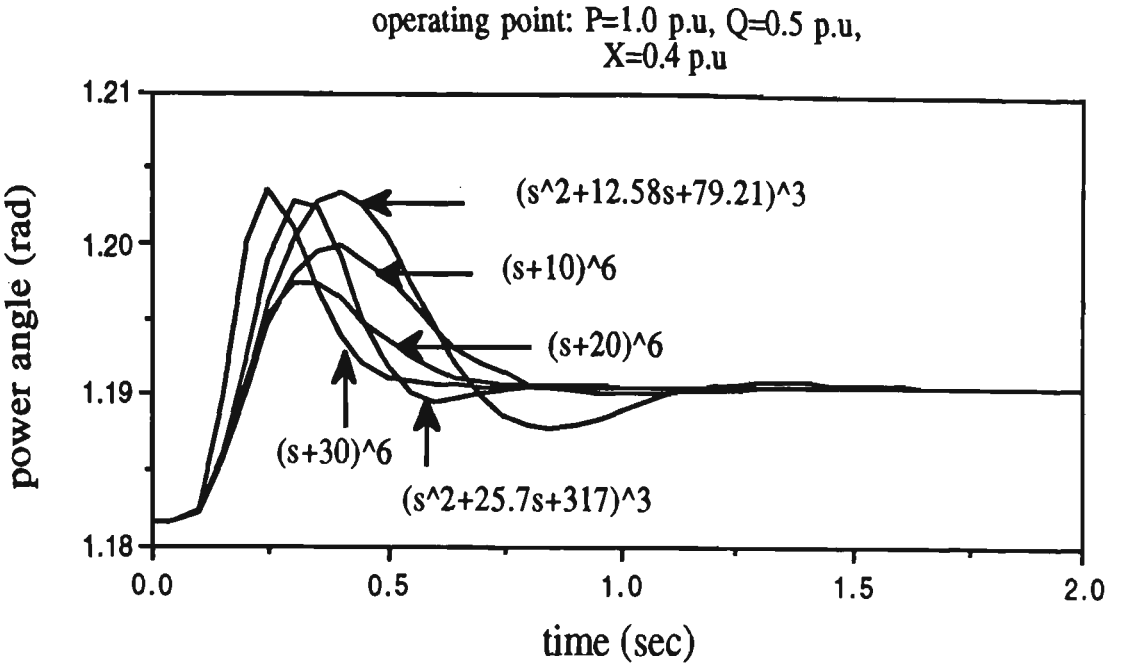

Figure 5.12: Time response of the system to a 1% step change in load

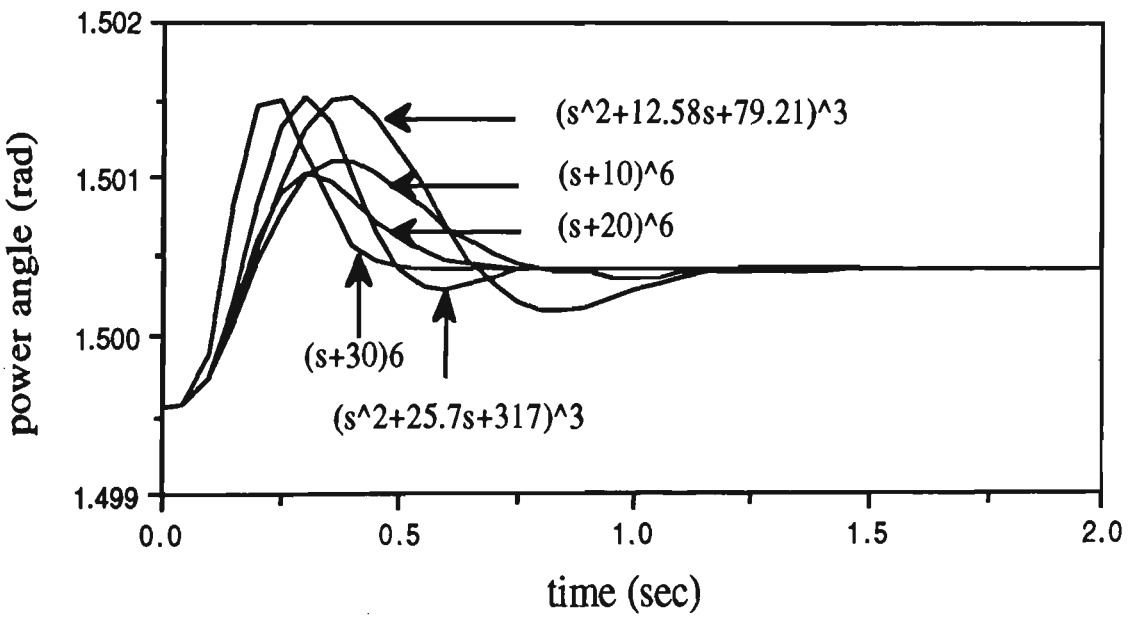

Figure 5.13 (a): Time response of the system to a 1% step change in load for Australian system

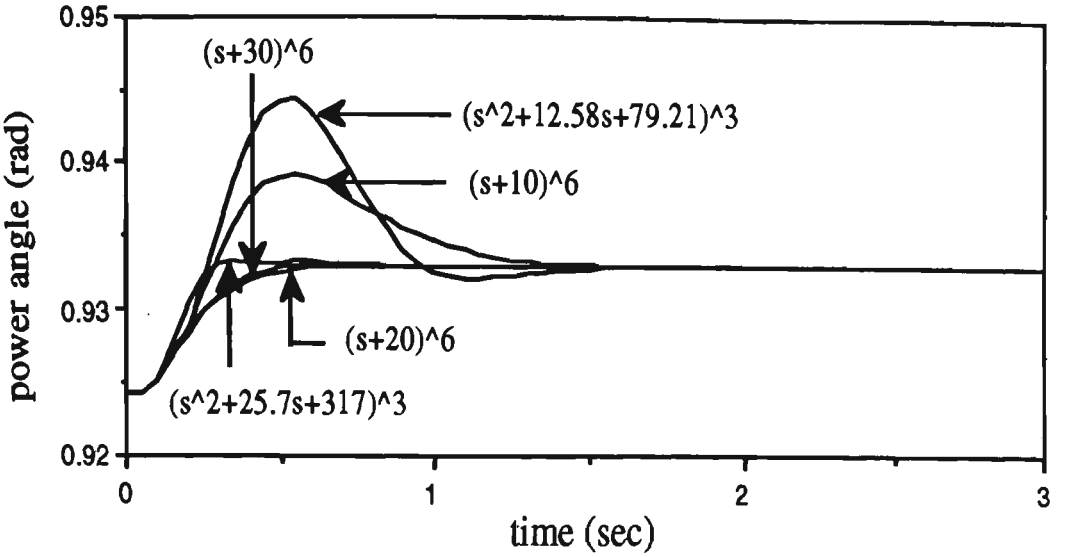

Figure 5.13 (b): Time response of the system to a 1% step change in load for Hydro system (reactance line = 0.4 p.u)

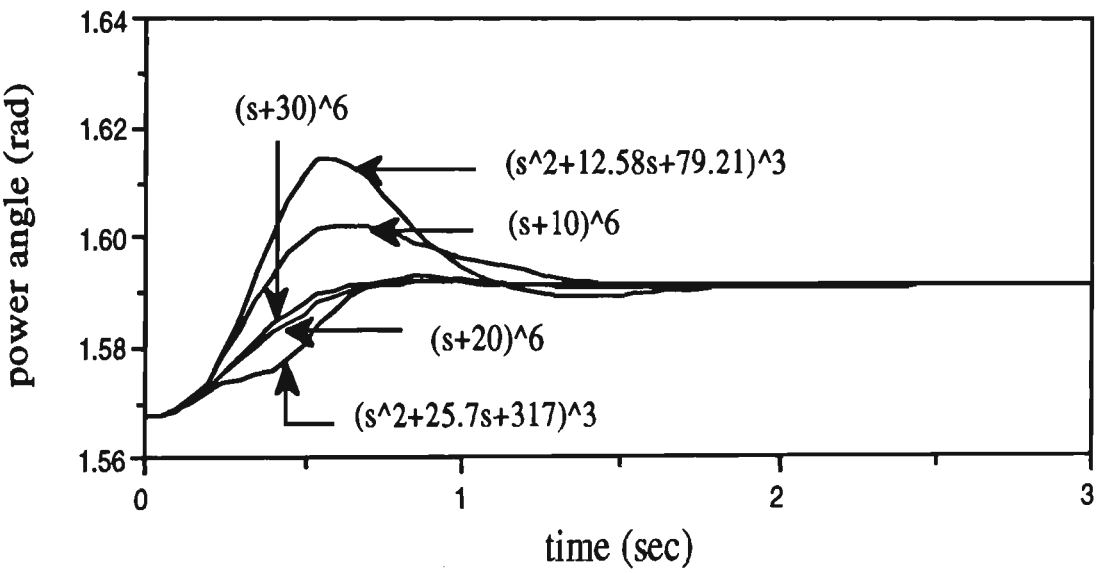

Figure 5.13 (c): Time response of the system to a 1% step change in load for Hydro system (reactance line = 1.0 p.u)

5.4.6 Comparison with fixed gain stabiliser

The power angle variation following a 1% step change in load is shown in Figure 5.14 where the PA stabiliser is compared with fixed gain

stabiliser deriving its input from rotor speed as designed in Section 5.3.1. The effect of both stabilisers on voltage regulator action following a 1% step change in voltage reference is also obtained and shown in Figure 5.15. It can be seen from Figures 5.14 and 5.15 that although PA controller is a little inferior in overshoot than a fixed gain stabiliser, it has faster settling time. The behaviour of the identified parameters are given in Figures 5.16 (a) and (b) showing a fast parameter convergence.

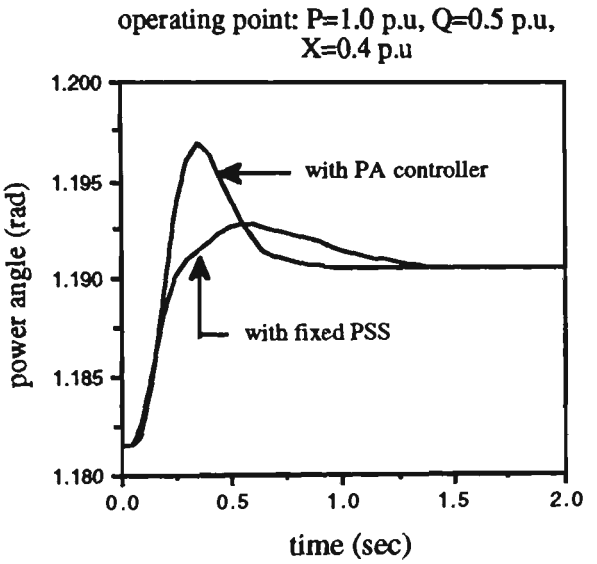

Figure 5.14 Power angle variation following a 1% step change in load

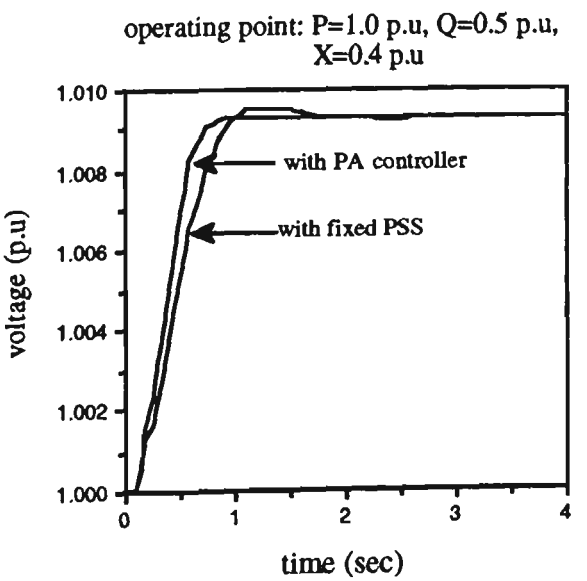

Figure 5.15 The changes in terminal voltage following a 1% step change in voltage reference

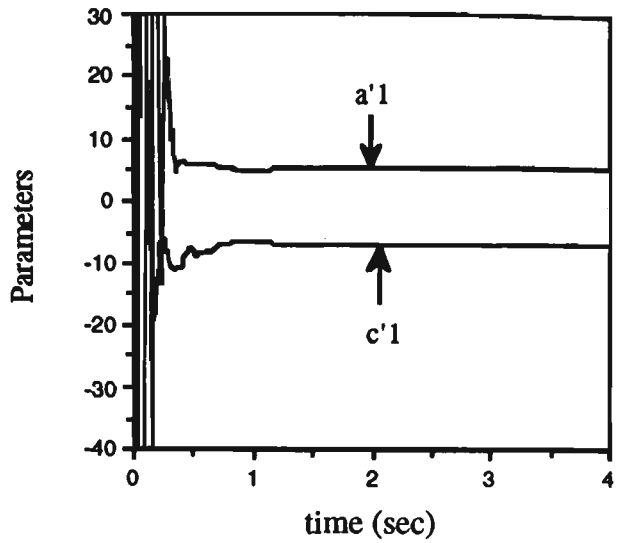

(a)

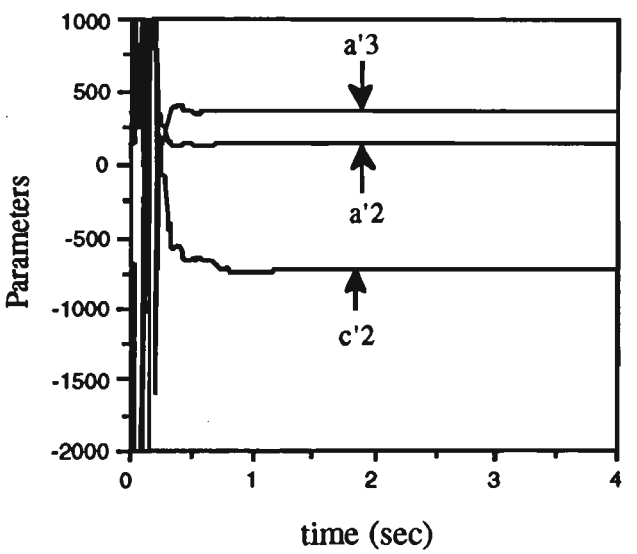

(b)

Figure 5.16: Parameter convergence

As shown earlier a fixed "parameter" PSS does not provide an acceptable response as the operating point changes. The behaviour of the power angle for two other different operating points following a 1% step change in load is shown in Figures 5.17 and 5.18. The effect of the controllers on voltage regulator action following a 1% step change in voltage reference is also shown in Figures 5.19 and 5.20 for both operating

points. As can be seen from Figures 5.17 to 5.20, the PA controller has much faster settling time than the fixed gain stabiliser.

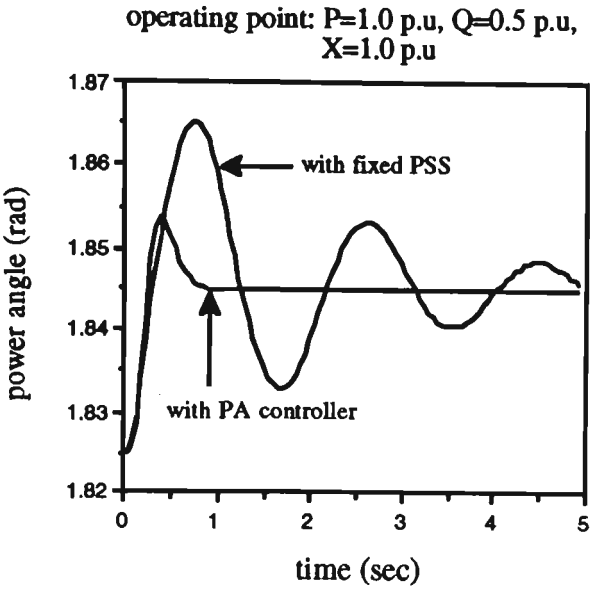

Figure 5.17: Power angle variation following a 1% step change in load

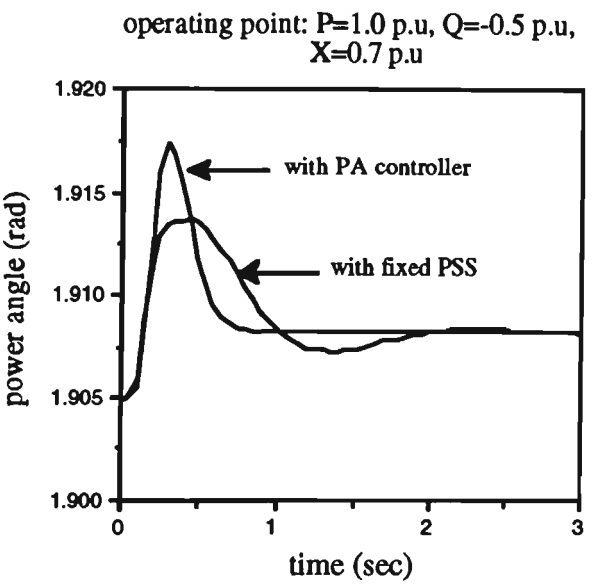

Figure 5.18: Power angle variation following a 1% step change in load

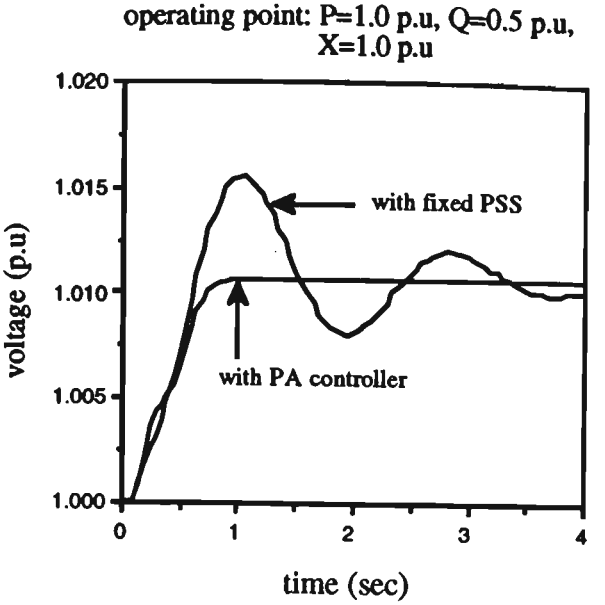

Figure 5.19: The changes in terminal voltage following a 1% step change in voltage reference

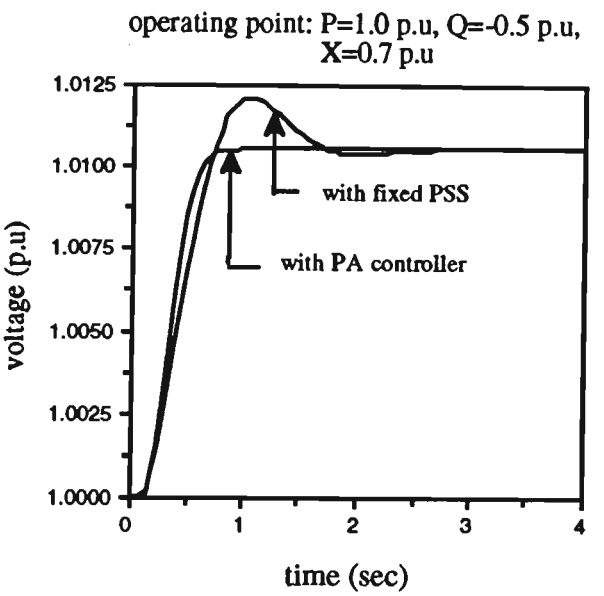

Figure 5.20: The changes in terminal voltage following a 1% step change in voltage reference

For large disturbance studies in order to restrict the level of generator terminal voltage fluctuations during transient conditions, limits are imposed on the controller output. It has been suggested by Kundur, et al [3] that the controller output be limited by a limiter in the range of [-0.1,0.2] p.u and this limiter will be also used here. Figure 5.21 shows

the time response of the system to a three phase fault close to generator bus with a successful reclosure. The controller output is also shown in Figure 5.22.

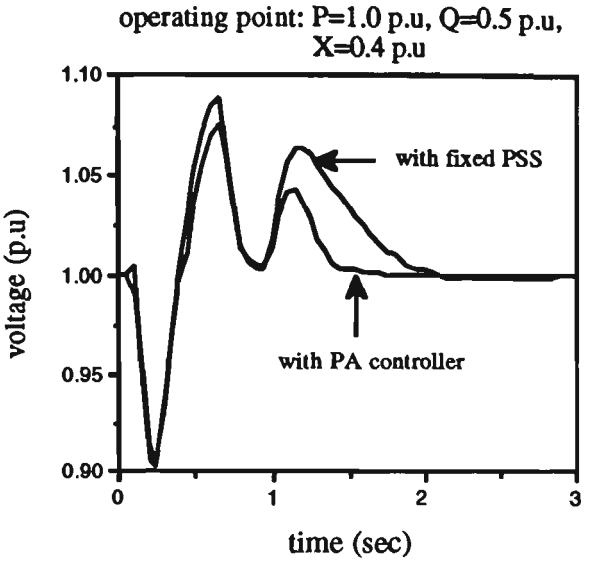

Figure 5.21: Time response of the system to a 3ϕ fault

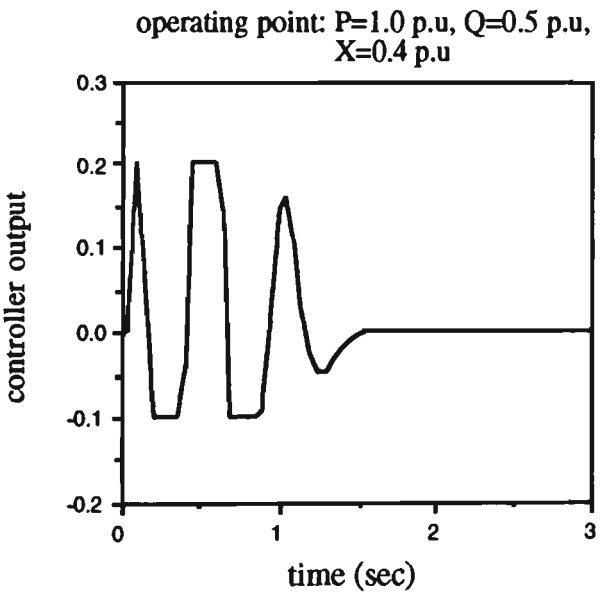

Figure 5.22: Controller output following a 3ϕ fault

It can be seen from Figure 5.21 that the PA controller gives a faster settling time than the conventional stabiliser.

The performance of the system is now examined for the case where the excitation system is shown by K_e. Figure 5.23 shows the time response

of this model with the case where the excitation system is $[K_e/(1+ T_e s)]$ to a 1% step change in load.

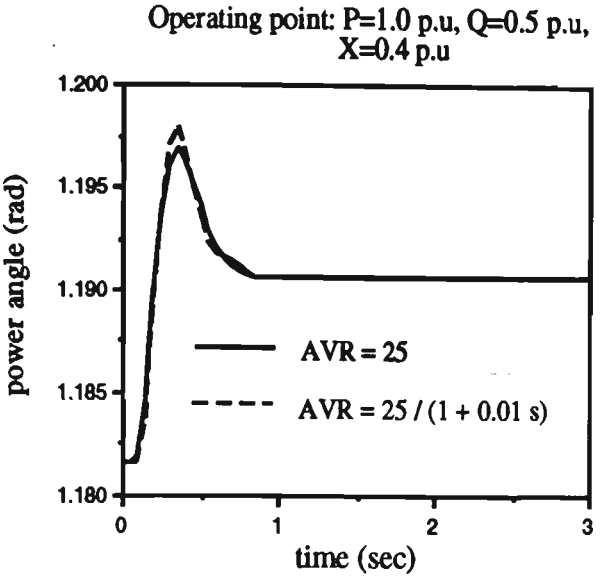

Figure 5.23 : Power angle variation following a 1% step change in load

As can be seen from Figure 5.23 both excitation system models provide a very close damping characteristics.

5.4.7 Stability of feedback controller

It is important to check whether the feedback controller is stable or not. The roots of the polynomial F for a wide range of operating points taken from [3] are given in Table II. The polynomial F has roots in the left hand side of the delta-plane confirming its stability for all cases. Therefore, with suitable choice for the roots of the polynomial T closed-loop stability can be guaranteed.

Table II

P + jQ (p.u)	X=0.1 p.u	X=0.4 p.u	X=0.7 p.u	X=1.0 p.u
0.5+j0.0	-23.56±j45.58 -45.52	-24.58±j35.71 -43.46	-24.72±j35.38 -43.3	-24.64±j35.62 -43.56

Table II (continued)

P + jQ (p.u)	X=0.1 p.u	X=0.4 p.u	X=0.7 p.u	X=1.0 p.u
1.0+j0.5	-24.36±j32.31 -42.83	-25.98±j27.2 -40.61	-25.55±j32.07 -42.27	-24.82±j40.82 -44.42
1.0-j0.5	-22.8±j49.24 -45.13	-25.06±j29.2 -41.63	-27.9±j24.26 -38.96	-29.18±j22 -37.07

5.5 CONCLUSIONS

The small disturbance stability characteristics of a single machine infinite bus system have been studied by means of a transfer function relating power angle to mechanical power disturbance. It has been shown that although fixed gain PSS improves the damping of the system for one operating point, the damping diminishes as operating point changes. The Pole Assignment adaptive stabiliser has been shown to enhance the damping of the power system for all operating points. The design of the controller has been simplified by the use of the delta operator form of transfer function. It gives an order reduction in the numerator of the open-loop system which helps to reduce the computation burden. The delta operator also allows to ignore the use of the washout circuit. A particular choice of poles has been shown to give a good response over a wide range of operating points for different generator inertias. Comparative results showed that the adaptive controller based on a low order model of the open-loop system where the excitation system had been considered by a dc gain would provide a desirable damping characteristics when applied to the actual open-loop system.

CHAPTER 6

Chapter 6

MODEL REFERENCE ADAPTIVE CONTROLLER

6.1 INTRODUCTION

In Chapter 5 an adaptive Pole Assignment controller was demonstrated. In this algorithm, the desired system closed-loop poles are specified and the updating of the controller parameters is based on explicit system identification. It was shown that by using this method the settling time of the system was fixed over a wide range of operating points.

In all STR techniques there is no effort to fix the zeros of the closed-loop system and, therefore, the system response is somewhat variable. This problem can be resolved by modifying the PA controller such that the location of both the zeros and the poles of a particular transfer function is specified. This chapter describes the derivation of a new type of Model Reference Adaptive Controller (MRAC) using the delta operator achieving this. The usual approach in the MRAC is to adjust the parameters of the regulator in such a way that the error between the controlled plant output and that of the model converges to zero. However, in the MRAC given in this work controller parameters are so designed that the poles and zeros of the closed-loop system transfer function ($G_d(s)$) are located at preselected locations using an explicit system identification without the need to compare the actual plant and the model outputs. Controller design is simplified based on a continuous-time control strategy by the use of the delta operator rather than the shift

operator. It will be shown that this adaptive controller provides a better damping characteristic than the Pole Shifting adaptive controller or a fixed gain stabiliser.

In Chapter 3 it was shown that there was a close resemblance between the coefficients of the continuous-time and discrete-time systems when the delta operator was used instead of the shift operator. This allows one to ignore sampling zeros arising in discretization and, therefore, the order of polynomials in both denominators and numerators of continuous-time and discrete-time system transfer functions will be the same. It will be shown that this advantage allows the designer to use a more simplified MRAC with an approximate discrete model. This in turn reduces the number of controller parameters to be identified. Comparative results for a multimachine power system (two-machine case) will be given for the adaptive stabiliser and for a fixed parameter stabiliser. The results clearly show the benefit of the proposed adaptive stabiliser to enhance the damping of the system, especially where the operating point changes.

6.2 MODEL REFERENCE ADAPTIVE CONTROLLER

6.2.1 Adaptive controller scheme

The philosophy of the design in this approach is to select the poles and zeros of the closed-loop system in such a manner that the specifications for steady-state accuracy as well as a good transient response are satisfied. A compensator is then designed to force the closed-loop system to have this transfer function. The transfer function to be considered here is $G_d(s) = \frac{\Delta\delta}{\Delta P_m}$. In Chapter 5 it was shown that the dynamic stability of the power system could be readily analysed by using this

transfer function. The general scheme of the controller that will achieve this is shown in Figure 6.1, in which ΔP_m, ΔV_{ref} and $\Delta\delta$ are the changes in load, voltage reference and power angle respectively. The choice of a common denominator F(s) in the two controller blocks gives full scope to modify $G_d(s)$ with the minimum number of adjustable controller parameters. This needs a slight modification when a discrete-time mathematical model is used instead of the continuous-time system as will be discussed in Section 6.2.3.

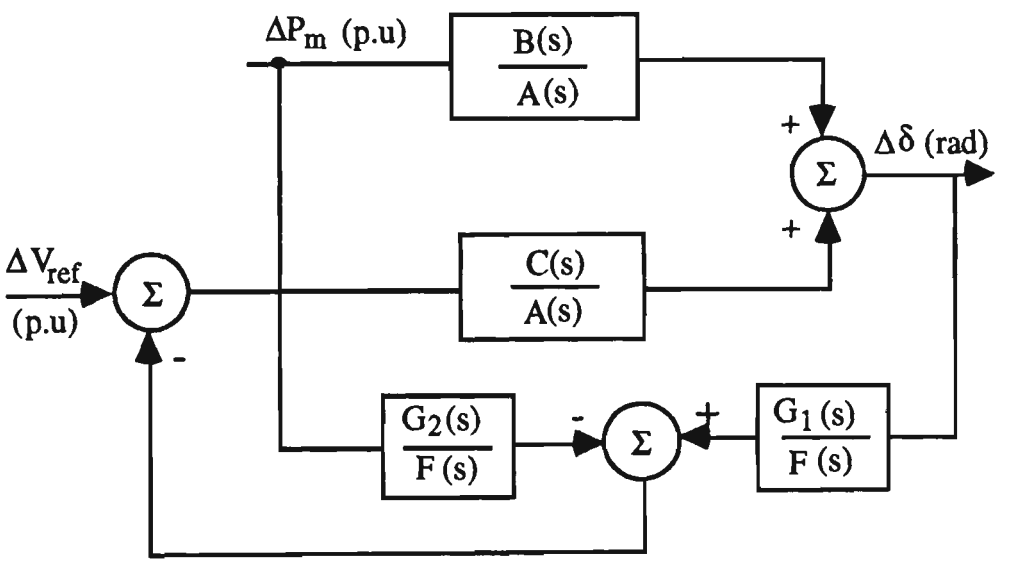

Figure 6.1: Block diagram of the proposed closed-loop system

Using Superposition, one can obtain

$$\Delta\delta = \frac{BF + G_2C}{AF + G_1C}\Delta P_m + \frac{CF}{AF + G_1C}\Delta V_{ref} \qquad (6\text{-}1)$$

For clarity, the polynomial argument s has been dropped from Equation (6-1). The polynomials F, G_1 and G_2 will be given further.

Considering the desired closed-loop transfer function as $G_d(s)=\frac{\Delta\delta}{\Delta P_m} = \frac{R}{T}$

and Equation (6-1) imply that:

$$\begin{cases} B\ F + G_2\ C = R \\ A\ F + G_1\ C = T \end{cases} \qquad (6\text{-}2)$$

Since deg $G_1 \leq$ deg F, deg C < deg A and deg B = deg A - 2 (see equations given in Appendix VII), it follows that

deg AF = deg (AF + G_1C) = deg T and,

deg BF = deg (BF + G_2C) = deg R.

Note that deg C < deg B and deg G_2 < deg F. Hence

deg T - deg R = deg A - deg B = 2.

Moreover, since B(s) = $b_1 s + b_2$ (see equations given in Appendix VII) and the first coefficient of polynomial F as will be shown further is 1, the first coefficient of polynomial R should also be a constant value of $b_1 = \frac{1}{M}$ (see Equation (6-2), in which the polynomial B is multiplied by the polynomial F in the numerator of $G_d(s)$) where M is the inertia constant of the machine. Therefore, the forms of polynomials R and T will be;

$$R(s) = b_1\, s^{n_t-2} + r_1\, s^{n_t-3} + \ldots + r_{n_t-2}$$

$$T(s) = s^{n_t} + t_1\, s^{n_t-1} + t_2\, s^{n_t-2} + \ldots + t_{n_t} \qquad (6\text{-}3)$$

6.2.2 Choice of a desirable closed-loop transfer function

The purpose of this design is to choose a closed-loop transfer function which gives a desirable response. The design begins with the selection of a conventional second-order transfer function having a desirable

characteristic. This will be modified to a higher order to match Equations (6-2) and (6-3).

Consider, for example, a conventional second-order system as

$$\frac{\omega_n^2}{s^2 + 2\zeta\omega_n s + \omega_n^2} \qquad (6\text{-}4)$$

Suppose that Equation (6-4) should have desirable characteristics as follows;

$$t_p = 0.25 \text{ sec}, \zeta = 0.707$$

where t_p and ζ are the time required to reach the first peak and damping ratio respectively.

Considering the equation

$$t_p = \frac{\pi}{\omega_n \sqrt{1 - \zeta^2}} \qquad (6\text{-}5)$$

leads to the following transfer function.

$$\frac{317}{s^2 + 25.7\, s + 317} \qquad (6\text{-}6)$$

The dc gain of the system changes when the operating point changes. Therefore, Equation (6-6) needs to be premultiplied by the dc gain of the system which is 0.91 for the power system example given in Section 5.3.1.

$$\frac{0.91 \text{ X } 317}{s^2 + 25.7\, s + 317} \qquad (6\text{-}7)$$

As explained earlier a first degree polynomial $B(s) = b_1 s + b_2$ is multiplied by the polynomial F in Equation (6-2). This implies that

regardless of the degree of the polynomial F there would be one additional zero and this should be added to Equation (6-7) in the form:

$$(b_1 s + \beta)$$

Combining Equations (6-7) and the above additional polynomial results in:

$$\frac{R}{T} = \frac{0.91 \text{ X } 317 (b_1 s + \beta)}{(s^2 + 25.7 s + 317)} \qquad (6\text{-}8)$$

In order to keep the first coefficient of the polynomial R as b_1 (see Equation (6-3)), Equation (6-8) should be modified:

$$\frac{R}{T} = \frac{0.91 \text{ X } 317 (\frac{b_1}{0.91 \text{ X } 317} s + \beta)}{(s^2 + 25.7 s + 317)(s + \beta)} \qquad (6\text{-}9)$$

The polynomial $(s + \beta)$ was added to the denominator in Equation (6-9) because the degree difference between denominator and numerator should be equal to 2. The step response of the transfer function given in Equation (6-9) has been calculated for three different values of $\beta = 5$, 13 and 20 and the results are shown in Figure 6.2. It can be seen from Figure 6.2 that the best choice for β is 13 because it has less overshoot and faster settling time in comparison with the other cases. In fact $\beta = 13$ is very close to the real part of the conjugate poles $(-12.85 \pm j12.33)$ of the second-order transfer function given in Equation (6-6).

It will be shown further in Section 6.2.5 that the desirable closed-loop transfer function has degree of more than 1 and 3 for the numerator and denominator respectively. Therefore, some poles and zeros should be added to Equation (6-9). In order to have the required characteristics, the same poles and zeros are used so that they cancel each other:

$$\frac{R}{T} = \frac{0.91 \text{ X } 317 \left(\frac{b_1}{0.91 \text{ X } 317} s + \beta\right)}{(s^2 + 25.7\, s + 317)(s + \beta)} \text{ X } \frac{(s + \eta)^n}{(s + \eta)^n} \qquad (6\text{-}10)$$

Choice of η should result in a stable feedback controller and this will be explored further using simulation results.

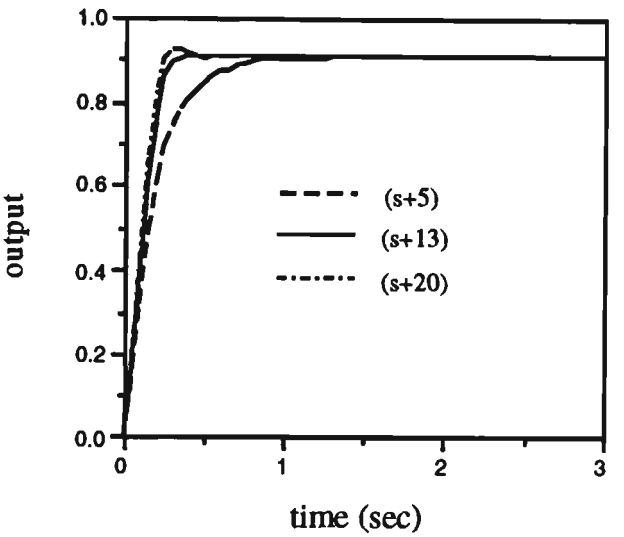

Figure 6.2 : Step response of Equation (6-9) for three different cases

6.2.3 Determination of controller parameters

Digital devices are normally used to implement adaptive control algorithms. Thus, the computations are done in discrete-time. The same discrete-time transfer functions of Equations (5-5) are also used here. Because the delta model is used for discretization the degrees of polynomials in both the continuous and discrete models of the transfer function $G_d(s)$ are the same, i.e., n(A) = n(T) and n(R) = n(B) where n(.) shows the degree of the polynomial (see Equations (5-5) and (6-9)). This enables the form of desirable transfer function used for continuous-time system to be used in the discrete-time system as well. It should be

mentioned that such an assumption will be impossible if the shift operator is used.

The polynomials F, G_1 and G_2 are chosen in the form of

$$F(\delta) = \delta^{n_f} + f_1 \delta^{n_f-1} + f_2 \delta^{n_f-2} + \ldots + f_{n_f}$$

$$G_1(\delta) = \delta (g_1 \delta^{n_f-1} + g_2 \delta^{n_f-2} + \ldots + g_{n_f})$$

$$G_2(\delta) = \delta (g'_1 \delta^{n_f-2} + g_2 \delta^{n_f-3} \ldots + g'_{n_f-1}) \qquad (6\text{-}11)$$

The degree of polynomial G_2 is less than the degree of polynomial G_1 in Equation (6-11) because if the same form of polynomial G_1 is used, that is

$$G'_2(\delta) = \delta (g'_1 \delta^{n_f-1} + g'_2 \delta^{n_f-2} + \ldots + g'_{n_f}) \qquad (6\text{-}12)$$

this implies that

$$b_1 + c_1 g'_1 = b_1 \qquad (6\text{-}13)$$

where b_1 is the first coefficient of polynomial R in Equation (6-3). Equation (6-13) will be satisfied if and only if g'_1 is always equal to zero and this cannot be true.

The next step is to choose the coefficients of F, G_1 and G_2 such that the Diophantine equations (6-2) are satisfied. The degrees of polynomials F, G_1 and G_2 can be obtained by solving the following equations:

$$\begin{cases} \deg A + \deg F = \deg T \\ 3 \deg F - 1 = 2 \deg T - 3 \end{cases} \qquad (6\text{-}14)$$

For clarity, the polynomial argument δ has been dropped from Equation (6-14). This will also be the case elsewhere provided there is no ambiguity. The second relationship in Equation (6-14) shows the number

of the unknown coefficients to be calculated and has been determined using the same procedure as given in Section 5.4.2. By keeping the dc gain of the system constant (dc gain = $\frac{r_{n_{t-2}}}{t_{n_t}}$), the number of known coefficients will be reduced from (2 deg T-2) to (2 deg T -3).

By considering Equations (5-5) and (6-11), the solution of Equation (6-2) takes the form of

$$\begin{pmatrix} 1 & 0 & 0 & 0 & 0 & 0 & 0 & 0 & 0 & 0 & 0 \\ a_1 & 1 & 0 & 0 & c_1 & 0 & 0 & 0 & 0 & 0 & 0 \\ a_2 & a_1 & 1 & 0 & c_2 & c_1 & 0 & 0 & 0 & 0 & 0 \\ a_3 & a_2 & a_1 & 1 & 0 & c_2 & c_1 & 0 & 0 & 0 & 0 \\ 0 & a_3 & a_2 & a_1 & 0 & 0 & c_2 & c_1 & 0 & 0 & 0 \\ 0 & 0 & a_3 & a_2 & 0 & 0 & 0 & c_2 & 0 & 0 & 0 \\ 0 & 0 & 0 & a_3 & 0 & 0 & 0 & 0 & 0 & 0 & 0 \\ b_1 & 0 & 0 & 0 & 0 & 0 & 0 & 0 & c_1 & 0 & 0 \\ b_2 & b_1 & 0 & 0 & 0 & 0 & 0 & 0 & c_2 & c_1 & 0 \\ 0 & b_2 & b_1 & 0 & 0 & 0 & 0 & 0 & 0 & c_2 & c_1 \\ 0 & 0 & b_2 & b_1 & 0 & 0 & 0 & 0 & 0 & 0 & c_2 \end{pmatrix} \begin{pmatrix} f_1 \\ f_2 \\ f_3 \\ f_4 \\ g_1 \\ g_2 \\ g_3 \\ g_4 \\ \dot{g}_1 \\ \dot{g}_2 \\ \dot{g}_3 \end{pmatrix} = \begin{pmatrix} t_1 - a_1 \\ t_2 - a_2 \\ t_3 - a_3 \\ t_4 \\ t_5 \\ t_6 \\ t_7 \\ r_1 - b_1 \\ r_2 \\ r_3 \\ r_4 \end{pmatrix} \qquad (6\text{-}15)$$

Equation (6-15) can be written as

$$N X = Y \qquad (6\text{-}16)$$

The solution of Equation (6-16) is

$$X = N^{-1} Y \qquad (6\text{-}17)$$

where X gives the controller parameters.

Equation (6-17) cannot be solved because matrix N is singular. The singularity may be realised by considering Equation (6-18) which has been obtained by combining the equations of Equation (6-2).

$$ACG_2 - BCG_1 = AR - BT \qquad (6\text{-}18)$$

It can be seen from the Diophantine equation (6-18) that there is a common factor (polynomial C) in the left hand side only. This shows that there would be no solution for the adaptive controller unless it is modified [81]. Notice that there is no such problem with the continuous-time system shown in Figure 6.1 because polynomial C is a pure number (see equations given in Appendix VII). The solution for the discrete-time model is to replace polynomial $C(\delta) = c_1\delta + c_2$ by the constant coefficient c_2 in the second equation of Equation (6-2) ensuring that there is no common factor in the left hand side of Equation (6-18). This can be obtained by modifying the adaptive control scheme as shown in Figure 6.3.

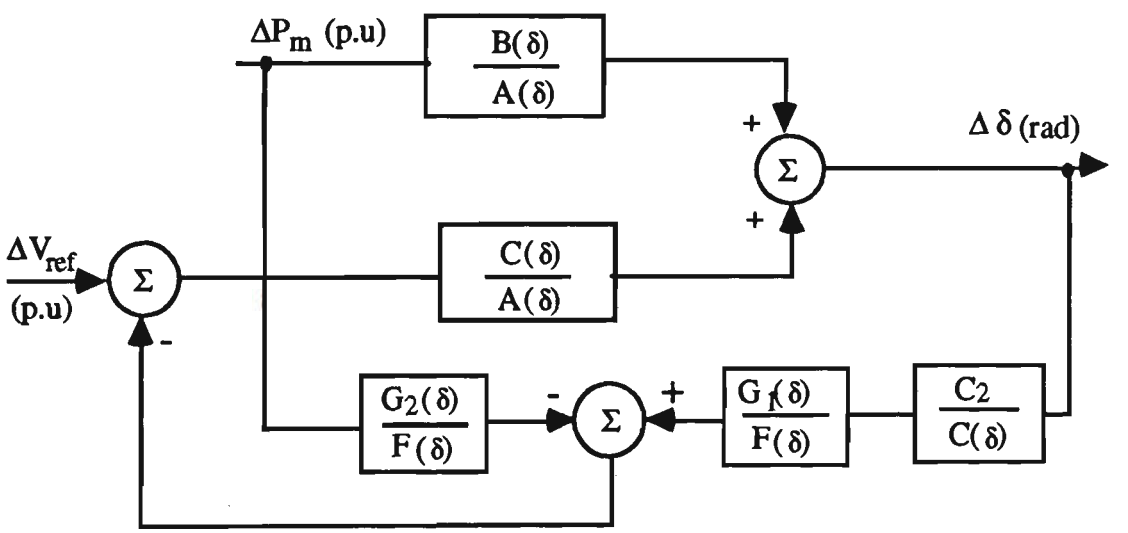

Figure 6.3: Modified scheme for MRAC

For discrete model Equation (6-1) is modified as :

$$\Delta\delta(t_k) = \frac{BF + G_2C}{AF + G_1c_2}\Delta P_m(t_k) + \frac{CF}{AF + G_1c_2}\Delta V_{ref}(t_k) \quad (6\text{-}19)$$

Equation (6-15) can be rewritten as:

$$\begin{pmatrix} 1 & 0 & 0 & 0 & 0 & 0 & 0 & 0 & 0 & 0 & 0 \\ a_1 & 1 & 0 & 0 & 0 & 0 & 0 & 0 & 0 & 0 & 0 \\ a_2 & a_1 & 1 & 0 & c_2 & 0 & 0 & 0 & 0 & 0 & 0 \\ a_3 & a_2 & a_1 & 1 & 0 & c_2 & 0 & 0 & 0 & 0 & 0 \\ 0 & a_3 & a_2 & a_1 & 0 & 0 & c_2 & 0 & 0 & 0 & 0 \\ 0 & 0 & a_3 & a_2 & 0 & 0 & 0 & c_2 & 0 & 0 & 0 \\ 0 & 0 & 0 & a_3 & 0 & 0 & 0 & 0 & 0 & 0 & 0 \\ b_1 & 0 & 0 & 0 & 0 & 0 & 0 & 0 & c_1 & 0 & 0 \\ b_2 & b_1 & 0 & 0 & 0 & 0 & 0 & 0 & c_2 & c_1 & 0 \\ 0 & b_2 & b_1 & 0 & 0 & 0 & 0 & 0 & 0 & c_2 & c_1 \\ 0 & 0 & b_2 & b_1 & 0 & 0 & 0 & 0 & 0 & 0 & c_2 \end{pmatrix} \begin{pmatrix} f_1 \\ f_2 \\ f_3 \\ f_4 \\ g_1 \\ g_2 \\ g_3 \\ g'_1 \\ g'_2 \\ g'_3 \end{pmatrix} = \begin{pmatrix} t_1 - a_1 \\ t_2 - a_2 \\ t_3 - a_3 \\ t_4 \\ t_5 \\ t_6 \\ t_7 \\ r_1 - b_2 \\ r_2 \\ r_3 \\ r_4 \end{pmatrix} \qquad (6\text{-}20)$$

6.2.4 Estimation of plant transfer functions

The same procedure given in Section 5.4.3.1 is used here to estimate the closed-loop transfer function $G_d(s) = \frac{R}{T}$. Consider the block diagram of Figure 6.4 where A_1, B_1 and C_1 are the polynomials at the new operating point:

$$A_1(\delta) = \delta^3 + a'_1\,\delta^2 + a'_2\,\delta + a'_3$$

$$B_1(\delta) = b'_1\,\delta + b'_2$$

$$C_1(\delta) = c'_1\,\delta + c'_2 \qquad (6\text{-}21)$$

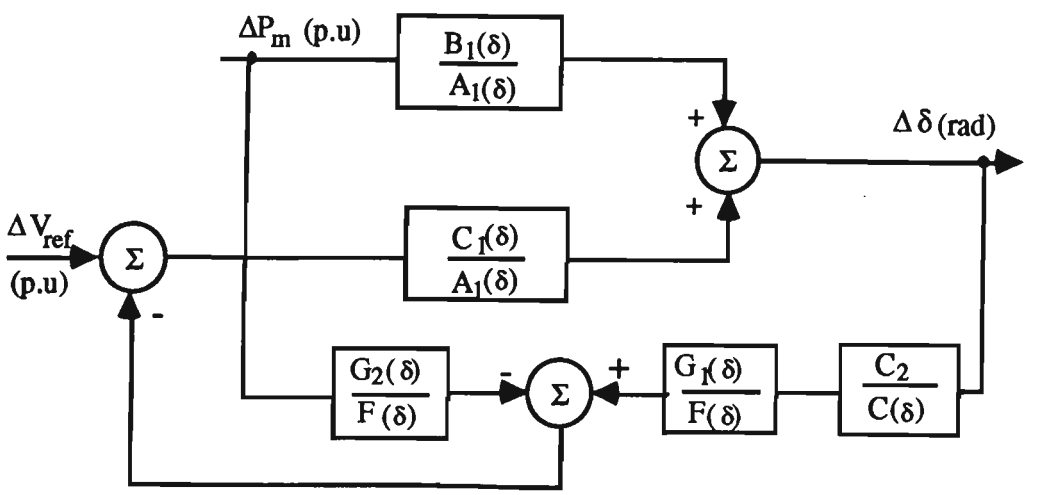

Figure 6.4: The block diagram of the system at new operating point

Let the identified polynomials R' and T' be as

$$R'(\delta) = b_1 \delta^6 + r'_1 \delta^5 + \ldots + r'_6$$

$$T'(\delta) = \delta^8 + t'_1 \delta^7 + t'_2 \delta^6 + \ldots + t'_8 \qquad (6\text{-}22)$$

By considering Equation (6-20) the parameters of the open-loop system can be calculated by the following equation:

$$\begin{pmatrix} a_1 \\ a_2 \\ a_3 \\ b_2 \\ c_1 \\ c_2 \end{pmatrix} = \begin{pmatrix} 1 & 0 & 0 & 0 & 0 & 0 \\ f_1 + \frac{c_2}{c_1} & 1 & 0 & 0 & 0 & 0 \\ 0 & 0 & f_4 \frac{c_2}{c_1} & 0 & 0 & 0 \\ 0 & 0 & 0 & f_4 \frac{c_2}{c_1} & 0 & 0 \\ 0 & f_4 \frac{c_2}{c_1} & f_4 + f_3 \frac{c_2}{c_1} & 0 & 0 & g_4 \frac{c_2}{c_1} \\ f_4 \frac{c_2}{c_1} & f_4 + f_3 \frac{c_2}{c_1} & f_3 + f_2 \frac{c_2}{c_1} & 0 & g_4 \frac{c_2}{c_1} & g_3 \frac{c_2}{c_1} \end{pmatrix}^{-1} \begin{pmatrix} t_1 - f_1 - \frac{c_2}{c_1} \\ t_2 - f_2 - f_1 \frac{c_2}{c_1} \\ t_8 \\ r_6 \\ t_7 \\ t_6 \end{pmatrix}$$

(6-23)

Since the delta model with a short sampling time is used, the coefficient b'_1 which corresponds to the constant value of $b_1 = \frac{1}{M}$ (M is the inertia of machine in seconds) is almost the same at all operating points. Note that, as for the PA controller, the parameters of the controller are fixed during the identification process.

The steps involved in the Model Reference Adaptive Controller (MRAC) are summarised as follows:

(i) The linearized model of Figure 2.1 is rearranged in the modified block diagram as shown in Figure 6.3.

(ii) At each sample interval, the coefficients of polynomials A, B and C are estimated by recursive least-squares method.

(iii) Obtain dc gain of the system which is equal to $\frac{b_2}{a_3}$. Then update the coefficients of the numerator (R) of the desired closed-loop transfer function.

(iv) Compute the control which will then place poles and zeros to preselected locations.

6.2.5 Simulation results

The same excitation control system given in Section 5.3.1 is used here. Regarding the closed-loop system bandwidth shown in Figure 6.5, the sampling time is chosen as 10 msec. The equivalent discrete-time model of Equation (6-10) is then considered as follows;

$$\frac{R}{T} = \frac{0.91 \text{ X } 278.8 \left(\frac{b_1}{0.91 \text{ X } 278.8}\delta + 9.52\right)}{(\delta^2 + 25.45\,\delta + 278.8)(\delta + 9.52)} \text{ X} \frac{(\delta + \lambda)^n}{(\delta + \lambda)^n} \quad (6\text{-}24)$$

Since the degree of the polynomial T has been calculated as 7, the value of n in Equation (6-24) is 4. As mentioned earlier the choice of λ depends on the stability of the feedback controller. The value of $\lambda = 26$, which corresponded to the root $\eta = 30$ in continuous-time system, gave a stable polynomial F over a wide range of operating points. Choosing a larger value than 26 for λ is not necessary for the power system example given in this work. Figures 6.6 and 6.7 show the time response of the system to a 1% step change in load and a 1% step change in voltage reference respectively.

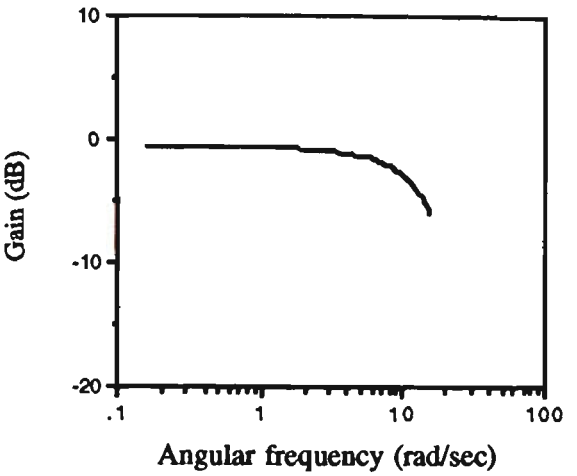

Figure 6.5: The gain characteristics of the closed-loop system $G_d(s)$

Referring to Figures 6.6 and 6.7 it is clear that MRAC significantly improves system damping. The settling time is reduced to 0.3 seconds which is faster than the PA and fixed gain stabilisers, and there is no overshoot. It is also clear from Figure 6.5 that the transfer function $G_d(s) = \frac{\Delta\delta}{\Delta P_m}$ almost has a flat gain characteristics over the most frequency range of concern (1-16 rad/sec). As explained in [34] this confirms that the controller can provide the same damping characteristics for both local and inter-area modes. The behaviour of the identified parameters are also shown in Figures 6.8 (a) and (b) showing a fast convergence. Transient performance of the system to a three phase fault with a successful reclosure is also tested and the results are shown in Figure 6.9.

The response of the power system to a 1% step change in load for two other operating points are also shown in Figures 6.10 and 6.11. Transient performance of the system was also tested following a 1% step change in voltage reference and shown in Figures 6.12 and 6.13.

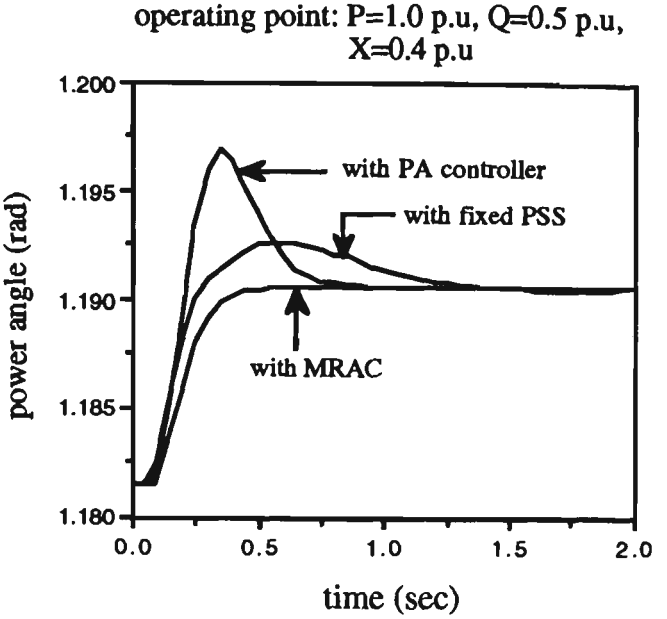

Figure 6.6: Power angle variation following a 1% step change in load

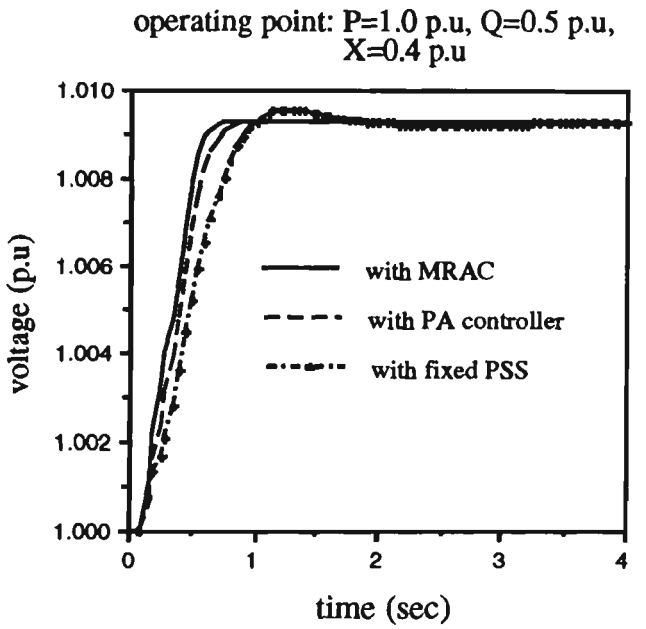

Figure 6.7 The changes in terminal voltage following a 1% step change in voltage reference

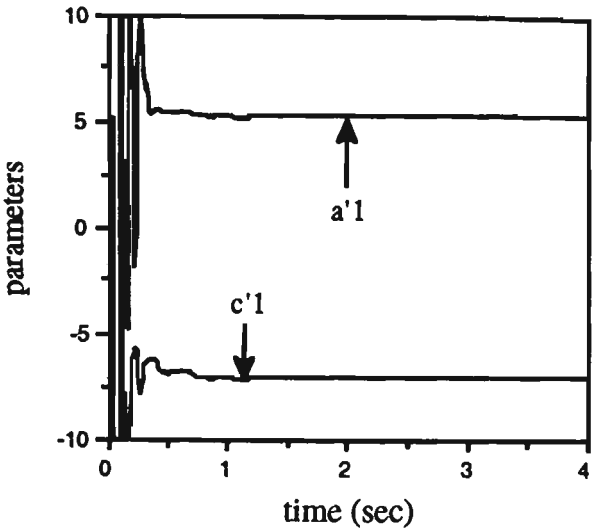

(a)

Figure 6.8: Parameter convergence

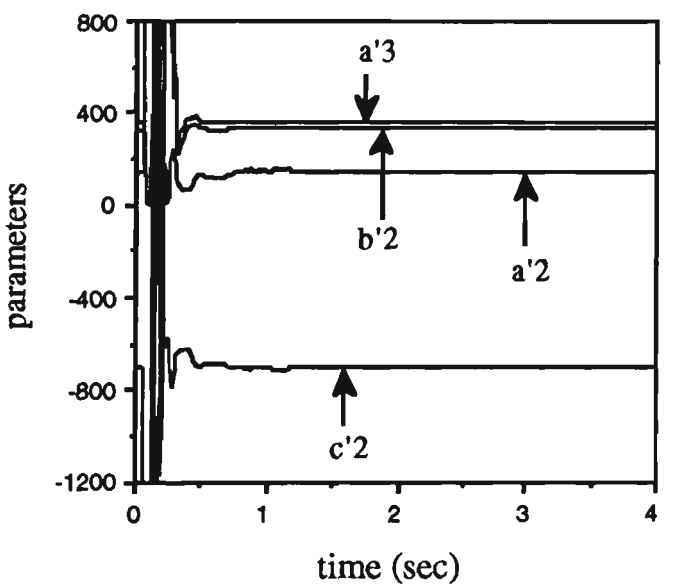

(b)

Figure 6.8: Parameter convergence

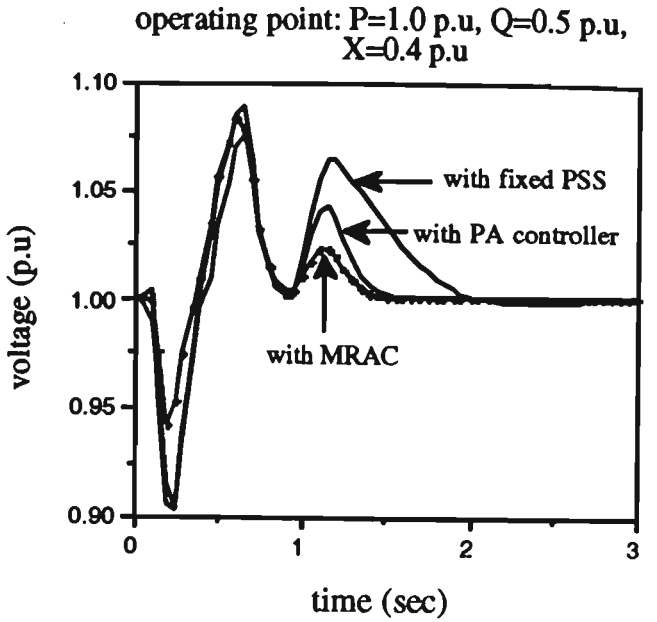

Figure 6.9: Time response of the system to a 3ϕ fault

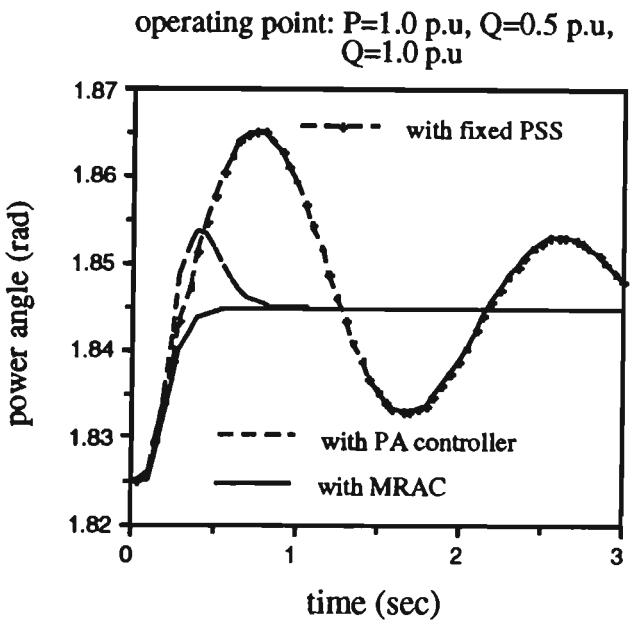

Figure 6.10: Power angle variation following a 1% step change in load

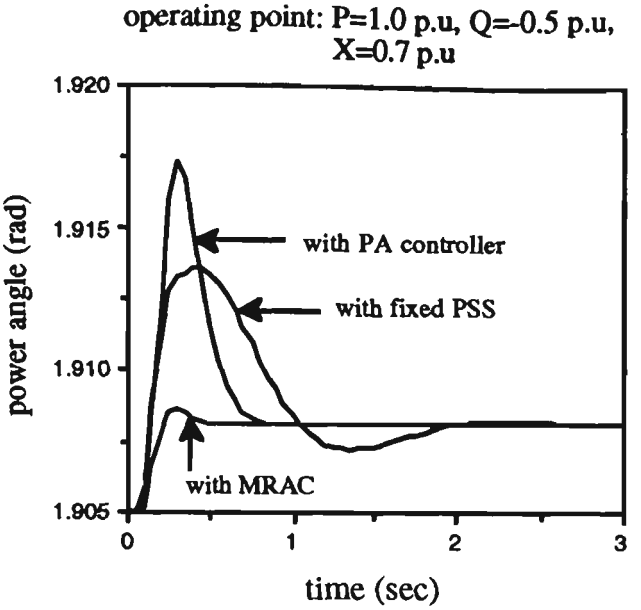

Figure 6.11: Power angle variation following a 1% step change in load

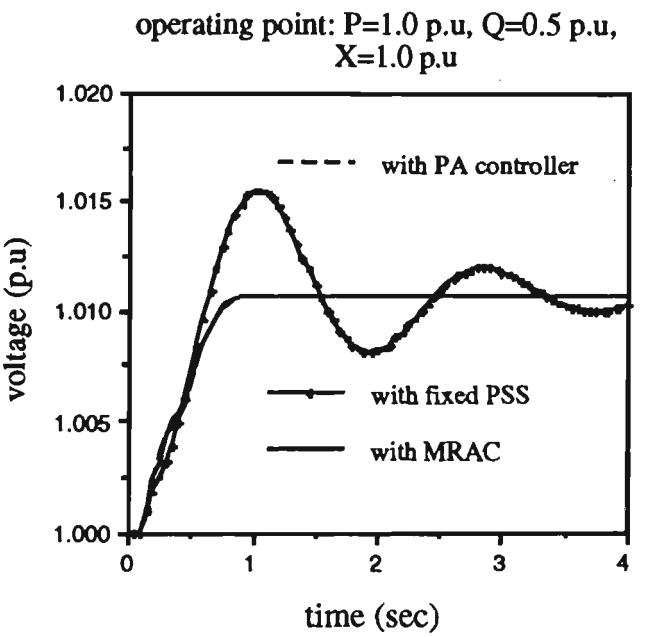

Figure 6.12 The changes in terminal voltage following a 1% step change in voltage reference

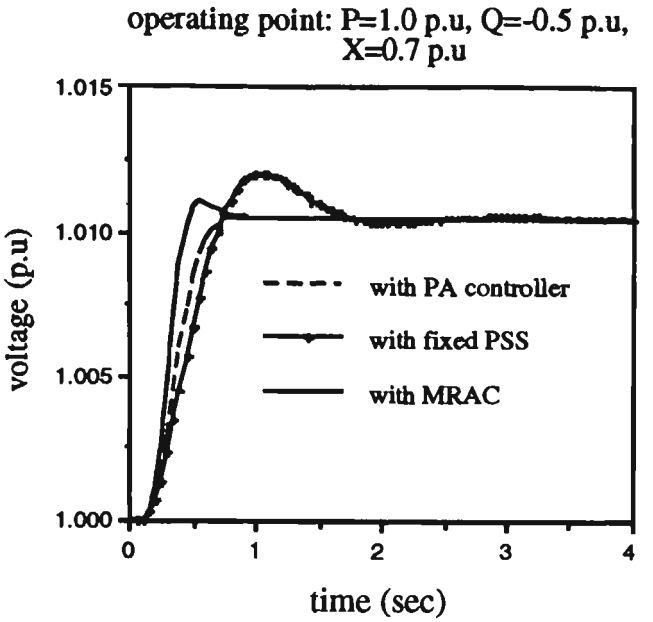

Figure 6.13 The changes in terminal voltage following a 1% step change in voltage reference

It can be seen from Figures 6.10 to 6.13 that the damping of the power system has been significantly improved when compared with the other cases. The additional zero introduced in Equation (6-9) will change when the dc gain of the system changes. Therefore, as can be seen from Figures 6.11 and 6.13 there might be a small overshoot for some cases. However, since the dc gain does not change significantly, for instance for this system dc gain is in the range of (0.3-2), the overall performance of the system would not be appreciably affected.

The performance of the system is now examined when the excitation system is represented by a dc gain K_e. Figure 6.14 shows the time response of this model in comparison with the case where the excitation system is given by $[K_e/(1+ T_e s)]$ to a 1% step change in load.

As can be seen from Figure 6.14 both excitation system models provide a very close damping characteristics.

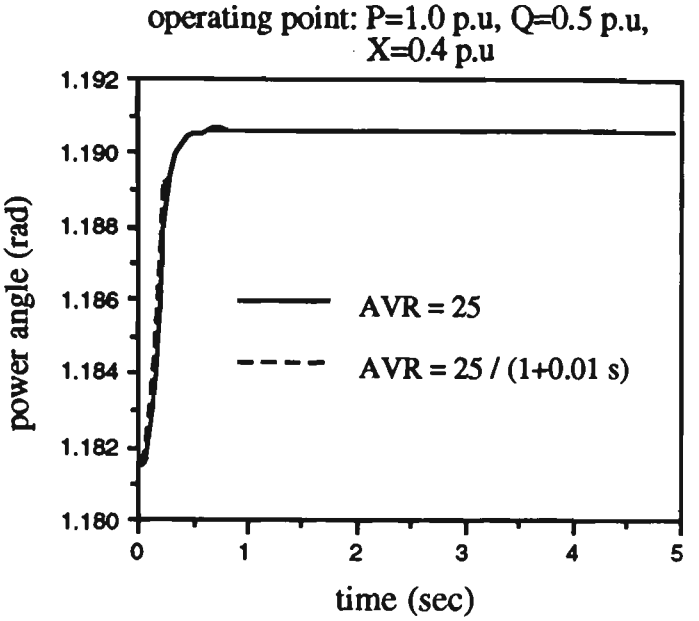

Figure 6.14 : Power angle variation following a 1% step change in load

6.2.6 Stability of feedback controller

The stability of the feedback controller has also been checked for a wide range of operating points and shown in Table I. As can be seen from Table I polynomial F has roots in the left hand side of the delta-plane confirming its stability for all cases.

Table I

P + jQ (p.u)	X=0.1 p.u	X=0.4 p.u	X=0.7 p.u	X=1.0 p.u
0.5+j0.0	-61.42±j25.52 -5.58±j39.48	-55.75±j21.68 -11.01±j34.84	-54.21±j17.01 -12.47±j37.3	-12.72±j38.76 -53.94±j8.11
1.0+j0.5	-59.1±j32.5 -7.64±j29.1	-55.22±j30.31 -11.55±j27.64	-53.37±j21.6 -13.5±j32.72	-11.52±j43.04 -45.83, -65.13
1.0-j0.5	-64.96±j32.15 -2.0±j38.93	-60.33±j37.68 -7.16±j27.3	-59.34±j38.83 -8.41±j23.54	-58.9±j39.4 -9.02±j22.38

6.3 MODEL REFERENCE ADAPTIVE CONTROLLER USING APPROXIMATE MODEL

6.3.1 Discrete time transfer function

In Chapter 3, it was pointed out that the shift form of the discrete-time model bore no resemblance to the continuous-time model. On the other hand, the coefficients in the delta form are very close to the corresponding coefficients in the continuous model when a short sampling time is used. It is relatively easy to check this similarity by considering Table II for initial operating point of P+jQ=1+j 0.5 p.u and X=0.4 p.u.

Table II

Parameters	a_1	a_2	a_3	b_0	b_1	b_2	c_0	c_1	c_2
Continuous-time system	3.9	130	365	0	125	333	0	0	-722
Discrete-time system	5.12	133	358	0.5	126	326	-.01	-7.1	-707

Since the coefficient $-c_1$ (7.1) in polynomial $C(\delta)$ is much smaller than $-c_2$ (707), polynomial $C(\delta)$ can be written as follows;

$$C(\delta) = c_2 \qquad (6\text{-}25)$$

Equation (6-25) corresponds to the corresponding polynomial in the continuous-time model given in Appendix VII. The time response of the open-loop transfer function $G_c(\delta) = \frac{\Delta\delta}{\Delta V_{ref}}$ to a 1% step change in voltage reference is shown in Figure 6.15 for two different forms of the polynomial $C(\delta)$. This figure shows the resemblance between the two cases. This allows one to draw an approximate MRAC as given in the following Section.

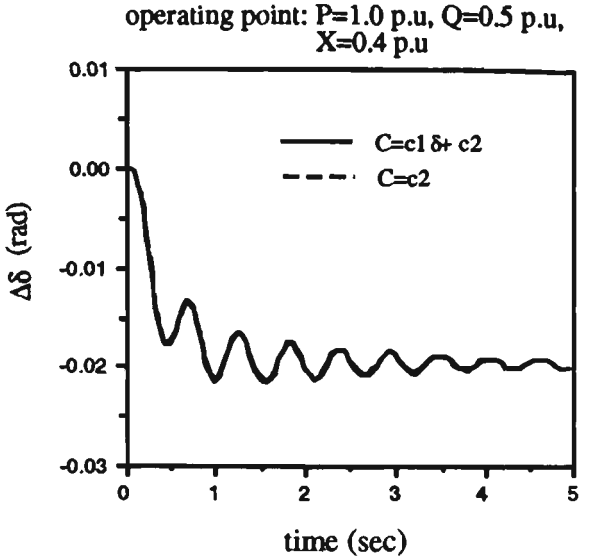

Figure 6.15: Time response of the open-loop system to a 1% step change in voltage reference

6.3.2 Determination of controller parameters

By considering the adaptive controller scheme given in Figure 6.1, the polynomials F, G_1 and G_2 are selected as:

$$F(\delta) = \delta^{n_f} + f_1 \delta^{n_f-1} + f_2 \delta^{n_f-2} + \ldots + f_{n_f}$$

$$G_1(\delta) = \delta (g_1 \delta^{n_f-1} + g_2 \delta^{n_f-2} + \ldots + g_{n_f})$$

$$G_2(\delta) = \delta (g'_1 \delta^{n_f-1} + g'_2 \delta^{n_f-2} + \ldots + g'_{n_f}) \qquad (6\text{-}26)$$

The degrees of polynomials F, G_1 and G_2 can be calculated by solving the following equations.

$$\begin{cases} \deg A + \deg F = \deg T \\ 3 \deg F = 2 \deg T - 3 \end{cases} \qquad (6\text{-}27)$$

Since there is no polynomial as a common factor in the left hand side of Equation (6-18) by using this method there is no need to modify the adaptive controller scheme given in Figure 6.1 and this reduces the

number of controller parameters to be identified (see Equations (6-20) and (6-28)).

By considering Equations (5-5), (6-26) and (6-27), the solution of Equation (6-2) can be found as:

$$\begin{pmatrix} 1 & 0 & 0 & 0 & 0 & 0 & 0 & 0 & 0 \\ a_1 & 1 & 0 & 0 & 0 & 0 & 0 & 0 & 0 \\ a_2 & a_1 & 1 & c_2 & 0 & 0 & 0 & 0 & 0 \\ a_3 & a_2 & a_1 & 0 & c_2 & 0 & 0 & 0 & 0 \\ 0 & a_3 & a_2 & 0 & 0 & c_2 & 0 & 0 & 0 \\ 0 & 0 & a_3 & 0 & 0 & 0 & 0 & 0 & 0 \\ b_1 & 0 & 0 & 0 & 0 & 0 & c_2 & 0 & 0 \\ b_2 & b_1 & 0 & 0 & 0 & 0 & 0 & c_2 & 0 \\ 0 & b_2 & b_1 & 0 & 0 & 0 & 0 & 0 & c_2 \end{pmatrix} \begin{pmatrix} f_1 \\ f_2 \\ f_3 \\ g_1 \\ g_2 \\ g_3 \\ g'_1 \\ g'_2 \\ g'_3 \end{pmatrix} = \begin{pmatrix} t_1 - a_1 \\ t_2 - a_2 \\ t_3 - a_3 \\ t_4 \\ t_5 \\ t_6 \\ r_1 - b_2 \\ r_2 \\ r_3 \end{pmatrix} \qquad (6\text{-}28)$$

Equation (6-28) can be written as

$$Z\,X = L \qquad (6\text{-}29)$$

The solution of Equation (6-29) is

$$X = Z^{-1}\,L \qquad (6\text{-}30)$$

6.3.3 Estimation of plant transfer functions

The same procedure given in Section 5.4.3.1 is used here to estimate the closed-loop transfer function $G_d(s) = \frac{R}{T}$. Let the identified polynomials R' and T' be as

$$R'(\delta) = b_1\,\delta^4 + r'_1\,\delta^3 + \ldots + r'_4$$

$$T'(\delta) = \delta^6 + t'_1\,\delta^5 + t'_2\,\delta^4 + \ldots + t'_6 \qquad (6\text{-}31)$$

By considering Equation (6-28) the parameters of the open-loop system can be calculated by the following equation.

$$\begin{pmatrix} \dot{a}_1 \\ \dot{a}_2 \\ \dot{a}_3 \\ \dot{b}_2 \\ \dot{c}_2 \end{pmatrix} = \begin{pmatrix} 1 & 0 & 0 & 0 & 0 \\ f_1 & 1 & 0 & 0 & 0 \\ f_2 & f_1 & 1 & 0 & g_1 \\ 0 & 0 & 0 & f_3 & 0 \\ 0 & 0 & f_3 & 0 & 0 \end{pmatrix}^{-1} \begin{pmatrix} \dot{t}_1 - f_1 \\ \dot{t}_2 - f_2 \\ \dot{t}_3 - f_3 \\ \dot{r}_4 \\ \dot{t}_6 \end{pmatrix} \qquad (6\text{-}32)$$

As can be seen from Equations (6-23) and (6-32) there is much less computational burden to be taken for calculating the open-loop system parameters in the case of approximate MRAC.

6.3.4 Simulation results

The same excitation control system used in Section 5.3.1 is used. Figures 6.16 and 6.17 show the time response of the system to a 1% step change in load and a 1% step change in voltage reference respectively for two MRACs. Transient performance of the system to a three phase fault with a successful reclosure is also tested and the results are shown in Figure 6.18. It is clear from Figures 6.16 to 6.18 that although the system performance is better in MRAC case, the approximate MRAC still works satisfactorily with the advantage that there is no need to modify the adaptive controller scheme given in Figure 6.1.

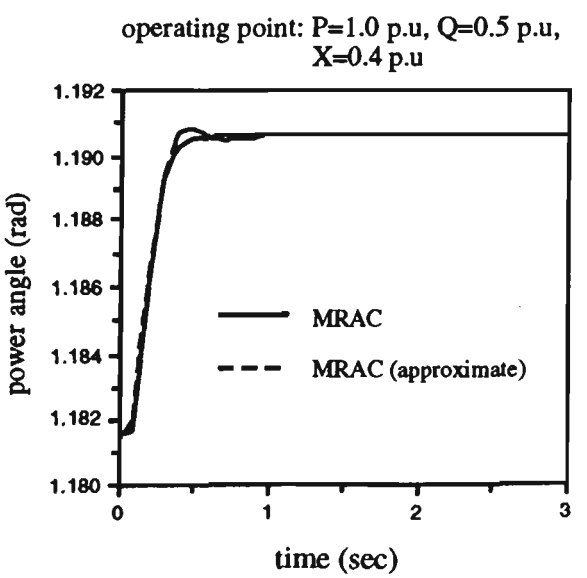

Figure 6.16: Power angle variation following a 1% step change in load

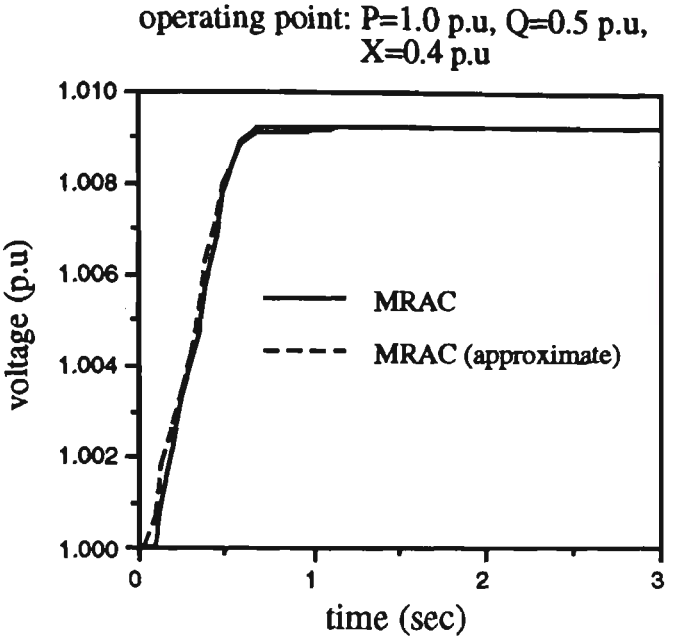

Figure 6.17: The changes in terminal voltage following a 1% step change in voltage reference

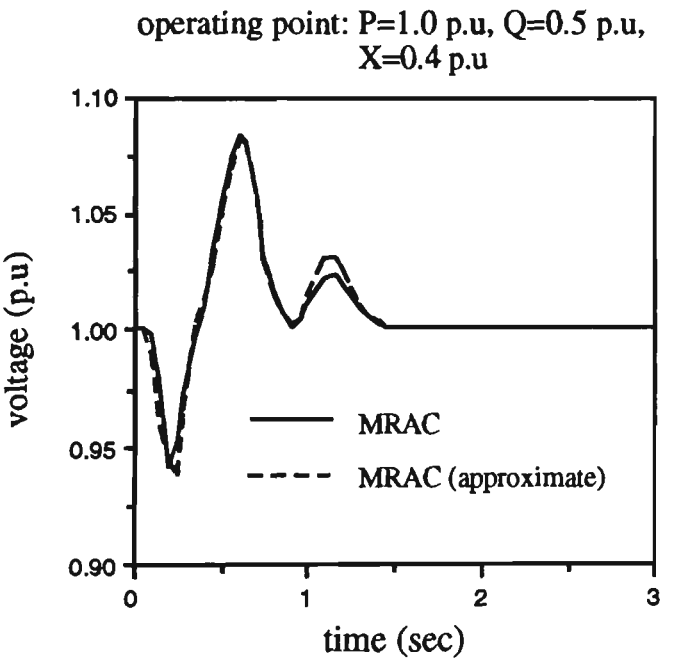

Figure 6.18: Time response of the system to a 3ϕ fault

6.3.5 Stability of feedback controller

The roots of the polynomial F are shown in Table III. The location of roots show the stability of feedback controller for all cases.

Table III

P + jQ (p.u)	X=0.1 p.u	X=0.4 p.u	X=0.7 p.u	X=1.0 p.u
0.5+j0.0	-8.76±j54.03 -90.55	-14.22±j47.1 -79.15	-14.48±j45.88 -78.47	-13.82±j47.95 -79.75
1.0+j0.5	-15.68±j42.84 -77.2	-19.63±j38.77 -68.34	-17.82±j43.33 -74.19	-11.93±j50.72 -84.2
1.0-j0.5	-7.56±j57.6 -94.87	-17.82±j43.33 -74.19	-22.77±j37.08 -64.05	-25±j35.46 -59.92

6.4 POLE SHIFTING ADAPTIVE CONTROLLER

A self tuning controller based on Pole Assignment had the advantage of overcoming the drawbacks of Minimum Variance control and of incorporating a comparatively simple calculation algorithm. In addition, it always produces a much smoother control action which is more acceptable [44]. Based on the PA control technique, a Pole Shifting controller has been proposed by [32] to simplify the selection of the closed-loop poles while retaining the basic advantages. In this technique the closed-loop poles of the system are shifted radially towards the origin of the unit circle in the z-domain by a preselected constant factor (α) less than one [32]. This method will now be compared with the new method presented earlier in this chapter.

6.4.1 Determination of controller parameters

Consider, for example, an open-loop system can be represented by the transfer function

$$y(k) = \frac{B(q^{-1})}{A(q^{-1})}\ u(k) \tag{6-33}$$

where y(k) and u(k) are the sampled output of the system and the computed control at sample instants respectively, and q^{-1} is the backward shift operator. Polynomials A and B are given by

$$A(q^{-1}) = 1 + a_1 q^{-1} + a_2 q^{-2} + \ldots + a_{n_a} q^{-n_a}$$

$$B(q^{-1}) = b_1 q^{-1} + b_2 q^{-2} + \ldots + b_{n_a} \tag{6-34}$$

It should be noted that in this section the aim is to compare the same Pole Shifting controller appeared in the literature with the proposed adaptive controllers in this work. Therefore, the shift operator is used instead of the delta operator.

The control is computed from [44]

$$u(k) = \frac{G(q^{-1})}{F(q^{-1})}\ y(k) \tag{6-35}$$

where polynomials F and G are given by

$$F(q^{-1}) = 1 + f_1 q^{-1} + f_2 q^{-2} + \ldots + f_{n_f} q^{-n_f}$$

$$G(q^{-1}) = g_1 q^{-1} + g_2 q^{-2} + \ldots + g_{n_f} \tag{6-36}$$

The closed-loop system is shown in Figure 6.19. From Figure 6.19 the closed-loop transfer function will be

$$\frac{y(k)}{e(k)} = \frac{B(q^{-1})\,F(q^{-1})}{A(q^{-1})\,F(q^{-1}) + G(q^{-1})\,B(q^{-1})} \tag{6-37}$$

By choosing the closed-loop poles as the roots of the polynomial T

$$T(q^{-1}) = 1 + t_1 q^{-1} + t_2 q^{-2} + \ldots + t_{n_t} q^{-n_t} \tag{6-38}$$

the control parameters f_i and g_i are computed from

$$A(q^{-1})\,F(q^{-1}) + G(q^{-1})\,B(q^{-1}) = T(q^{-1}) \qquad (6\text{-}39)$$

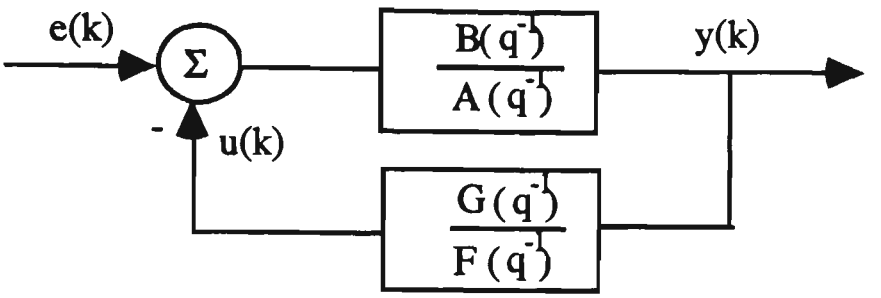

Figure 6.19 The closed-loop system

Although the actual system is of a high order, it is identified as if $n_a=3$ [32]. By using the same method given in Section 5.4.2 it can be seen that $n_f = 3$. Considering Equations (6-34), (6-36) and (6-38) the solution of Equation (6-39) takes the form of

$$\begin{pmatrix} 1 & 0 & 0 & 0 & 0 & 0 \\ a_1 & 1 & 0 & b_1 & 0 & 0 \\ a_2 & a_1 & 1 & b_2 & b_1 & 0 \\ a_3 & a_2 & a_1 & 0 & b_2 & b_1 \\ 0 & a_3 & a_2 & 0 & 0 & b_2 \\ 0 & 0 & a_3 & 0 & 0 & 0 \end{pmatrix} \begin{pmatrix} f_1 \\ f_2 \\ f_3 \\ g_1 \\ g_2 \\ g_3 \end{pmatrix} = \begin{pmatrix} t_1 - a_1 \\ t_2 - a_2 \\ t_3 - a_3 \\ t_4 \\ t_5 \\ t_6 \end{pmatrix} \qquad (6\text{-}40)$$

The open-loop poles of the system are obtained by solving the characteristics roots of the polynomial

$$A(q^{-1}) = 0 \qquad (6\text{-}41)$$

If all roots of Equation (6-40) are within the unit circle in the z-domain, the system is stable. Obviously, the system is more stable the closer the poles are to the origin of the unit circle. The function of the Pole Shifting Self Tuning Regulator is to shift all roots of Equation (6-41) towards the origin of the unit circle by a factor α such that T becomes

$$T(q^{-1}) = A(\alpha q^{-1}) = 1+\alpha a_1 q^{-1}+\alpha^2 a_2 q^{-2}+\ldots+\alpha^{n_a} a_{n_a} q^{-n_a}$$

$$= 1+\alpha a_1 q^{-1}+\alpha^2 a_2 q^{-2}+\alpha^3 a_3 q^{-3} \qquad (6\text{-}42)$$

Considering Equations (6-40) and (6-42) implies that

$$\begin{pmatrix} 1 & 0 & 0 & 0 & 0 & 0 \\ a_1 & 1 & 0 & b_1 & 0 & 0 \\ a_2 & a_1 & 1 & b_2 & b_1 & 0 \\ a_3 & a_2 & a_1 & 0 & b_2 & b_1 \\ 0 & a_3 & a_2 & 0 & 0 & b_2 \\ 0 & 0 & a_3 & 0 & 0 & 0 \end{pmatrix} \begin{pmatrix} f_1 \\ f_2 \\ f_3 \\ g_1 \\ g_2 \\ g_3 \end{pmatrix} = \begin{pmatrix} (\alpha - 1)\, a_1 \\ (\alpha^2 - 1)\, a_2 \\ (\alpha^3 - 1)\, a_3 \\ 0 \\ 0 \\ 0 \end{pmatrix} \qquad (6\text{-}43)$$

Equation (6-43) can be written as

$$Q\,X = I \qquad (6\text{-}44)$$

The solution of Equation (6-44) is

$$X = Q^{-1}\, I \qquad (6\text{-}45)$$

6.4.2 Estimation of plant transfer function

System identification can be represented by considering the rotor speed (ω) and the control input u as shown in Figure 6.20.

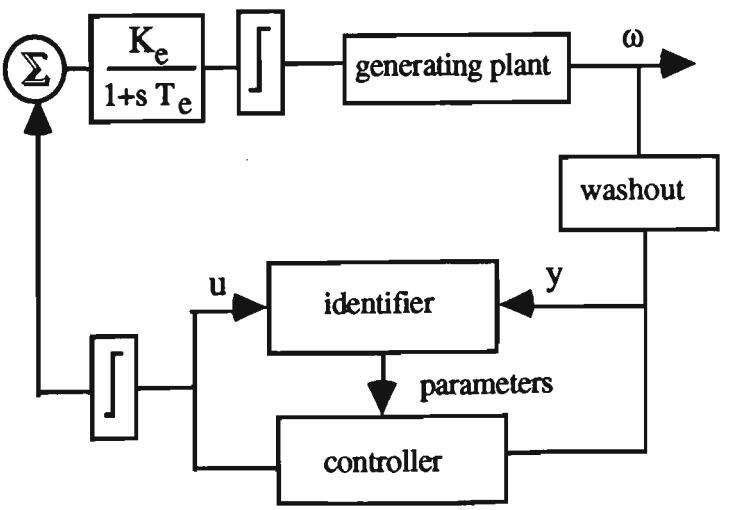

Figure 6.20: Proposed scheme for identification and adaptive controller

A sequence of psedurandom noise is superimposed with the control input u to perform the identification process.

6.4.3 Simulation results

The same excitation control system used in Section 6.2.5 is used. Figure 6.21 shows the time response of the system to a 1% step change in load for the Pole Shifting (PS) controller and the PA and MRAC given before.

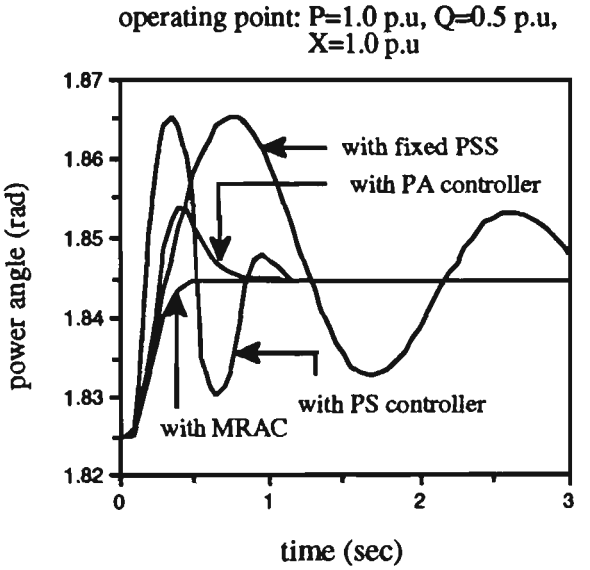

Figure 6.21: Power angle variation following a 1% step change in load

It is clear from Figure 6.21 that both PA controller and MRAC given in this work have better performance than PS controller.

6.5 MULTIMACHINE CASE

6.5.1 System block diagram

The same linearized model of Figure 2.2 is used here.

6.5.2 A simplified block diagram

For the analysis purposes of this work the block diagram of the linearized model shown in Figure 2.2 may be reconfigured to a simplified diagram

as shown in Figure 6.22. This figure shows the effect of disturbances such as a small change in load (ΔP_m) and power swing disturbances (ΔP_d). The denominator of $G_{b_i}(s)$ is the same as the denominator of $G_{d_i}(s)$. Each transfer function given in Figure 6.22 represents the individual ith machine. Therefore, the coefficients of all polynomials are the same as the ones given for a single-machine infinite-bus model in Appendix VII with the exception that the "K_{ii}" parameters are obtained from the linearized model of the entire system.

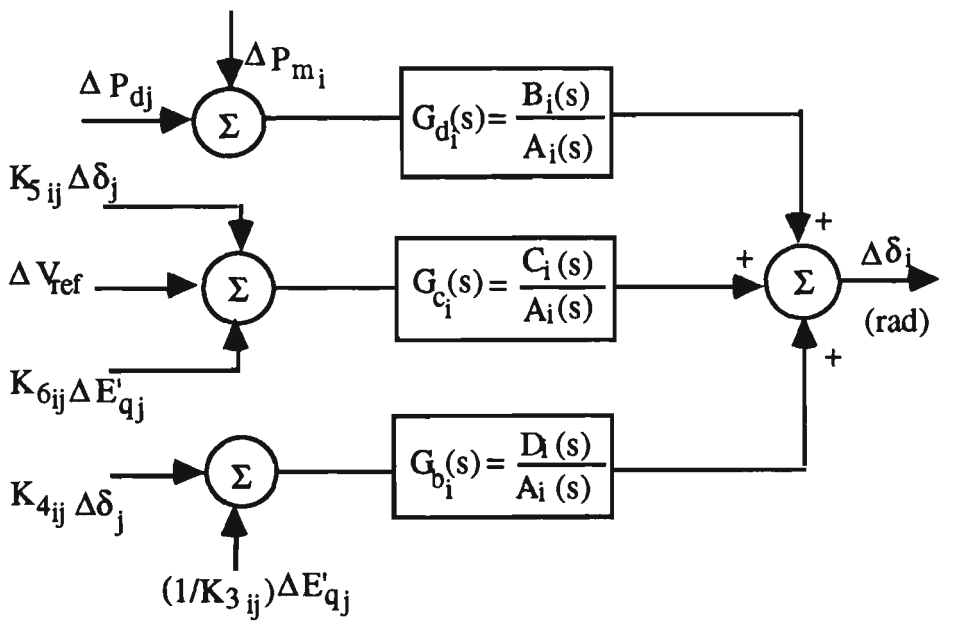

Figure 6.22: A modified block diagram of Figure 2.2

6.5.3 Fixed gain PSS for design operating point

The same example given in Chapter 4 is used here.

6.5.4 MRAC using approximate model

6.5.4.1 Adaptive controller scheme

By using a decentralised structure each generator is equipped by the adaptive controller shown in Figure 6.23 where the effect of other machines on the power system is also included.

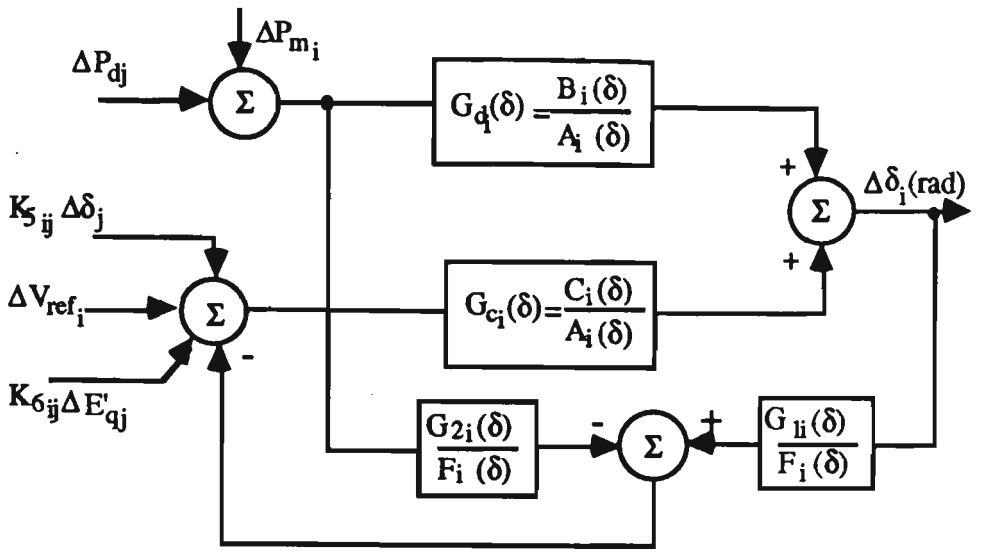

Figure 6.23: Block diagram of the closed loop of the ith machine

The coefficients of transfer functions G_{di} and G_{ci} for the two-machine system are given in Table IV (see Equations (5-5)). A delta operator discrete model has been calculated using a sampling time of 0.01 sec.

Table IV (generator #1)

Parameters	a_1	a_2	a_3	b_0	b_1	b_2	c_0	c_1	c_2
Continuous-time system	20.9	73.1	730	0	159	3087	0	0	-1902
Discrete-time system	19.6	75.9	658	0.8	165	2783	-.03	-17.4	-1714

Table IV (generator #2)

Parameters	a_1	a_2	a_3	b_0	b_1	b_2	c_0	c_1	c_2
Continuous-time system	27.8	12.5	124	0	43	1177	0	0	-1493
Discrete-time system	24.4	12.5	109	0.2	45	1028	-.02	-13	-1303

6.5.4.2 Determination of controller parameters

The same reference model used in Section 6.2.2 is also used here. In order to design the adaptive controller it is assumed that the excitation system is given simply by its dc gain. Therefore, the same Equations of

(6-26) and (6-28) can be used to obtain the controller parameters. Although this model is assumed in setting up the identification algorithm, simulation studies have represented the actual excitation system by the more accurate model $[K_{e_i}/(1+T_{e_i}s)]$.

6.5.4.3 Estimation of plant transfer functions

The same procedure given in Section 5.4.3.1 is used to estimate the transfer function $G_{d_i}(\delta)$. The open-loop system of ith machine can be obtained using Equation (6-32). The effect of other machines on the ith machine due to dynamic interaction will be considered by measuring the signal ΔP_{d_j} and $\Delta\delta_i$. The $\Delta\delta_i$ is also affected by the other signals such as $\sum K_{5ij}\Delta\delta_j$ and $\sum K_{6ij}\,\Delta E'_{qj}$. However, the latter signals are not necessary to be measured because they do not have any effect on the identified transfer function $G_{d_i}(\delta)$ (see Figure 6.22). The ΔV_{ref_i} is considered to be zero [45].

6.5.5 Simulation results

Figures 6.24 (a) and (b) show the response of the system to a small step change in load for approximate MRAC and fixed PSS for generators 1 and 2 respectively. The behaviour of the identified parameters is also shown in Figures 6.25 (a) and (b). The transient response of the system is also tested for another operating point (see Appendix VI) where the designed fixed PSS has been used and shown in Figures 6.26 (a) and (b) for generators 1 and 2 respectively.

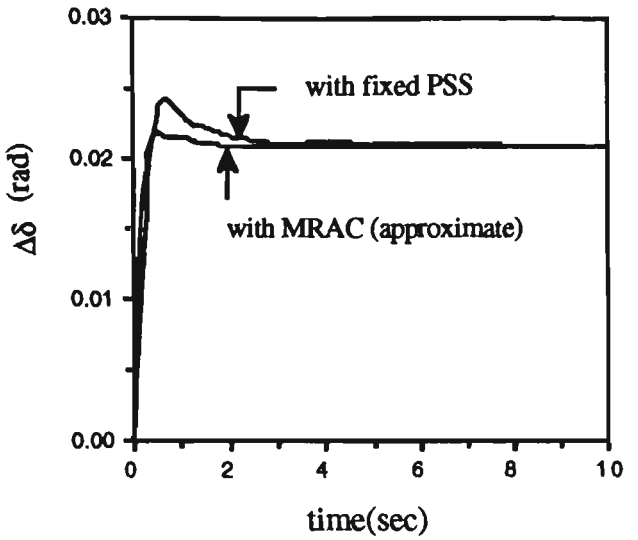

(a) generator #1

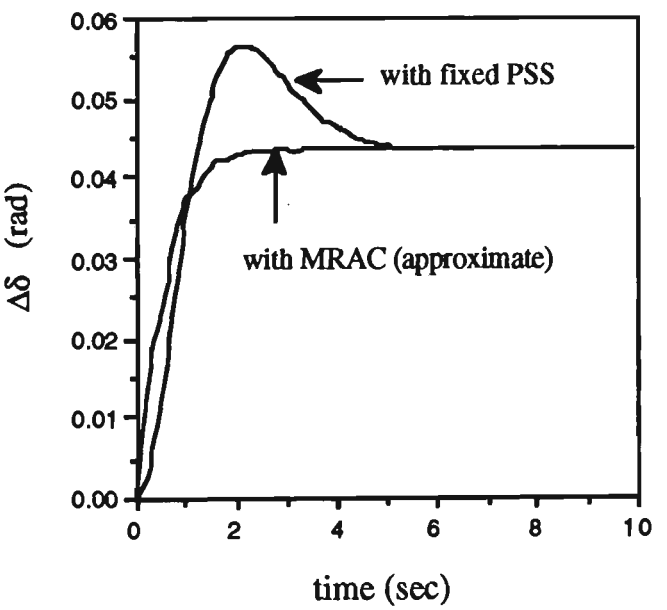

(b) generator #2

Figure 6.24: Power angle variation following a small change in load

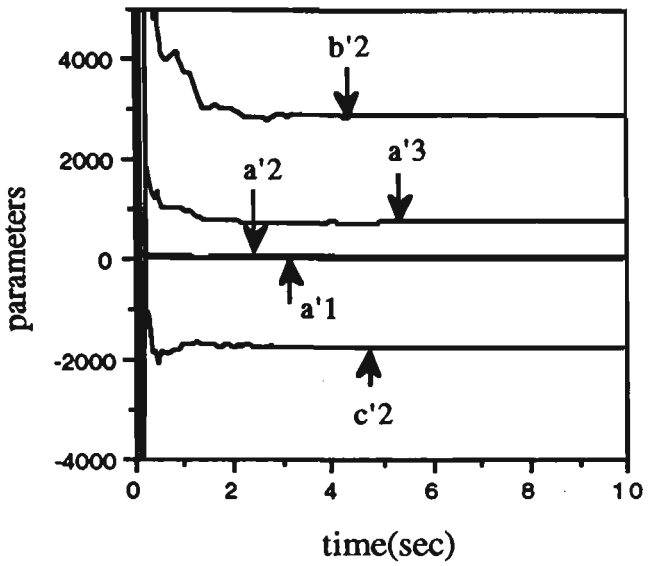

(a) generator #1

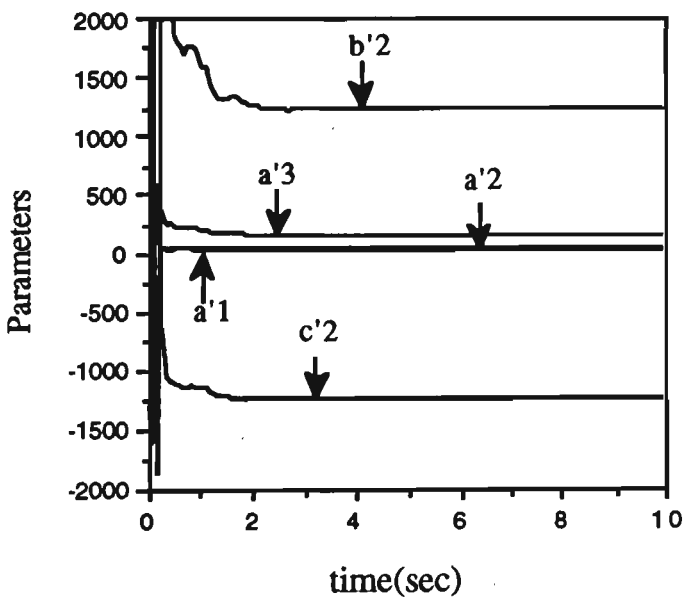

(b) generator #2

Figure 6.25: Parameter convergence

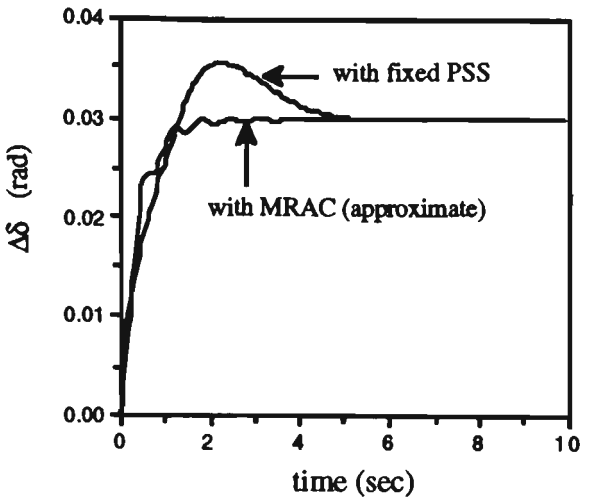

(a) generator #1

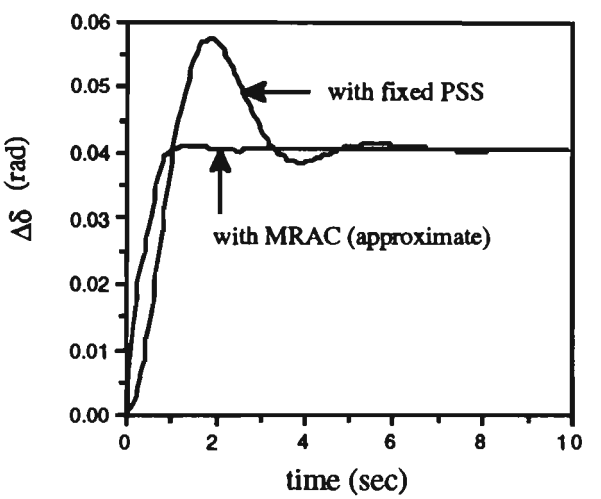

(b) generator #2

Figure 6.26: Power angle variation following a small change in load

As can be seen from Figures 6.24 and 6.26 the adaptive controller performance is superior to the fixed PSS, especially where the operating point changes.

6.5.6 Stability of feedback controller

The roots of the polynomial F are shown in Table V. The location of roots show the stability of the feedback controller for two operating points.

Table V

Normal operating point		Other operating point	
Generator #1	Generator #2	Generator #1	Generator #2
-20.06±j16.86	-2.335±j26.9	-21.94±j17.82	-4.1±j24.9
-6.49	-37.1	-5.01	-34.34

6.6 CONCLUSIONS

A new type of Model Reference Adaptive Controller using an explicit system identification which does not require calculation of the error between the plant output and that of model has been presented. In this algorithm the controller parameters have been adjusted so that the poles and zeros of the closed-loop system are placed at desirable locations. It has been shown that using the delta operator in discretization allows the designer to use a more simplified controller with an approximate discrete model as this needs less computational time. It also simplifies the controller algorithm based on a continuous-time control strategy by reducing the number of controller parameters to be identified. The MRACs given in this chapter have provided desirable performance over a wide range of operating points. A comparison of the proposed controllers given in this work with the PS controller appeared in the literature has been also given. The results confirmed the superiority of the PA controller and MRAC. The proposed adaptive controller is also tested for a multimachine case where the results show a better performance of approximate MRAC than the fixed PSS.

CHAPTER 7

Chapter 7

CONCLUSIONS

The goal throughout this thesis has been to search for an adaptive controller which is able to provide a desirable response over a wide range of operating points.

It was shown that a low order model of the open-loop system including the generator model and the excitation system could sufficiently represent the actual system for the design of the adaptive controller.

When adaptive controllers are to be applied to power systems, it is essential that the continuous-time system be discretized by using a suitable mathematical model. A comparison between two mathematical models for discretizing power system transfer functions showed that the shift model representation was very sensitive to numerical round-off when short sampling time was used. This had several undesirable results such as incorrect steady state response, frequency response and difficulties in identifying power system parameters. The delta operator was used to solve these problems. It not only gave more accurate results but had the added advantage that its transfer function bore a close correspondence to the continuous-time system by ignoring sampling zeros from discretization. This advantage allowed to use a more simplified adaptive controller such that the less controller parameters had to be identified and this reduced the computational time.

Adaptive controllers based on Pole Assignment and model reference

adaptive techniques using the delta operator were then proposed. In the Pole Assignment adaptive controller the controller parameters were so designed that the poles of the closed-loop system were placed at well-damped locations.

In all STC techniques the exact desirable response does not always follow because there is no effort to fix the location of the zeros as well as the poles. Accordingly, the PA controller was modified by using a new type of Model Reference Adaptive Controller. This algorithm, in which the poles and zeros are located at preselected locations using an explicit system identification, gives the specified desirable response for all operating points. In this model reference adaptive technique there was no need to obtain the error between the plant and model outputs. The results of a SMIB and two-machine power systems showed that the proposed adaptive controller would provide better damping characteristics than a fixed PSS, especially where the operating point changed.

Author's publications

[55] Khodabakhshian, A., Gosbell, V. J. and Elshafei, A. L., "New adaptive stabilisers, Part I- Pole Assignment adaptive controller using delta operator", under review by IEEE Power System Engineering Committee

[65] Khodabakhshian, A., Gosbell, V. J. and Elshafei, A. L., "New adaptive stabilisers, Part II- Model Reference Adaptive Controller using delta operator", under review by IEEE Power System Engineering Committee

[84] Khodabakhshian, A., Gosbell, V. J. and Coowar, F., "Discretization of power system transfer functions", IEEE Tans. on Power Systems, Vol. 9, No. 1, Feb. 1994, pp. 255-261

[85] Khodabakhshian, A. and Gosbell, V. J., "A new model for identifying adaptive control of power system", International Power System Engineering Conference, Singapore, March 1993

APPENDICES

APPENDICES

Appendix I: The synchronous generator equations [4]

The synchronous generator equations in per unit form in terms of Park's d-q axes are:

$$p\delta = \omega - \omega_o$$

$$p\omega = (\omega_o/(2\,H))\,(T_m - T_e - D\,(\omega - \omega_o))$$

$$pe'_q = (1/T'_{do})\,(V_f - e'_q - (x_d - x'_d)\,i_d)$$

$$V_f = V_q + x_d\,i_d$$

$$e'_q = V_q + x'_d\,i_d$$

$$V_t^2 = V_d^2 + V_q^2$$

$$T_e = V_d\,i_d + V_q\,i_q$$

$$V_d = x_q\,i_q$$

where p stands for derivative.

The limiter values for excitation system and stabiliser are $\pm$ 7 and + 0.2, -0.1 p.u respectively.

Appendix II: Design of simplified and conventional stabilisers [3,4]

The objective of a power system stabiliser (PSS) is to add damping to rotor oscillations. This is achieved by modulating the voltage regulator set point

to produce torque variation in phase with speed. Power system stabiliser transfer function may have two forms of

1- Conventional PSS [3,4]

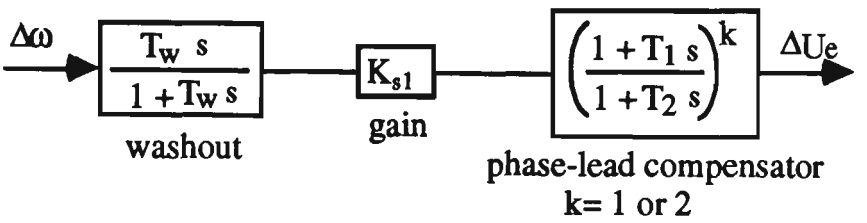

2- Simplified PSS [5]

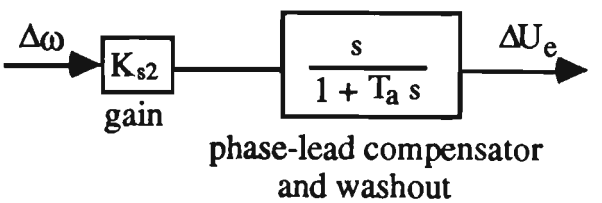

In order to obtain the PSS parameters a general procedure may be outlined as follows [3,4];

a) The undamped natural frequency of oscillation ω_n is obtained from the torque angle characteristic equation derived from mechanical loop as shown in Figure A.1.

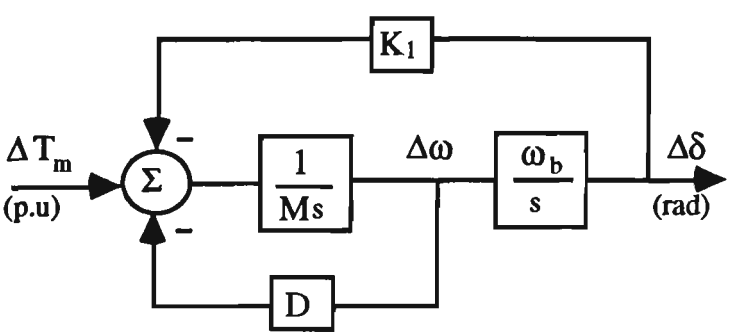

Figure A.1

The characteristic equation would then be

$$s^2 + (D / M)\, s + (K_1\, \omega_b / M) = 0 \qquad (1)$$

This gives rise to damped oscillation with frequency $\omega_n \sqrt{1-\zeta^2}$ and damping ration ζ where

$$\omega_n = \sqrt{\frac{K_1\, \omega_b}{M}} \quad \text{and} \quad \zeta = \frac{1}{2}\, D \,/ \sqrt{K_1\, M\, \omega_b} \qquad (2)$$

b) The phase lag produced by voltage regulator loop as well as the reciprocal of its magnitude for the undamped natural frequency $\omega_n = \sqrt{\frac{K_1\, \omega_b}{M}}$ rad/sec is calculated as follows (see Figure A.2);

$$-\angle \frac{\Delta T_s}{\Delta U_e} = -\angle \frac{K_3\, K_2\, K_e}{1 + K_e\, K_3\, K_6 + T'_{d0}\, K_3\, s} \Big|_{s = j\, \omega_n} \qquad (3)$$

It should be noted that since the feedback path through K_4 provides a small positive damping component, it is considered negligible [3].

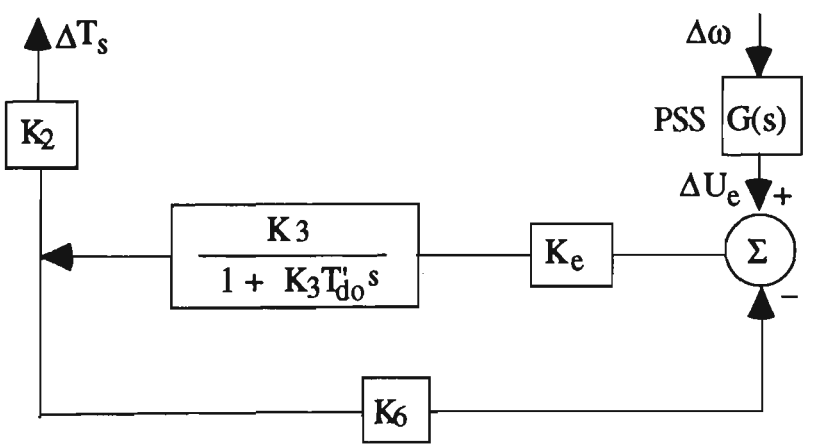

Figure A.2: Component of torque produced by voltage regulator action

c) Considering a suitable value for damping ratio ζ , the damping coefficient would be

$$D = 2\, \zeta\, \sqrt{K_1\, \omega_b\, M} \qquad (4)$$

From Figure A.2 it can be seen that

$$|\Delta T_S| = D|\Delta\omega| = \left|\frac{\Delta T_S}{\Delta U_e}\right|_{s=j\omega n} |G(s)|_{s=j\omega n} |\Delta\omega| \quad (5)$$

Therefore, the gain of G(s) can be calculated as follows;

$$K_S = \frac{D}{\left|\frac{\Delta T_S}{\Delta U_e}\right|_{s=j\omega n} |G(s)|_{s=j\omega n}} \quad (6)$$

Now one example is taken from [3] where the generator parameters are

x_d = 1.6 p.u, x_q = 1.55 p.u, x'_d= 0.32 p.u, T'_{do} = 5.0 sec, H = 1.5 and K_d=0.01.

The exciter gain is considered as K_e = 25 [5]. By considering operating point

$P + jQ = 1.0 + j\,0.5$ p.u and Terminal voltage, V_t = 1.0 p.u

the "K" parameters of linear model of Figure 2.1 would then be K_1=1.01, K_2=1.17, K_3=0.36, K_4=1.47, K_5=-0.097, K_6=0.417. Then by using the procedure explained earlier the PSS parameters for such a system are obtained as follows;

1- simplified PSS: K_{S2} = 10, T_a = 0.05 sec

2- conventional PSS: K_{S1} = 7.2, T_w = 10, T_1= 1.32, T_2 = 0.05, k = 1

Transient performance of the power system to a 5% step change in load, a 5% step change in voltage reference and a three phase fault close to generator bus with a successful reclosure was tested for both kinds of PSSs and shown in Figures A.3 (a), (b) and A.4 respectively.

Referring to figures A.3 and A.4, it can be seen that the results are almost the same for both kinds of PSSs.

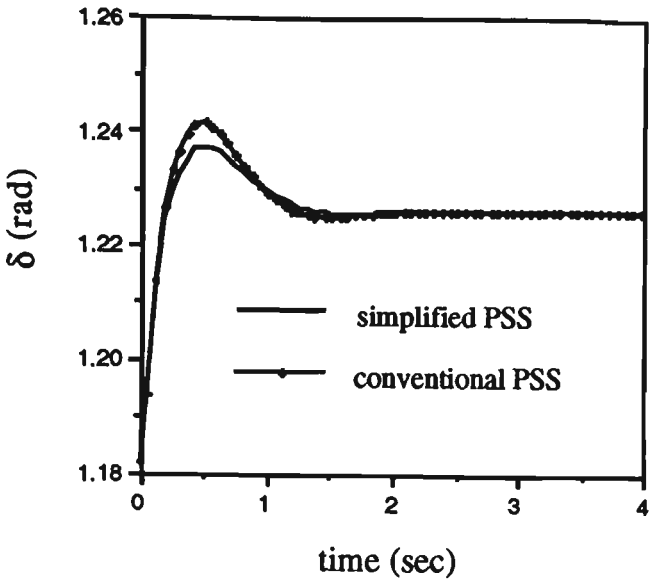

Figure A.3 (a): Time response of the system to a 5% step change in load

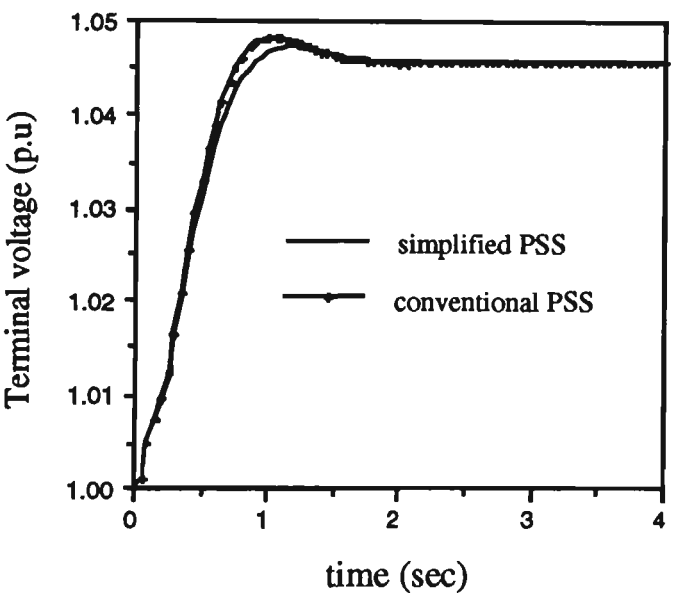

Figure A.3 (b): Time response of the system to a 5% step change voltage reference

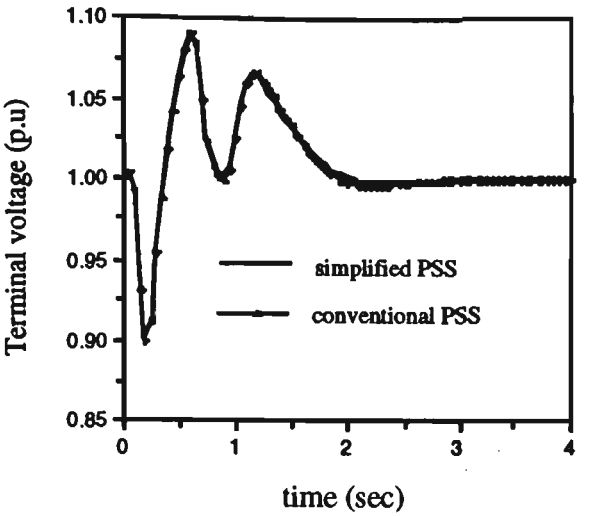

Figure A.4: Time response of the system to a three phase fault close to generator bus after a successful reclosure

The parameters of the exciter and PSS for the case of high order model have been obtained as follows;

$K_e = 25$, $T_e = 0.01$ [34,49], $K_s = 8.5$, $T_w = 10$, $T_1 = 1$, $T_2 = 0.02$, $k = 1$

Appendix III: Derivation of transfer function $G_d(s)$ with stabiliser

For low frequency oscillations produced by a disturbance ΔP_d, the change in the power angle $\Delta\delta$ can be modelled as follows;

(i) high order model

$$G_d(s)=\frac{\Delta\delta(s)}{\Delta P_d(s)} = \frac{B_1s^4 + B_2s^3 + B_3s^2 + B_4s + B_5}{s^6 + A_1s^5 + A_2s^4 + A_3s^3 + A_4s^2 + A_5s + A_6} \qquad (7)$$

where

$A_0 = K_3\, T'_{do}\, T_e\, M\, T_W\, T_2$

$A_1 = (K_3\, T'_{do}\, TE\, (M\, (T_W + T_2) + K_d\, T_w\, T_2) + (K_3\, T'_{do} + T_e)\, M\, T_w\, T_2)/A_0$

$A_2 = (K_3\, T'_{do}\, T_e\, (M + K_d\, (T_2 + T_w) + K_1\, T_w\, T2) + (K_3\, T'_{do} + T_e)\, (M\, (T_w + T_2) + K_d\, T_w\, T_2) + (1 + K_6\, K_e\, K_3)\, M\, T_w\, T_2) / A_0$

$A_3 = (K_3\, T'_{do}\, T_e\, (K_d + K_1\, (T_w + T_2)) + (K_3\, T'_{do} + T_e)\, (M + K_d\, (T_2 + T_w) + K_1\, T_w\, T_2) + (1 + K_6\, K_e\, K_3)\, (M\, (T_2 + T_w) + K_d\, T_2\, T_w) + K_2\, K_3\, (-K_4\, Te\ T_2\, T_w + K_s\, K_e\, T_w\ T_1))\ /\ A_0$

$A_4 = (K_3\, T'_{do}\, T_e\, K_1 + (K_3\, T'_{do} + T_e)\, (K_d + K_1\, (T_2 + T_w)) + (1 + K_6\, K_e\, K_3)\, (M + K_d\, (T_2 + T_w) + K_1\, T_2\, T_w) + K_2\, K_3\ (K_s\, K_e\, T_w - K_5\, K_e\, T_2\, T_w - K_4\, (T_e\, (T_2 + T_w) + T_2\, T_w)))\ /\ A_0$

$A_5 = (K_1\, (K_3\, T'_{do} + T_e) + (1 + K_6\, K_e\, K_3)\, (K_d + K_1\, (T_2 + T_w)) + K_2\, K_3\, (-K_4\, (T_2 + T_w + T_e) - K_5\, K_e\, (T_2 + T_w)))\ /\ A_0$

$A_6 = (K_1\, (1 + K_6\, K_e\, K_3) + K_2\, K_3\ (-K_4 - K_5\, K_e))\ /\ A_0$

$B_1 = (K_3\ T'_{do}\, T_e\, T_2\, T_w)\ /\ A_0$

$B_2 = (K_3\, T'_{do}\, T_e\, (T_2 + T_w) + T_2\, T_w\, (K_3\, T'_{do} + T_e))\ /\ A_0$

$B_3 = (K_3\, T'_{do}\, T_e + (K_3\, T'_{do} + T_e)\, (T_2 + T_w) + T_2\, T_w\, (1 + K_6\, K_e\, K_3))\ /\ A_0$

$B_4 = ((1 + K_6\, K_e\, K_3)\, (T_2 + T_w) + T_e + K_3\, T'_{do})\ /\ A_0$

$B_5 = (1 + K_6\, K_e\, K_3)\ /A_0$

(ii) low order model

$$G_d(s) = \frac{\Delta\delta(s)}{\Delta P_d(s)} = \frac{B_1 s^2 + B_2 s + B_3}{s^4 + A_1 s^3 + A_2 s^2 + A_3 s + A_4} \qquad (8)$$

where

$B_1 = (K_3\, T'_{d0}\, T_a)\ /\ (K_3\, T'_{d0}\, T_a\, M)$

$B_2 = ((1 + K_e K_3 K_6) T_a + K_3 T'_{d0})\ /\ (K_3\, T'_{d0}\, T_a\, M)$

$B_3 = (1 + K_e K_3 K_6)\ /\ (K_3\, T'_{d0}\, T_a\, M)$

$A_1 = (K_3 T'_{d0} M + (1 + K_e K_3 K_6) T_a M + K_d K_3 T_a T'_{d0})\ /\ (K_3\, T'_{d0}\, T_a\, M)$

$A_2 = ((1 + K_e K_3 K_6) M + K_d K_3 T'_{d0} + (1 + K_e K_3 K_6) K_d T_a + K_1 K_3 T_a T'_{d0} + K_e K_3 K_2 K)\ /\ (K_3\, T'_{d0}\, T_a\, M)$

$$A_3=((1+K_eK_3K_6)K_d+K_1K_3T'_{d0}+(1+K_eK_3K_6)K_1T_a-K_2K_3T_a\,(K_4+K_eK_5))\,/\,(K_3\,T'_{d0}\,T_a\,M)$$

$$A_4=((1+K_eK_3K_6)K_1-K_2K_3\,(K_4+K_eK_5))\,/\,(K_3\,T'_{d0}\,T_a\,M)$$

Appendix IV: The condition for significant numerical difficulties of the shift operator

The discussion in this Appendix closely follows that in Middleton [83]. Let $\rho(x) = \sum_{i=0}^{n} a_i x^i$ denote a polynomial in a complex variable x. Assume that each coefficient has similar relative accuracy as would occur when the numbers are represented in a computer in floating point format. Individual terms may be positive or negative and the relative accuracy will be worse when the polynomial consists of large terms which almost cancel. Following this concept, reference [83] defines the "numerical conditioning" associated with the polynomial as:

$$\nu(x) = \frac{\Sigma(\text{absolute terms})}{\Sigma(\text{signed terms})} = \frac{\sum_{i=0}^{n} |a_i x^i|}{\sum_{i=0}^{n} a_i x^i} \qquad (9)$$

A large value of Equation (9) suggests that the polynomial will be sensitive to numerical round-off. The relative robustness of the δ and q representations can be compared by examining the ratio $\frac{\nu_\delta(\omega)}{\nu_q(\omega)}$ for the characteristic equations, i.e. the denominator of the transfer functions. These are taken to be $\rho_\delta(\delta) = \delta^n + a_{n-1}\,\delta^{n-1} + \ldots + a_0$ for the delta model and $\rho_q(q) = q^n + b_{n-1}\,q^{n-1} + \ldots + b_0$ for the shift model. These coefficients are related to the sums of the products of roots. For example, if the roots of $\rho_q(q)$ are $q_{i_1}, \ldots, q_{i_n}$ then

$$|b_k| = \sum_{i_1 \neq i_2 \neq \ldots i_{n-k}} |q_{i_1} \ldots q_{i_{n-k}}| \qquad (10)$$

Using $\delta = \frac{e^{j\omega h} - 1}{h}$ and $q = e^{j\omega h}$ one can show:

$$\frac{v_\delta(\omega)}{v_q(\omega)} = \frac{\sum_{k=0}^{n} |h^{n-k} a_k| (2 - 2\,\mathrm{Cos}\,(\omega h))^{k/2}}{\sum_{k=0}^{n} |b_k|} \qquad (11)$$

where b_k has been given above and

$$h^{n-k} |a_k| = h^{n-k} \sum_{i_1 \neq i_2 \neq \ldots i_{n-k}} |\delta_{i_1}| \ldots |\delta_{i_{n-k}}|$$

$$= h^{n-k} \sum_{i_1 \neq i_2 \neq \ldots i_{n-k}} \left|\frac{q_{i_1} - 1}{h}\right| \ldots \left|\frac{q_{i_{n-k}} - 1}{h}\right|$$

$$= \sum_{i_1 \neq i_2 \neq \ldots i_{n-k}} |q_{i_1} - 1| \ldots |q_{i_{n-k}} - 1| \qquad (12)$$

Let suppose the system is at least a fourth order system with four poles as is reasonable for a power system transfer function. Considering $\omega_s = 50\,\omega$ implies that

$$(2 - 2\,\mathrm{Cos}\,(\omega\, h))^{k/2} << 1 \qquad (13)$$

for $k \geq 1$ and

$$(2 - 2\,\mathrm{Cos}\,(\omega\, h))^{k/2} = 1 \qquad (14)$$

when k = 0. For the δ form to be more robust:

$$\nu_\delta(\omega) << \nu_q(\omega) \tag{15}$$

To satisfy Equation (15), the following Equation has to be satisfied when k=0:

$$h^{n-k} |a_k| << |b_k| \text{ or } h^{n-k} |a_k| < 0.1 |b_k| \tag{16}$$

For a system having four poles Equation (16) can be written as follows:

$$|q_{i_1} - 1||q_{i_2} - 1||q_{i_3} - 1||q_{i_4} - 1| < 0.1 |q_{i_1} q_{i_2} q_{i_3} q_{i_4}| \tag{17}$$

It is assumed that all poles are in the right hand side of the unit circle and therefore have the same sign. Considering the pole with smallest magnitude (q_k) and Equation (17) implies that

$$|q_k - 1| < (0.1)^{1/4} |q_k| \text{ or } |q_k - 1| < \frac{1}{2} |q_k| \tag{18}$$

For the other terms in numerator and denominator of Equation (11) (i.e., k≥1), by considering Equations (13) and (18), Equation (15) will be seen to be satisfied.

Appendix V: Australian power system

The generator parameters using 100 MVA base are

H = 16.5 sec, $x_d = x_q = 0.476$ p.u, $x'_d = 0.05$ p.u, $T'_{do} = 5.3$ sec and

the operating points for two different cases are

	1993 high load	1993 medium load
P	8.7	4.4
Q	1.206	0.326
Vt	0.9789 + j 0.2045	0.9803 + j 0.1977
Vo	0.9962 - j 0.0872	1.0288 - j 0.0503
Z	0.0024+ j 0.03539	0.00401+j0.04941
Y	0.208 - j 1.939	-0.682 - j 0.709

All parameters have been given in p.u. on 100 MVA base.

The parameters of the Hydro system taken from [3] are as follows;

H = 5.0 sec, x_d = 1.14, x_q = 0.66 p.u, x'_d = 0.24 p.u, T'_{do} = 12 sec and the operating point is P+jQ=1.0+j0.5 p.u and V_t=1.0 p.u.

Appendix VI: Multimachine system

The generator parameters are as follows;

Frequency=60 Hz, MVA base=3000

	Generator #1	Generator #2
MVA base	700	2600
P(MW)	600	2400
Q(MVAr)	103.45	1335.9
T'_{do}	7.6	7.6
x_d	0.9	0.9
x'_d	0.3	0.3
x_q	0.68	0.68
H	5.07	5.07
V_t	1.0	1.05
angle	0.0	38.89
D	1	5

V_3=0.986 $\angle$ -11.7, P_{load}=3000 MW, Q_{load} = 1000 MVAr, X_C = -j1.48, and reactance lines are both j1 p.u. All parameters have been given in p.u

except machine inertia H and time constants which are in seconds. The exciter gain and its time constant are 250 and 0.01 sec respectively for each generator.

The linearized equations are obtained as follows [4];

$$A=\begin{bmatrix} -0.42265 & -0.11204 & -0.15337 & 0 & 0 & 0.10781 & -0.00831 & 0 \\ 377 & 0 & 0 & 0 & 0 & 0 & 0 & 0 \\ 0 & -0.05722 & -0.25589 & 0.13158 & 0 & 0.05722 & 0.07274 & 0 \\ 0 & -1111 & -14528 & -100 & 0 & 1111 & -8195.25 & 0 \\ 0 & 0.00148 & -0.03587 & 0 & -0.56896 & -0.00159 & -0.12043 & 0 \\ 0 & 0 & 0 & 0 & 377 & 0 & 0 & 0 \\ 0 & 0.01688 & -0.0036 & 0 & 0 & -0.01688 & -0.18085 & 0.13158 \\ 0 & -1773.5 & -1269 & 0 & 0 & 1773.5 & -20720.25 & -100 \end{bmatrix}$$

$$B=\begin{bmatrix} 0 & 0 & 0 & 25000 & 0 & 0 & 0 & 0 \\ 0 & 0 & 0 & 0 & 0 & 0 & 0 & 25000 \end{bmatrix}^T$$

The eigenvalue analysis of the above equations shows that the lightly damped mode is -0.1624±j6.6626. A participation factor analysis given in [28] shows that both generators are effective in this mode. Therefore, the PSSs are so designed that the phase lag produced by this mode in each excitation system is compensated by using the same method given in Appendix II [4,102]. The PSS parametrs are obtained as follows;

Generator #1: $$10\ \frac{2\,s}{1+2\,s}\ \frac{1+0.1\,s}{1+0.02\,s}$$

Generator #2: $$3\ \frac{2s}{1+2\,s}\ \frac{1+0.06\,s}{1+0.02s}$$

The other operating point is given as follows;

$V_1=0.95 \angle 2$, $V_3=1.02 \angle -20$, $P_{load}=3800$ MW, Q_{load} = 190 MVAr. It is assumed that the terminal voltage of the second generator with a higher inertia remains constant.

Appendix VII: Derivation of transfer function $G_d(s)$ and $G_c(s)$ with no stabiliser

For the power system without PSS $G_d(s)$ and $G_c(s)$ can be modelled as follows;

$$G_d(s)=\frac{\Delta\delta(s)}{\Delta P_m(s)}=\frac{E_1 s+E_2}{s^3+F_1 s^2+F_2 s+F_3}$$

$$G_c(s)=\frac{\Delta\delta(s)}{\Delta V_{ref}(s)}=\frac{G_1}{s^3+F_1 s^2+F_2 s+F_3}$$

$$G_b(s)=\frac{H_1}{s^3+F_1 s^2+F_2 s+F_3} \qquad (19)$$

where

$E_1=(K_3 T'_{d0}) / (K_3 T'_{d0} M)$

$E_2=(1+K_eK_3K_6) / (K_3 T'_{d0} M)$

$F_1=((1+K_eK_3K_6) M + K_dK_3T'_{d0}) / (K_3 T'_{d0} M)$

$F_2=((1+K_eK_3K_6)K_d+K_1K_3T'_{d0}) / (K_3 T'_{d0} M)$

$A_4=((1+K_eK_3K_6)K_1-K_2K_3 (K_4+K_eK_5)) / (K_3 T'_{d0} M)$

$G_1=-(K_eK_3 K_2) / (K_3 T'_{d0} M)$

$H_1= -(K_3 K_2) / (K_3 T'_{d0} M)$

REFERENCES

REFERENCES

[1] Larsen, E.V. and Swann, D.A. "Applying power system stabilisers, Pts I, II, & III", IEEE Trans. on PAS, Vol. 100, 1981, pp. 3017-3046

[2] Kundur, P., Kelin, M., Rogers, G.J. and Zywno, M.S., "Application of power system stabilisers for enhancement of overall system stability", IEEE Trans. on PAS, PWRS-2, 1989, pp. 614-626

[3] Demello, F.P. and Concordia, C., "Concepts of synchronous machine stability as affected by excitation control", IEEE Trans. on PAS, PAS-88, 1969, pp.316-326

[4] Yu,Y.N. "Electric power system dynamics" (Academic Press, 1983)

[5] Bergen, A.R. "Power System Analysis", (Prentice-Hall,1986)

[6] Anderson, P.M. and Fouad, A.A., "Power system control and stability", (Iowa state University Press, 1977)

[7] Demello, F.P., Hannett, L. N. and Undrill, J. M., "Practical approaches to supplementary stabilising from accelerating power", IEEE Trans. on PAS, Vol. PAS-97, Sept./Oct. 1978, pp.1515-1522

[8] Pierre, D.A., "A perspective on adaptive control of power systems", IEEE Trans. on Power Systems, Vol. PWRS-2, No.2, pp. 387-396, May 1987

[9] Byerly, R.T., Bennon, R.J., and Sherman, D.E., "Eigenvalue analysis of synchronising power flow oscillations in large electric power systems", IEEE Trans. on PAS, Vol. PAS-101, No. 1, pp: 235-243, 1982

[10] Gove, R.M., "Geometric construction of the stability limits of synchronous machines", IEE Proceedings, Vol. 112, No. 5, pp: 977-985, 1965

[11] Booth, R.R., and Dillon, G.L., "The use of digital computers for steady state stability calculations", Electrical and Mechanical Engineering Transactions, IE Aust., pp: 12-22, 1968

[12] Bollinger, K., Laha, A., Hamilton, R., and Harras T., "Power stabiliser design using Root-Locus methods", IEEE Trans. on PAS, Vol. PAS-94, No. 5, pp: 1484-1488, 1975

[13] Oradat, C.P. and Fitzer, J., "Determining power system stabiliser parameters by the Root-Locus method", Proceedings of the 1977 control of power systems conference and exposition, pp: 44-48, 1977

[14] Stapleton, "Root-Locus study of synchronous machine regulation", IEE Proceedings, Vol. 3, No. 4, pp: 761-768, 1964

[15] Ogata, K., "Modern control engineering", 2nd. Ed., Prentice-Hall, 1990

[16] Ewart, D.N., and Demello, F.P., "A digital computer program for the automatic determination of dynamic stability limits", IEEE Trans. on PAS, Vol. PAS-86, No. 7, pp: 867-875, 1967

[17] Aldred, A.S., and Shackshaft, G., "A frequency response method for the predetermination of synchronous machine stability", IEE Proceedings, Vol. 107, Part C, pp: 2-10, 1960

[18] Newcomb, R.W., "Concepts of linear systems and controls", Brooks/Cole publishing company, 1968

[19] Heffron, W.G., Philips, R.A., "Effect of a modern amplidyne on under-excited operation of large turbine generators", AIEEE Transactions, Prt III, Vol. 71, pp: 692-697, 1952

[20] Venikov, V.A., "Transient phenomena in electric power systems", Pergamon Press, 1964

[21] Yu, Y.N., and Vongsuriya, K., "Steady state stability of a regulated synchronous machine connected to an infinite system", IEEE Trans. on PAS, Vol. PAS-85, No. 7, pp: 12-22, 1966

[22] Surana, S., and Harihan, M.V., "Transient response and transient stability of a power system", IEE Proceedings, Vol. 115, pp: 114-120, 1968

[23] Van, Ness J.E., Brasch, F.H., Landgren, G.L., and Naumann, S.T., "Analytical investigation of dynamic instability occurring at power station", IEEE Trans. on PAS, Vol. PAS-99, pp: 1386-1395, 1980

[24] Obata, Y., Takeda, S., and Suzuki, H., "An efficient eigenvalue technique for multimachine power system dynamic stability analysis", IEEE Trans. on PAS, Vol. PAS-100, No.1, pp: 259-263, 1966

[25] Martins. N., "Efficient eigenvalue and frequency response methods applied to power system small signal stability studies" , IEEE Trans. on Power Systems, Vol. PWRS-1, No. 1, pp: 217-226, 1986

[26] Ajjarapu, V., "Reducibility and eigenvalue sensitivity for identifying critical generators in multimachine power systems", IEEE Trans. on Power Systems, Vol. PWRS-5, No. 3, pp: 712-719, 1990

[27] Yu, Y.N., and Li, Q.H., "Pole placement power system stabilisers design of an unstable nine-machine system", IEEE Trans. on Power Systems, Vol. 5, No. 2, pp: 353-358, May 1990

[28] Perez-Arriaga, I.J., Verghese, G.C., and Schweppe, F.C., "Selective model analysis with applications to electric power systems", IEEE Trans. on PAS, Pt. I & II, pp: 3117-3134, Sept. 1982

[29] Yu, Y.N., Vongsuriya, K., and Wedman, L.N., "Application of an optimal control theory to a power system", IEEE Trans. on PAS, pp: 55-62, Jan. 1970

[30] Yu, Y.N., Moussa, H.A.M., "Optimal stabilisation of a multimachine system", IEEE Trans. on PAS, pp: 1174-1182, 1972

[30a] Aldeen, M., and Crusca, F., "A new LQR approach to the design of power system stabilisers", Procceding of the 12 IFAC world congress, Sydney, Australia, 1993, Vol. 8, pp: 21-26

[30b] Moore, B.C., "Principle components analysis in linear systems: controllability, observability, and model reduction" , IEEE Trans. on Automation and Control, AC-26, pp 17-31

[31] Habibullah, B., and Yu, Y.N., "Physically realisable wide power range optimal controllers for power system", IEEE Trans. on PAS, pp: 1498-1506, Sept./Oct. 1974

[32] Ghosh, A., Ledwich, G., Malik, O.P., G.S., "Power system stabiliser based on adaptive control techniques", IEEE Trans., Vol. PAS-103, No. 8, pp: 1983-1988, August 1984

[33] Gu, W. and Bollinger, K.E., "A self-tuning power system stabiliser for wide-range synchronous generator operation", IEEE Trans. on Power System, Vol. 4, No.3, August 1989, pp.1191-1199

[34] Cheng, S.J., Chow, Y.S., Malik, O. P. and Hope, G. S., "An adaptive synchronous machine stabiliser", IEEE Trans. on Power Systems, Vol. PWRS-1, No. 3, August 1986, pp. 101-109

[35] Ghandakly, A. A. and Farhoud, A. M., "A parametrically optimised Self-Tuning Regulator for power system stabilisers", IEEE Trans. on Power Systems, Vol. 7, No. 3, August 1992, pp. 1245-1250

[36] Chandra, A., Malik, O.P. and Hope, G.S., "A Self-Tuning Controller for the control of multimachine power systems", IEEE Trans. on Power Systems, Vol. 3, August 1988, pp.1065-1071

[37] Whitaker, H. P., Yamron, J. and Kezer, A., "Design of Model Reference Adaptive Control systems for aircraft", Report R-164, Instrumentation laboratory, MIT, 1958

[38] Isermann, R., "Parameter adaptive control algorithms-a tutorial", Automatica, Vol. 18, No. 5, pp: 513-528, 1982

[39] Kalman, R. E., "Design of a self-optimising control system", ASME Transactions, Vol. 80, pp. 468-478, 1958

[40] Wieslander, J. and Wittenmark, B., "An approach to adaptive control using real time identification", Automatica 7, 211-217, 1971

[41] Astrom, K. J., Wittenmark, B., "On Self-Tuning Regulators", Automatica, Vol. 9, 1973, pp. 185-199

[42] Clarke, D. W. and Gawthrop, P. J., "A Self-Tuning Controller", IEE Proceedings, Pt. D., Vol. 122, 1975, pp. 929-933

[43] Clarke, D. W. and Gawthrop, P. J., "Self-Tuning Controller", IEE Proceedings, Pt. D., Vol. 126, 1979, pp. 633-640

[44] Wellstead, P.E., Prager, D. and Zanker, P., "Pole Assignment Self-Tuning Regulators", Proc. IEE, Vol. 126, No. , August 1979, pp.781-787

[45] Kanniah, J., Malik, O. P. and Hope, G.S, "Excitation control of synchronous generators using adaptive regulators, Part I-Theory and simulation results", IEEE Trans. on Power Systems, Vol. PAS-103, No. 5, May 1984, pp. 897-903

[46] Kanniah, J., Malik, O. P. and Hope, G.S, "Excitation control of synchronous generators using adaptive regulators, Part II-Implementation and test results", IEEE Trans. on Power Systems, Vol. PAS-103, No. 5, May 1984, pp. 904-910

[47] Harris, C. J. and Billings (Eds), S. A., "Self-Tuning and adaptive control: Theory and applications" (Peter Peregrines Ltd. 1985)

[48] Xia, D. and Heydt, G. T., "Self-Tuning Controller for generator excitation control", IEEE Trans. on Power Systems, Vol. PAS-102, No. 6, June 1983, pp. 1877-1885

[49] Bollinger, K.E. and Gu, W., "A comparison of rotor damping from adaptive and conventional PSS in a multimachine power system", IEEE Trans. on Energy Conversion, Vol. 5, No. 3, Sep. 1990, pp: 453-461

[50] Bollinger, K.E., Mister, Jr. A.F., "PSS tuning at the Virginia Electric and Power Co. Bath County Pumped Storage Plant", IEEE PAS Trans., Vol. 4, No. 2, pp: 566-574, May 1989

[51] Bollinger, K.E., Chapin, M.V., "Stability tests and tuning the PSS at Battle River Plant of Alberta Power Ltd.", IEEE PAS Trans., Vol. 3, No. 1, pp: 956-962

[52] Bollinger, K.E., Winsor, R. and Campbell, A., "Frequency response methods for tuning stabiliser to damp out tie-line power oscillations: Theory and field test results", IEEE Trans., Vol. PAS-98, No. 5, pp: 1509-1515, Sep/Oct. 1979

[53] Norum, W.E., Bollinger, K.E., "Lab and field tests of a self-tuning power system stabiliser", IEEE Trans. on Energy Conversion, Vol. 8, No. 3, pp: 476-483, Sep. 1993

[54] Fan, J. Y., Ortmeyer, T. H., Mukundan, R. "Power system stability improvement with multivariable Self-Tuning Control" IEEE Trans. on Power Systems, Vol. 5, No.1, February 1990, pp. 227, 234

[55] Khodabakhshian, A., Gosbell, V. J. and Elshafei, A. L., "New adaptive stabilisers, Part I- Pole Assignment adaptive controller using delta operator", under review by IEEE Power System Engineering Committee

[56] Allidina, A.Y. and Hughes, F.M., "Generalised Self Tuning Controller with Pole Assignment", IEE Proceedings, Vol. 127, Part D, No. 1, pp: 13-18, Jan. 1980

[57] Wu, C.J. and Hsu, Y.Y., "Design of Self Tuning PID power system stabiliser for multimachine power systems", IEEE Trans. on Power Systems, August 1988, pp: 1059-1064

[58] Cheng, S.J., Malik, O.P. and Hope, G.S., "Self-Tuning stabiliser for a multimachine power system", IEE Proc., Pt. C., pp. 176-185, May 1986

[59] Chen, G.P., Malik, O.P., Hope, G.S., Qin, Y.H., and Xu, G.Y., "An adaptive power system stabiliser based on the self-optimising pole shifting control strategy", IEEE Trans. on Energy Conversion, Vol. 8, No. 4, pp: 639-645, Dec. 1993

[60] Malik, O.P., Chen, G.P., Hope, G.S., Qin, Y.H. and Xu, G.Y., "An adaptive self-optimising pole shifting control algorithm", IEE Proceedings-D, Vol. 139, No. 5, pp: 429-438, 1992

[61] Pahalawatha, N.C., Hope, G.S. and Malik, O.P., "Multivariable Self Tuning power system stabiliser simulation and implementation studies", IEEE Trans. on Energy Conversion, Vol. 6, No. 2, pp: 310-319, June 1991

[62] Pahalawatha, N.C., Hope, G.S., Malik, O.P. and Wong, K., "Real time implementation of a MIMO adaptive power system stabiliser", IEE Proceedings, Vol. 137, Pt. C, No. 3, pp: 186-194, May 1990

[63] Malik, O.P., Hope, G.S., Cheng, S.J. and Hancock, G., "A multi-microcomputer based dual-rate Self Tuning power system stabiliser", IEEE Trans., EC-2,(3), pp: 355-360, 1987

[64] Ghandakly, A. and Dai, J.J., "An adaptive synchronous generator stabiliser design by Generalised Multivariable Pole Shifting (GMPS)

technique", IEEE Trans. on Power Systems, Vol. 7, No. 3, pp: 1239-1244, August 1992

[65] Khodabakhshian, A., Gosbell, V. J. and Elshafei, A. L., "New adaptive stabilisers, Part II- Model Reference Adaptive Controller using delta operator", under review by IEEE Power System Engineering Committee

[66] Mao, C., Malik, O. P., Hope, G. S. and Fan, J. Y., "An adaptive generator excitation controller based on linear optimal control", IEEE Trans. on Energy Conversion, Vol. 5., No. 4, 1990, pp. 673-678

[67] Mao, C.X., Fan, J., Malik, O.P. and Hope, G.S., "Studies of real-time adaptive optimal excitation controller and adaptive optimal power system stabiliser", IEEE Trans. on Energy Conversion, Vol. 7, No. 3, pp: 598-605, Sep. 1992

[68] Mao, C.X., Prakash, K.S., Malik, O.P., Hope, G.S. and Fan, J., "Implementation and laboratory test results for an adaptive power system stabiliser based on linear optimal control", IEEE Trans. on Energy Conversion, Vol. 5, No. 4, pp: 666-672, Dec. 1990

[69] Lim, C.M, "A Self-Tuning stabiliser for excitation or governor control of power systems", IEEE Trans. on Energy Conversions, Vol. 4, No. 2, June 1989, pp. 152-159

[70] Goodwin, G.C and Kwai, S.S., "Adaptive filtering prediction and control", Prentice-Hall, New Jersey, 1984

[71] Wu, Q.H., and Hogg, B.W., "Self Tuning Control for turbogenerator in multimachine power systems", IEE Proceedings, Vol. 137, Pt. C, No. 2, pp: 146-158, March 1990

[72] Ghandakly, A. and Idowa, P., "Design of a model reference adaptive stabiliser for the exciter and governor loops of power generators", IEEE Trans. on Power Systems, Vol. 5, No. 3, pp: 887-893, August 1990

[73] Ghandakly, A., Kroneger, P., "Digital controller design method for synchronous generator excitation and stabiliser systems, Part I: methodology and computer simulation", IEEE Trans. on Power Systems, Vol. PWRS-2, No. 3, pp: 633-637, August 1987

[74] Irving, E., Barret, J. P., Charcossey, C. and Monville, J. P., "Improving power network stability and unit stress with adaptive generator control", Automatica, Vol. 15, No. 1, Jan. 1979, pp. 31-46

[75] Popov, V. M., "The solution of a new stability problem for controlled systems", Translated from Autom. Telemekh., No. 7, pp. 7-27, 1963

[76] Hsu, Y.Y. and Chen, C.R., "Tuning of power system stabilisers using an artificial neural network", IEEE Trans. on Energy Conversion, Vol. 6, No. 4, pp: 612-619, Dec. 1991

[77] Rumelhart, D.E., Hinton, G.E. and Williams, R.J., "Learning internal representations by error propagation", in D.E Rumelhart and J.L. McClelland, Parallel Distributed Processing, Vol. 1, ch. 8

[78] Zhang, Y., Chen, G.P., Malik, O.P. and Hope, G.S., "An artificial neural network based adaptive power system stabiliser", IEEE Trans. on Energy Conversion, Vol. 8, No. 1, pp: 71-77, March 1993

[79] Hiyama, T., "Application of neural network to real time tuning of fuzzy logic PSS", ANNPS'93, Proceedings of the second International Forum on Applications of Neural Networks to power systems

[80] Hsu, Y.Y., and Cheng, C.H., "Design of fuzzy power system stabilisers for multimachine power systems", IEE Proceedings, Vol. 137, Pt. C, No.3, pp: 233-238, May 1990

[81] Astrom, K.J. and Wittenmark, B. "Computer controlled systems, theory and design" (Prentice-Hall,1990)

[82] Middleton, R.H. and Goodwin, G.C. "Improved finite word length characteristics in digital control using delta operators", IEEE Trans. Automatica, Contr.Vol, AC-31, pp 1015-1021, Nov.1986

[83] Middleton, R.H. and Goodwin, G.C. "Digital control and estimation" (Prentice-Hall, 1990)

[84] Khodabakhshian, A., Gosbell, V. J. and Coowar, F., "Discretization of power system transfer functions", IEEE Tans. on Power Systems, Vol. 9, No. 1, Feb. 1994, pp. 255-261

[85] Khodabakhshian, A. and Gosbell, V. J., "A new model for identifying adaptive control of power system", International Power System Engineering Conference, Singapore, March 1993

[86] IEEE Committee report, "Excitation system models for power system stability studies", IEEE Trans. on PAS, Vol. PAS-100, No.2, Feb. 1981, pp. 494-509

[87] Koessler, R.J., "Techniques for tuning excitation system parameters", IEEE Trans. on Energy Conversion, Vol. 3, No. 4, Dec. 1988

[88] O'Brein, M., Ledwich, G., "Placement of static compensators for stability improvement", IEE Proc. C., Vol. 132, No. 1, Jan. 1985, pp. 30-35

[89] Martins, N. and Lima, L.T., "Determination of suitable locations for power system stabilisers and static var compensators for damping electromechanical oscillations in large scale power systems", IEEE Trans. on Power Systems, Vol. 5, No. 4, Nov. 1990, pp. 1455-1469

[90] Kothari, M.L. and Nanda, J., "Application of optimal control strategy to automatic generation control of a hydrothermal system", IEE, Proc.C, Vol. 135, No. 4, pp. 268-274, 1988

[91] Ljung, L. and Soderstrom, T. "Theory and practice of recursive identification" (The MIT Press series in signal processing, optimization, and control, 1983)

[92] Astrom, K.J. and Eykhoff, P. "System identification-A survey" Automatica, Vol. 7, pp. 123-162, 1971

[93] Franklin, G. F., Powell, J. D. and Workman, M. L., "Digital control of dynamic systems, Second Edition" (Addison-Wesley Publishing Company, 1990)

[92] Anon, "Digital control generators", ABB review, No. 1, pp: 27-32, 1990

[95] Bellman, R., "Introduction to matrix analysis" (McGraw-Hill, New York, 1970)

[96] Astrom, K.J., Hagander, P. and Sternby, J. "Zeros of sampled systems", Automatica, Vol. 20, pp. 31-39, 1984

[97] Demello, F.P., Hannet, L.N., Parkinson, DS.W. and Czuba, J.S."A power system stabiliser design using digital control", IEEE Trans. on PAS, Vol. 101, pp. 2860-2868, 1982.

[98] Golten and Verwer partners, "Control system design and simulation (CODAS II)" Version 1.1, 1989

[99] Astrom, K.J., "Theory and applications of adaptive control, A survey", Automatica, Vol. 19, No. 5, Sept. 1983, pp. 471-486

[100] Astrom,K J. and Wittenmark, B, "Adaptive control", (Addison-Wesley, 1989)

[101] Adkins, B. and Harley, H.G., "The general theory of alternating current machines" (Chapman and Hall, 1975)

[102] Moussa, H.A.M. and Yu, Y.N., "Dynamic interaction of multimachine power system and excitation control", IEEE Trans. om PAS, Vol. PAS-93, Jul/Dec 1974, pp. 1150-1158

[103] Mobarak, M., Thorne, D. and Hill, E., "Contrast of power system stabiliser performance on hydro and thermal units", IEEE Trans. on PAS, Vol. PAS-99(4), pp. 1522-1533, 1980

[104] Ostogic, D. and Kovacevic, B., "On eigenvalue control of electromechanical oscillations by adaptive power system stabiliser", IEEE Trans. on power systems, Vol. 5, No.3, 1990, pp. 1188-1125

[105] Malik, O.P., Hope, G.S., Cheng, S.J. and Hancock, G., "A multi-micro-computer based dual-rate self-tuning power system stabiliser", IEEE Trans. on EC, Vol. 2, pp.355-360, 1987

[106] Edmunds, J.M., "Digital adaptive pole-shifting regulators", Ph.D thesis, UMIST, 1976